

Combating Antimicrobial Resistance: Synthesis of Pantothenamide-Mimicking Compounds Containing a 4,5- Dihydroisoxazole Ring

Shannon Heans

Department of Chemistry

McGill University

Montreal, Quebec, Canada

H3A 0B8

July 2023

*A thesis submitted to McGill University in partial fulfillment
of the requirements of the degree of Master of Science*

© Shannon Heans, 2023 All rights reserved

Table of Contents

Abstract.....	4
Résumé.....	6
Acknowledgements.....	8
List of Figures.....	9
List of Schemes.....	11
List of Tables.....	12
Abbreviations.....	13
Chapter 1: Introduction	
1.1 Infectious Diseases and Antimicrobial Resistance.....	16
1.2 Bacteria and Antibiotics.....	17
1.3 Parasites, Malaria, and Antiplasmodials.....	21
1.4 Coenzyme A Biosynthesis.....	25
1.5 Pantothenamides.....	27
1.6 Research Objective.....	38
Chapter 2: Synthetic Design and Strategy	
2.1 Preface and Contributions.....	40
2.2 Introduction.....	40
2.3 Synthetic Design of PanMCs Containing a 4,5-Dihydroisoxazole Moiety.....	42
2.4 Objective.....	44
2.5 Synthetic Results and Discussion.....	45
2.6 Conclusion.....	47

Chapter 3: Antibacterial Results

3.1	Preface and Contributions.....	50
3.2.	Introduction.....	50
3.3	Evaluation of Antibacterial Activity.....	52
3.4	Conclusion.....	57

Chapter 4: Antiplasmodial Results

4.1	Preface and Contributions.....	59
4.2	Introduction.....	59
4.3	Evaluation of Antiplasmodial Results.....	60
4.4	Conclusion.....	66

Chapter 5: Contributions and Future Directions

5.1	Contributions.....	68
5.2	Future Directions.....	68

Chapter 6: Experimental Protocols

6.1	Chemistry.....	71
6.2	Biology.....	95

References	99
-------------------	-------	----

Appendix: NMR Spectra	116
------------------------------	-------	-----

Abstract

The prevalence of antimicrobial resistance has been steadily increasing since antibiotics were first introduced in the clinics. While the development of antimicrobial resistance is a natural part of evolution for microbes, it has been exacerbated exponentially by the misuse and overuse of antimicrobials. It is estimated that by 2050, antimicrobial resistance will become one of the world's leading healthcare challenges, exemplified by the World Health Organization's (WHO) 2019 declaration that estimates antimicrobial resistance to be in the top ten global public health threats facing humanity. Several different approaches to tackling this problem exist – with the development of small molecule drugs displaying novel mechanisms of action being among the leading approaches. Antimicrobials featuring novel mode(s) of action avoid cross-resistance issues, slowing antimicrobial resistance development.

About 9 % of all known enzymes, including over 100 enzymes involved in metabolism alone, require coenzyme A (CoA) as an important cofactor, making its biosynthesis/metabolism a desirable target for drug development. It has been shown that inhibition or modification of the CoA cycle could lead to microbicidal treatments. Pantothenamides are amide derivatives of pantothenate (vitamin B₅) displaying antimicrobial activity through a unique, and typically multiple, mechanism(s) of action, making them attractive new agents in the battle against antimicrobial resistance. They act via a prodrug strategy, by which bacterial or parasitic CoA biosynthetic enzymes transform the molecules into the corresponding CoA antimetabolites that can inhibit further downstream CoA-utilizing enzymes, resulting in bacterial or parasitic cell death. However, pantothenamides are susceptible to cleavage by serum enzymes called pantetheinases, that hydrolyze pantothenamides into pantothenate and the corresponding amine; therefore, rendering them inactive *in vivo*. Our group focuses on developing a chemically diverse library of pantothenamide-mimicking compounds (PanMCs) that exhibit enhanced potency and reduced pantetheinase-related degradation.

Herein, 6 PanMCs (containing a 4,5-dihydroisoxazole ring in replacement of the labile amide bond) were synthesized, 5 in which are novel. Antibacterial testing was

performed for the six PanMCs synthesized (containing a 4,5-dihydroisoxazole ring) as well as five PanMCs synthesized by group member Chunling Blue Lan (containing either a tetrahydrofuran ring, a 4,5-dihydrooxazole ring, a 4,5-dihydrothiazole ring, an oxazolidin-2-one ring, or a 1,3-dioxolane ring). Antiplasmodial activity was described for the six PanMCs (containing a 4,5-dihydroisoxazole ring) synthesized, as well as ten PanMCs synthesized by group member Victoria Virgilio, (containing either a thiazole ring, a 1,3,4-thiadiazole ring, or a 4,5-dihydroisoxazole ring).

While none of the PanMCs tested displayed significant activity against any of the bacterial strains, six PanMCs containing various ring mimics displayed marginal activity against intraerythrocytic *Plasmodium falciparum*. Although future investigation is needed, this work contributes insight into structural changes of PanMCs and their resulting biological properties.

Résumé

La prévalence de la résistance aux antimicrobiens n'a cessé d'augmenter depuis l'introduction des antibiotiques en clinique. Bien que le développement de la résistance aux antimicrobiens fasse naturellement partie de l'évolution des microbes, il a été exacerbé de façon exponentielle par le mauvais usage et la surutilisation des antimicrobiens. On estime que d'ici 2050, la résistance aux antimicrobiens deviendra l'un des principaux défis mondiaux en matière de santé, comme en témoigne la déclaration de l'Organisation mondiale de la santé de 2019, qui estime que la résistance aux antimicrobiens figure parmi les dix principales menaces mondiales pour la santé publique auxquelles l'humanité est confrontée. Il existe plusieurs stratégies pour résoudre ce problème - le développement de médicaments à petites molécules présentant de nouveaux mécanismes d'action étant parmi les principales approches. Les antimicrobiens dotés de nouveaux modes d'action évitent les problèmes de résistance croisée et ralentit le développement de la résistance antimicrobienne.

Environ 9 % de toutes les enzymes connues, dont plus de 100 enzymes impliquées dans le métabolisme de base, nécessitent la coenzyme A (CoA) comme cofacteur, faisant de sa biosynthèse ou de son métabolisme une cible intéressante pour le développement de médicaments. Il a été montré que l'inhibition ou la modification du cycle de la CoA pouvait conduire à des traitements microbicides. Les pantothénamides sont des dérivés amides de la pantothénate (vitamine B₅) affichant une activité antimicrobienne par un ou plusieurs mécanismes d'action uniques, ce qui en fait de nouveaux agents attractifs dans la lutte contre la résistance aux antimicrobiens. Ils agissent via une stratégie de promédicament, par laquelle les enzymes biosynthétiques bactériennes ou parasitaires de CoA transforment ces molécules en antimétabolites de la CoA qui peuvent inhiber les enzymes utilisant la CoA en aval, entraînant la mort des cellules bactériennes ou parasitaires. Cependant, les pantothénamides sont susceptibles d'être clivés par des enzymes sériques appelées pantéthénases, qui hydrolysent les pantothénamides en pantothénate et l'amine correspondante; par conséquent, les rendant inactifs *in vivo*. Notre groupe se concentre sur le développement d'une bibliothèque chimiquement diversifiée d'imitateurs des

pantothénamides qui présentent une puissance accrue et une dégradation réduite liée à la pantéthénase.

Ici, cinq nouvelles molécules imitant les pantothénamides (contenant un cycle 4,5-dihydroisoxazole en remplacement du lien amide labile) et un analogue précédent contenant le même cycle ont été synthétisés. Des tests antibactériens sont rapportés pour ces six molécules synthétisés ainsi que cinq autres molécules (contenant soit un cycle tétrahydrofurane, un cycle 4,5-dihydrooxazole, un cycle 4,5-dihydrothiazole, un cycle oxazolidine-2-one, ou un cycle 1,3-dioxolane) synthétisées par Chunling Blue Lan, un membre du groupe. L'activité antiplasmodiale est aussi décrite pour les six molécules contenant un cycle 4,5-dihydroisoxazole, ainsi que pour dix autres molécules imitant les pantothénamides synthétisés par la membre du groupe Victoria Virgilio (contenant soit un cycle thiazole, soit un cycle 1,3,4-cycle thiadiazole, ou un cycle 4,5-dihydroisoxazole).

Bien qu'aucun des imitateurs de pantothénamide testés n'ait montré d'activité significative contre les souches bactériennes, six de ces molécules ont montré une activité marginale contre *Plasmodium falciparum* intraérythrocytaire. Nonobstant le fait que des recherches futures soient nécessaires, ces travaux contribuent à mieux comprendre les changements structuraux des imitateurs de pantothénamide et les propriétés biologiques qui en résultent.

Acknowledgements

There are so many wonderful people that I am so lucky to have met, and it makes me so proud to be earning my Master of Science from McGill University. I want to sincerely thank my supervisor, Prof. Karine Auclair for her interdisciplinary expertise, kindness, and wisdom, but most of all her compassion and patience with me throughout this entire experience. To my mother, thank you for always making me laugh even when I wanted to cry and always telling me that doing my best will always be enough. Also, I want to thank my friends and my entire research group who have stood by me throughout this whole journey to success. I also want to specially thank Jake Pierscianowski for teaching me all the biological techniques that I now use every day, as well as Victoria Virgilio and Chunling Blue Lan for helping me hone my synthetic techniques.

My sincerest gratitude goes out to my wonderful committee members: Prof. Nathan Luedtke and Prof. Scott Bohle, as well as Dr. Alex Wahba and Dr. Nadim Saadé for running my high-resolution mass spectrometry samples, and the Lumb, Tsantrizos, Arndsten, and Moitessier research groups for lending me chemicals. Also, a huge thank you goes out to Dr. Danielle Vlaho and Mr. Mitchell Huot for being excellent mentors to me and teaching me how to be a better mentor for others. It was an absolute honour and pleasure to be a part of McGill's Chemistry Department and to work with the most brilliant young minds and professors. There are no words to describe how grateful and lucky I am to have had this opportunity and I will continue to strive for excellence with the tools McGill gave me on my future path.

List of Figures

Figure 1.1: Timeline of when antibiotics were introduced into clinics (green boxes) and when corresponding resistance to antibiotics were observed (red boxes).⁸ The golden age of antibiotics is highlighted in yellow.

Figure 1.2: Examples of different species of bacteria.

Figure 1.3: Structure of Gram-positive (left) and Gram-negative (right) bacterial cell envelope.

Figure 1.4: Examples of each class of parasite that causes disease in humans. From left to right: protozoa, helminths, and an ectoparasite.

Figure 1.5: Life cycle of a *Plasmodium* infection.^{29–32}

Figure 1.6: Examples of ACTs; artemisinin derivatives (first row) and known partner drugs for the treatment of malaria (second and third rows).²⁹

Figure 1.7: Comparison of CoA antimetabolites and CoA. CoA antimetabolites lack the terminal thiol group necessary for acyl group transfer.

Figure 1.8: Different regions of synthetic modifications on the pantothenamide scaffold.

Figure 1.9: Summarized SARs for activity against *E. coli*.

Figure 1.10: Summarized SARs for activity in *S. aureus*.

Figure 1.11: Summarized SARs for activity against *P. falciparum*.

Figure 2.1: Examples of pharmaceuticals exhibiting a 5-membered, non-aromatic, heteroatom-containing rings. Said ring structure are highlighted in pink.

Figure 2.2: Examples of fluorinated pharmaceuticals. Florinef acetate is used in the treatment of adrenogenital syndrome, adrenal insufficiency, and postural hypotension.⁶⁵ Levofloxacin is an antibiotic, and Lipitor is a cholesterol-lowering agent. Fluorine atoms are highlighted in blue.

Figure 2.3: The current library of PanMCs featuring a 4,5-dihydroisoxazole ring synthesized by Chunling Blue Lan (**1a**) and Victoria Virgilio (**2a–2h**) as diastereomeric mixtures.

Figure 2.4: PanMCs synthesized by the author in this thesis as diastereomeric mixtures. **3f** was originally synthesized by Victoria Virgilio⁶⁷ but was remade for the

biological testing. The pantoyl moiety is highlighted in green and the side chain is highlighted in yellow.

Figure 2.5: Retrosynthesis to accessing the PanMCs generated in this thesis. The common fragment, the pantoyl moiety, is highlight in green and the side chain is highlighted in yellow.

Figure 3.1: Examples of common sites of infection for the six bacterial species being explored.^{68–74}

Figure 3.2: Structures of the PanMCs synthesized by the author. **3f** was originally synthesized by Victoria Virgilio⁶⁷ but was remade for the biological testing.

Figure 3.3: Structures of the PanMCs synthesized by group member Chunling Blue Lan that were tested here for antibacterial activity.

Figure 3.4: Percent growth inhibition of *A. baumannii*, *E. coli*, *K. pneumoniae*, *P. aeruginosa*, *S. aureus*, and *S. Typhimurium* in the presence of compound (50 μ M). The first lane is the control experiment with no compound added and is adjusted to 100 % growth. All experiments were performed in triplicates. Standard error of mean was used to determine the error bars.

Figure 3.5: MIC curves of **1d** (left) and **3c** (right) for growth inhibition of *S. aureus*. The highest concentration of compound tested was 50 mM. All experiments were performed in triplicates. Standard error of mean was used to determine the error bars.

Figure 3.6: MIC curves of **1d** (left) and **3c** (right) for growth inhibition of *A. baumannii*. The highest concentration of compound tested was 50 mM. All experiments were performed in triplicates. Standard error of mean was used to determine the error bars.

Figure 4.1: PanMCs synthesized by previous group member Victoria Virgilio.⁶⁷

Figure 4.2: PanMCs synthesized by the author. **3f** was first synthesized by previous group member Victoria Virgilio.⁶⁷

Figure 5.1: Potential PanMCs featuring a 4,5-dihydroisoxazole ring to add to the library.

Figure 5.2: Potential PanMCs featuring a 4,5-dihydroisoxazole ring in a different orientation.

Figure 6.1: The structure of the PanMC used as a negative control.⁶

List of Schemes

Scheme 1.1: The biosynthesis of CoA. The traditional pathway starts with pantothenate (highlighted in green). The CoA salvage pathway begins with pantetheine (highlighted in blue).

Scheme 1.2: Pantothenamide hydrolysis catalyzed by pantetheinases.

Scheme 1.3: Bioactivation of a generic pantothenamide into a CoA antimetabolite.

Scheme 2.1: The synthetic route used to access PanMCs **3a–3f**. NaOAc: sodium acetate, EtOH: ethanol, NCS: *N*-chlorosuccinimide, DMF: dimethylformamide, TEA: triethylamine, EA: ethyl acetate, TFA: trifluoroacetic acid, DCM: dichloromethane, TBD: triazabicyclodecene.

Scheme 2.2: Formation of the side product during the intermolecular cyclization.

List of Tables

Table 1.1: Examples of antibiotics, categorized by their mechanism of action.

Table 1.2: Pantothenamides active against *E. coli*. Compounds with an MIC less than 10 μ M are shown.^{52–54}

Table 1.3: Pantothenamides and PanMCs active against *S. aureus*. Compounds with an MIC less than 10 μ M are shown.^{52,53}

Table 1.4: Pantothenamides and PanMCs active against *P. falciparum*. Compounds with an IC₅₀ less than 1 μ M are shown.^{43,48,49} The IC₅₀ values in red are from molecules tested in pantetheinase-inactivated media.^{40,49}

Table 2.1: The most potent PanMCs against *P. falciparum* featuring a triazole, thiazole, or isoxazole ring in place of the labile amide group. Only compounds with nanomolar activity are shown.

Table 4.1: IC₅₀ values for compounds **2a**, **2d**, **4a–4h**, and **3a–3f** against intraerythrocytic *P. falciparum* are highlighted in purple and blue, respectively. IC₅₀ values for the previously reported PanMCs^{50,64} featuring the same rings in replacement of the labile amide group (**5a–5r**) are also shown in black for the purpose of establishing broader SARs. Standard error of the mean was used to calculate error. PanMCs with activity in the nanomolar range are highlighted in red.

Table 6.1: HPLC methods for purity measurements of non-free amine containing compounds.

Table 6.2: HPLC methods for purity measurements of free amine-containing compounds.

Table 6.3: Linear equations for each bacterial strain used to determine bacteria concentration.

Abbreviations

<i>A. baumannii</i>	<i>Acinetobacter baumannii</i>
ACT	Artemisinin-based combination therapy
AIDS	Acquired Immunodeficiency Syndrome
CoA	Coenzyme A
DCM	Dichloromethane
DPCK	Dephospho-coenzyme A kinase
EtOH	Ethanol
EA	Ethyl acetate
<i>E. coli</i>	<i>Escherichia coli</i>
HIV	Human immunodeficiency virus
IC ₅₀	Half-maximal growth inhibition
<i>K. pneumoniae</i>	<i>Klebsiella pneumoniae</i>
MIC	Minimum inhibitory concentration
NCS	<i>N</i> -chlorosuccinimide
N5-pan	<i>N</i> -pentylpantothenamide
<i>P. aeruginosa</i>	<i>Pseudomonas aeruginosa</i>
PanK	Pantothenate kinase
PanMC	Pantothenamide-mimicking compound

<i>P. falciparum</i>	<i>Plasmodium falciparum</i>
PPAT	Phosphopantetheine adenylyltransferase
PPCDC	Phosphopantothenoylcysteine decarboxylase
PPCS	Phosphopantothenoylcysteine synthase
SAR	Structure activity relationship
<i>S. aureus</i>	<i>Staphylococcus aureus</i>
<i>S. Typhimurium</i>	<i>Salmonella enterica</i> serovar Typhimurium
TBD	Triazabicyclodecene
TEA	Triethylamine
TFA	Trifluoroacetic acid
WHO	World Health Organization

Chapter 1

Introduction

1.1. Infectious Diseases and Antimicrobial Resistance

Infectious diseases pose a significant threat to healthcare systems and continues to jeopardize modern medicine. They affect public health systems around the world, harming disadvantaged communities disproportionately.¹ Pathogenic microorganisms including bacteria, fungi, and parasites are known to cause infectious disease as they can enter the body, proliferate, and cause an illness.² The most fatal infectious diseases to date are lower respiratory tract infections, which encompass a variety of illnesses such as pneumonia, bronchitis, and bronchiolitis, and these infections kill over 2 million people per year.^{3,4}

Humans and microbes' evolutionary paths have always been intertwined.⁵ On one side, humans develop antimicrobials to fight infectious diseases, and on the other side, microbes evolve to evade these medicines designed to eliminate them.⁵ It is an eternal battle. Nevertheless, the introduction of antimicrobials into the healthcare systems has dramatically improved the lifespan and quality of life of humans, and animals alike.⁶ Despite this, microbes have kept pace with antimicrobial development by using several evolutionary tactics to gain resistance.

In recent years, humans have been struggling to keep up with the rate in which microbes develop resistance mechanisms to the antimicrobials on the market (Figure 1.1).⁸

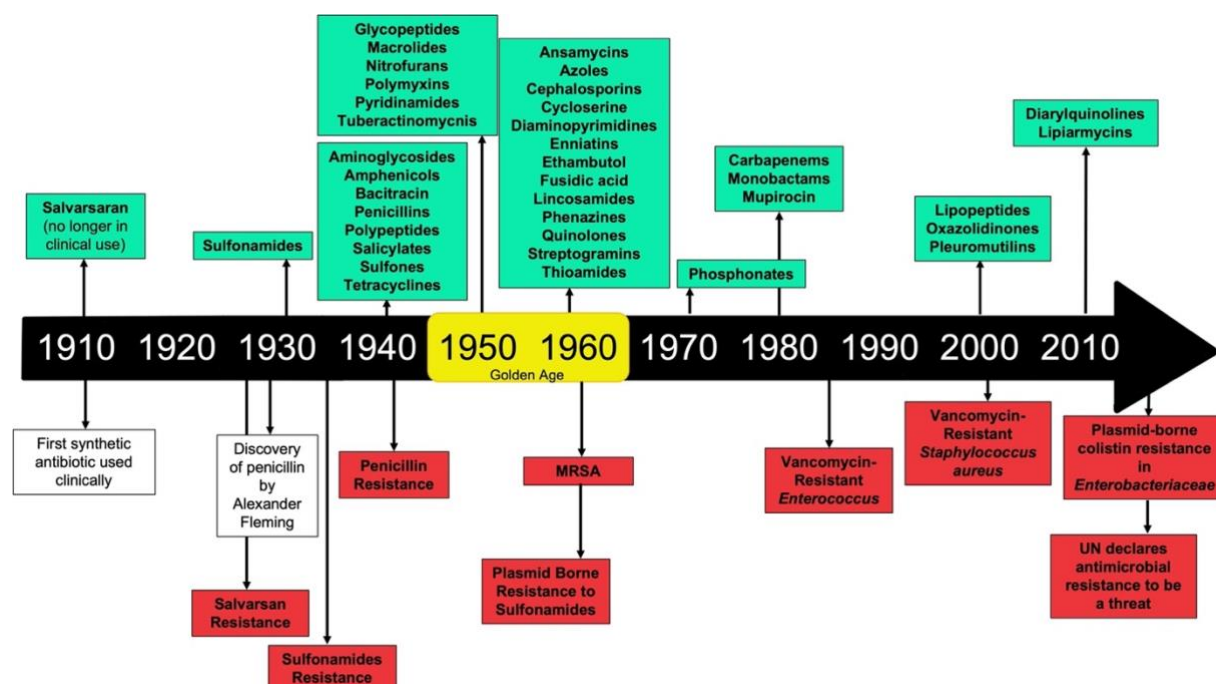


Figure 1.1: Timeline of when antibiotics were introduced into clinics (green boxes) and when corresponding resistance to antibiotics were observed (red boxes).⁸ The golden age of antibiotics is highlighted in yellow.

Drug resistant infectious diseases play a critical role in hospitals making undergoing procedures, even acute operations, a risky feat.^{7,9} Approximately 4 % of patients undergoing routine hospital procedures in the United States alone, acquire a drug-resistant microbial infection.⁹

The World Health Organization (WHO) currently estimates that 10 million people per year will succumb to antimicrobial resistant infections by 2050.¹⁰ The need for novel antimicrobials is dire.⁷⁻¹³ As such, the development of small molecule drugs displaying novel mechanisms of action is one of the major approaches to this problem.^{12,13}

1.2. Bacteria and Antibiotics

Bacteria are typically single-cell prokaryote microorganisms (Figure 1.2). They can survive in a myriad of diverse environments; from the soil, to acidic hot springs, to radioactive waste, to inside the human gut flora, and even in arctic snow.¹⁴ Bacteria are essential to life and the environment as they are heavily involved in the recycling of

nutrients and account for a large percentage of Earth's biomass.^{14,15} Remarkably, only a small subset of bacteria are disease-causing.¹⁴ Humans can contract bacterial infections through the air, food, living vectors, or water.^{14,15} However, the spread of drug resistant disease-causing bacteria is becoming increasingly alarming. In 2019, antimicrobial resistant bacterial infections caused 1.27 million deaths.¹⁶

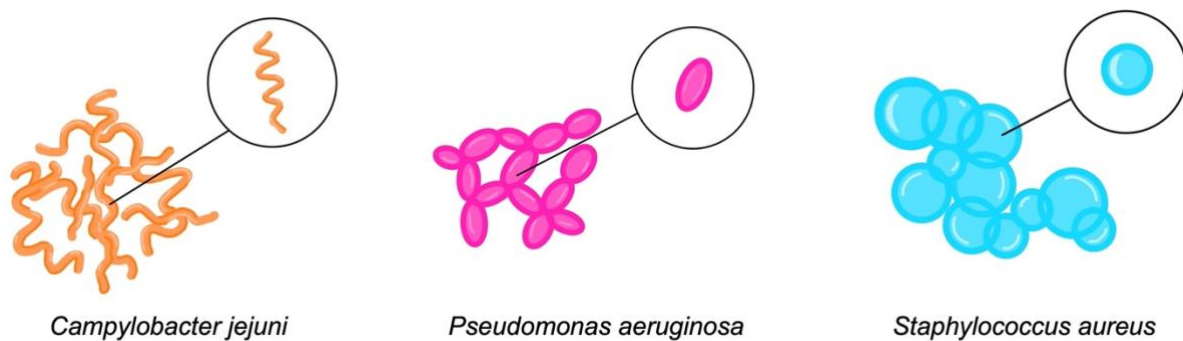


Figure 1.2: Examples of different species of bacteria.

Most bacterial species can be classified into one of two groups: Gram-negative or Gram-positive depending on the presence of an outer cell membrane or lack thereof (Figure 1.3).¹⁷ Gram-positive bacteria do not have an outer cell membrane, but instead have a thicker layer of peptidoglycan than Gram-negative bacteria.¹⁸ The former are also responsible for a large percentage of bloodstream infections in hospital.¹⁹ Gram-negative bacteria have a thin peptidoglycan cell wall, but they have an additional outer cell membrane containing lipopolysaccharides.¹⁸ They cause infections that are typically harder to treat than Gram-positive bacteria due to the very low permeability of their outer cell membrane to antibiotics.²⁰

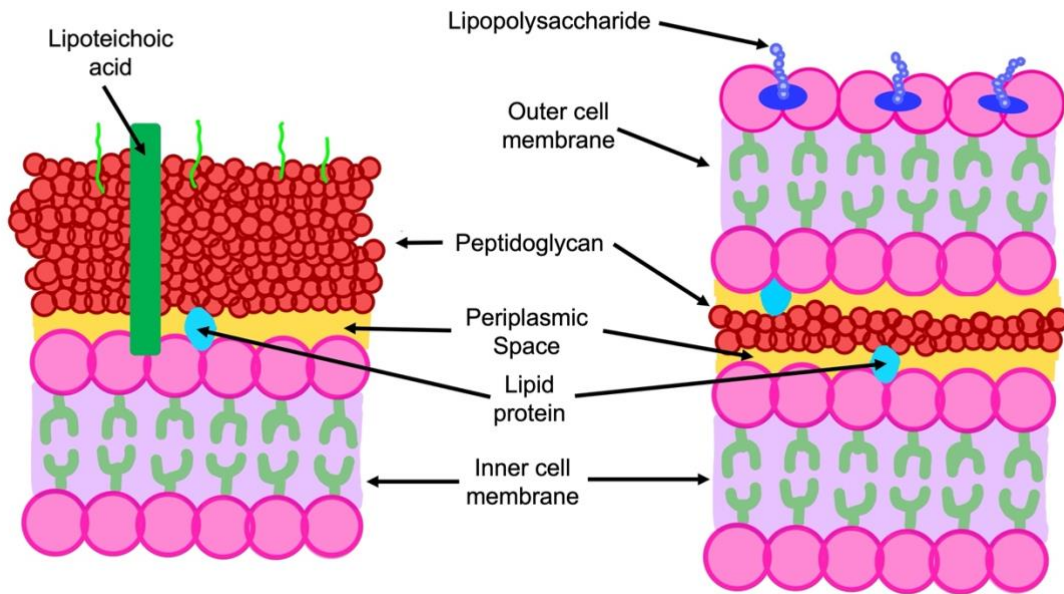
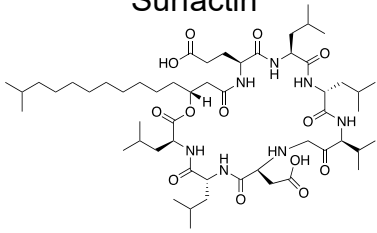
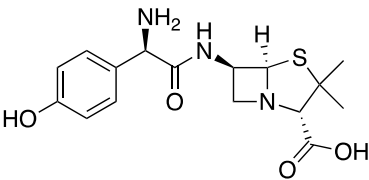
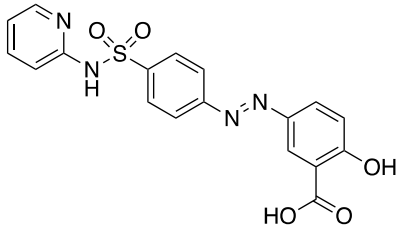
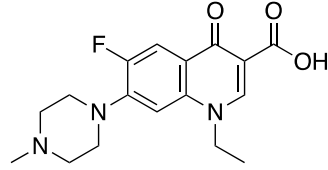


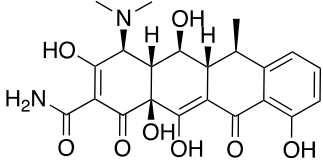
Figure 1.3: Structure of Gram-positive (left) and Gram-negative (right) bacterial cell envelope.

Antibiotics are medicines specifically used to treat and prevent bacterial infections while leaving the host unharmed. The “antibiotic era” started shortly after Paul Ehrlich originally had the idea of a “magic bullet”⁸ – a weapon that could meticulously target the microbe in the human body while leaving healthy cells alone.^{8,21–23} This philosophy led Ehrlich to develop a detailed screening procedure that ultimately lead to the discovery Salvarsan, a treatment for *Treponema pallidum*⁸ (the parasite that causes syphilis) and many others to follow.^{8,22} Then, the golden age of antibiotics dawned on society when Alexander Fleming discovered penicillin and it was introduced into the clinics.^{8,23} Several new classes of antibiotics were discovered during the golden age (1940–1970), but since then, the number of new antibiotics being discovered is less and less.^{8,21–24}

The antibiotics that are currently known, can be classified into categories based on their mechanism of action (Table 1.1).¹³

Table 1.1: Examples of antibiotics, categorized by their mechanism of action.

Mechanism of Action	Antimicrobial Class	Example
Disruption of cell membrane integrity	Lipopeptides	<p>Surfactin</p> 
Inhibit cell wall synthesis	<p>β-lactams</p> <p>Carbapenems</p> <p>Cephalosporins</p> <p>Monobactams</p> <p>Penicillins</p> <p>Glycopeptides</p>	<p>Amoxicillin, a penicillin</p> 
Inhibit metabolic pathways	<p>Sulfonamides</p> <p>Trimethoprim</p>	<p>Sulfalazine (Azulfidine), a sulfonamide</p> 
Inhibit nucleic acid synthesis	Quinolones	<p>Perfloxacin</p> 

Inhibit protein synthesis	Aminoglycosides	<p>Doxycycline, a tetracycline</p> 
	Tetracyclines	
	Chloramphenicol	
	Lincosamides	
	Macrolides	
	Oxazolidinones	
	Streptogramins	

Antimicrobial resistant bacteria continue to pose a significant threat to humanity, as humankind's discovery of new antibiotics has slowed considerably.

1.3. Parasites, Malaria, and Antiplasmodials

Parasites are organisms that infiltrate and inhabit a host organism, feeding at the expense of the host or off the host itself, forming an amensalism relationship.²⁵ Protozoa, helminths, and ectoparasites are the three different types of parasites that cause illness in humans (Figure 1.4).²⁵ Millions of people every year, predominately in the tropics and subtropics, contract a parasitic infection, with intestinal parasitic infections being among the most common class.^{26,27} These parasitic infections are frequently contracted through contaminated food or water.²⁸

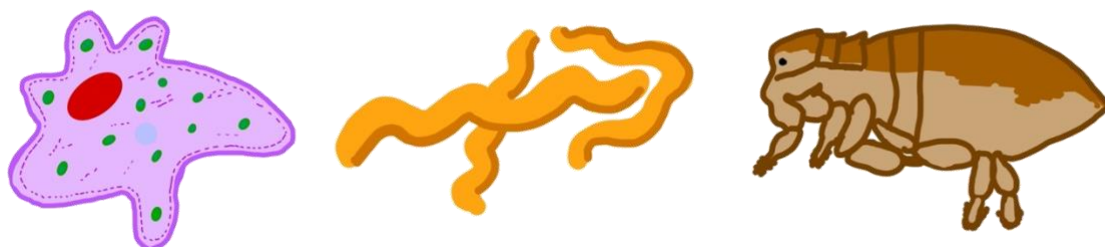


Figure 1.4: Examples of each class of parasite that causes disease in humans. From left to right: protozoa, helminths, and an ectoparasite.

Despite the high infection rate of intestinal parasitic infections, malaria is the most fatal parasitic infection globally with 241 million cases reported in 2020 and over 400 000 deaths estimated each year.^{27,29} Malaria is caused by a protozoan parasite of the genus *Plasmodium*, and is a vector borne disease, meaning that a living organism transmits the infection from one organism to another.²⁹ There are over 100 different species of *Plasmodium*; however, only 6 are known to infect humans with *Plasmodium falciparum* causing the most severe symptoms and the most fatalities.²⁹ Malaria is prevalent in countries lying close to the equator, particularly in sub-Saharan Africa, Central and Latin America, South-East Asia, and the Western Pacific region.³⁰ This parasitic infection poses a threat to about half of the world's population, with children under the age of 5, pregnant women, and people living with HIV/AIDS being the most at risk.^{29,30}

The life cycle of the *Plasmodium* species is elaborate and involves infections of humans and female *Anopheles* mosquitos (Figure 1.5).³¹ The cycle begins with an infected female *Anopheles* mosquito that bites and feeds on a human while injecting sporozoites into the human bloodstream.^{29–32} The sporozoites find their way to the liver where they undergo asexual reproduction forming schizonts.^{29–32} The schizonts then grow in size in the liver until they burst, releasing merozoites, or daughter cells, into the bloodstream.^{29–32} These merozoites are then able to infect the human blood cells, erythrocytes, and undergo asexual reproduction again.^{29–32} Eventually the erythrocytes will burst causing the host to experience clinical symptoms of malaria, and merozoites

will be released again into the bloodstream.^{29–32} Without treatment, this cycle of merozoites infecting erythrocytes, erythrocytes bursting, and the reintroduction of the merozoites into the bloodstream will continuously repeat.^{29–32} Sooner or later, a few asexual cells will travel from the bloodstream to the bone marrow, where they will mature into gametocytes and then return to the bloodstream.^{29–32} Then, when a mosquito takes a blood meal from an infected individual, it will ingest the *Plasmodium* gametocytes.^{29–32} These gametocytes will then differentiate into male and female gametes and undergo sexual reproduction to form zygotes in the insect's abdomen.^{29–32} Finally, the zygotes mature into sporozoites, travel to the salivary glands of the mosquito, and the cycle begins anew.^{29–32}

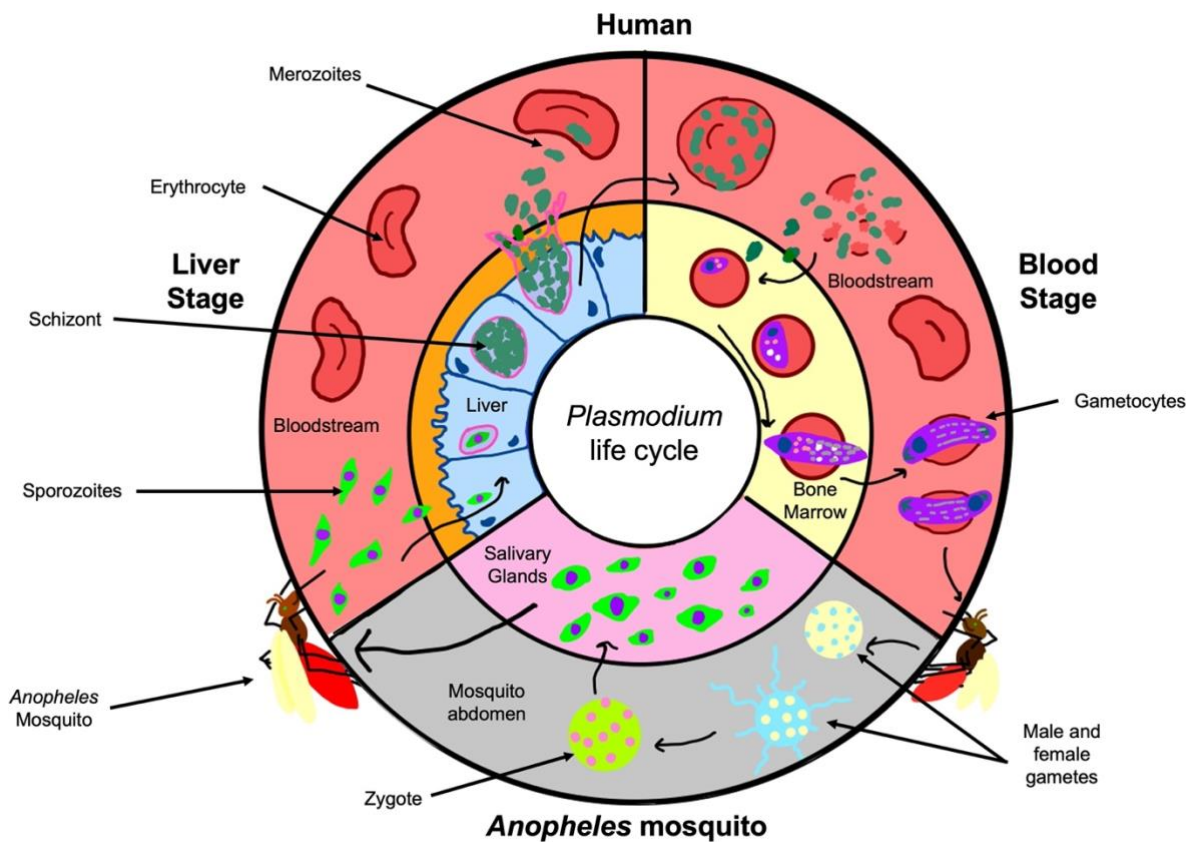


Figure 1.5: Life cycle of a *Plasmodium* infection.^{29–32}

To control the spread of malaria, insecticide-treated nets are used to prevent *Anopheles* mosquitos from encountering people.³³ The insecticides mainly used in these nets are pyrethroids, organochlorines, organophosphates, and carbamates, all

which *Anopheles* are rapidly gaining resistance to.³³ Other means of controlling malaria include the RTS,S/AS01 (Mosquirix™) vaccine, meant for children living in areas with high transmission of malaria and high mortality.³⁴ Despite the necessary 4 doses of the vaccine, it ultimately has a marginal efficacy of approximately 36 %.³⁴ The most effective treatments for individuals infected with *P. falciparum* are artemisinin-based combination therapies (ACTs) (Figure 1.6).²⁹ These therapies involve combining two active drugs with two different modes of action, where one of these drugs is an artemisinin derivative and the other is a partner drug.²⁹ During the first few days of treatment, the artemisinin derivative is administered to minimize the quantity of parasitic cells, then the partner drug is given later on in treatment to eliminate the remaining parasites.²⁹ However, similar to bacterial infections, *P. falciparum* is rapidly gaining resistance to both components of ACTs.²⁹

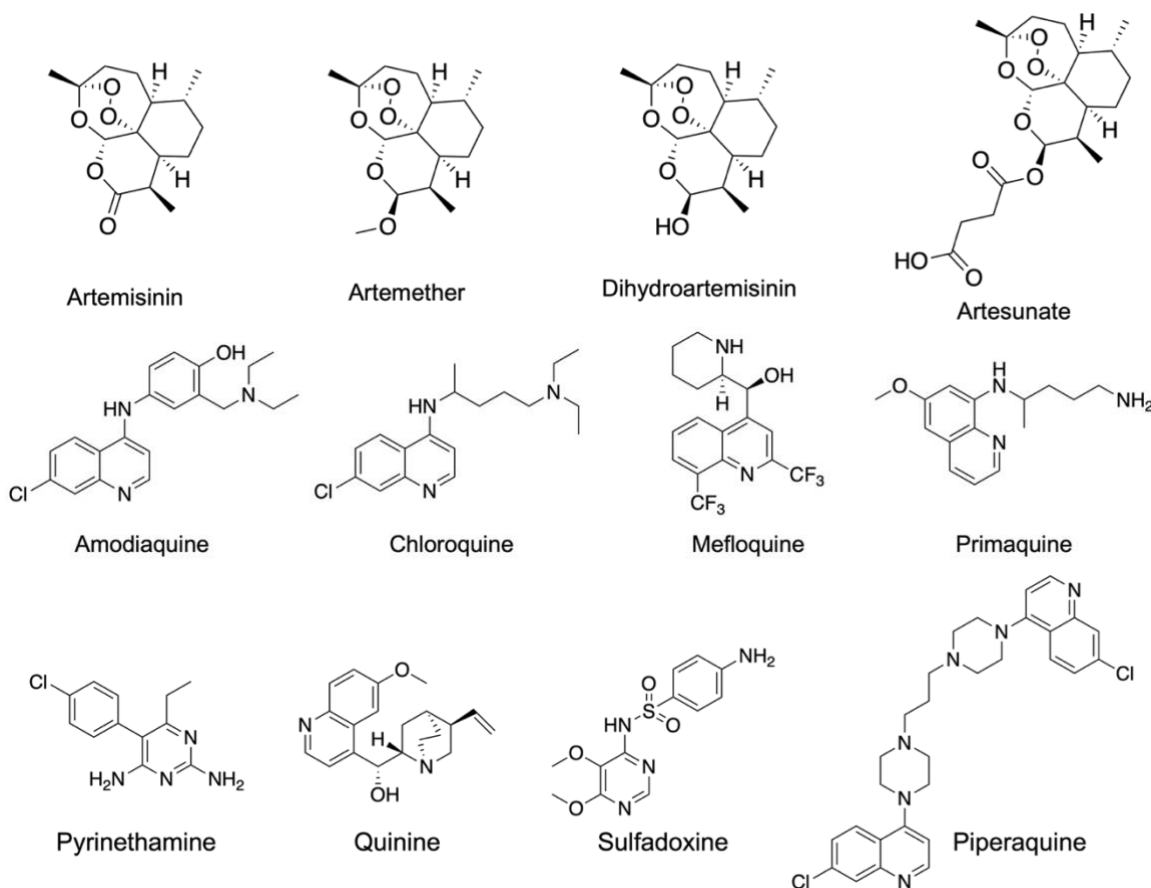


Figure 1.6: Examples of ACTs; artemisinin derivatives (first row) and known partner drugs for the treatment of malaria (second and third rows).²⁹

As the climate changes, malaria is expected to spread to more areas of the global, endangering even more lives.³⁵ With the growing resistance to insecticides and ACTs, people will soon be left defenseless against malaria, necessitating the discovery of novel antiparasmodial agents, preferably exhibiting a novel mechanism of action.

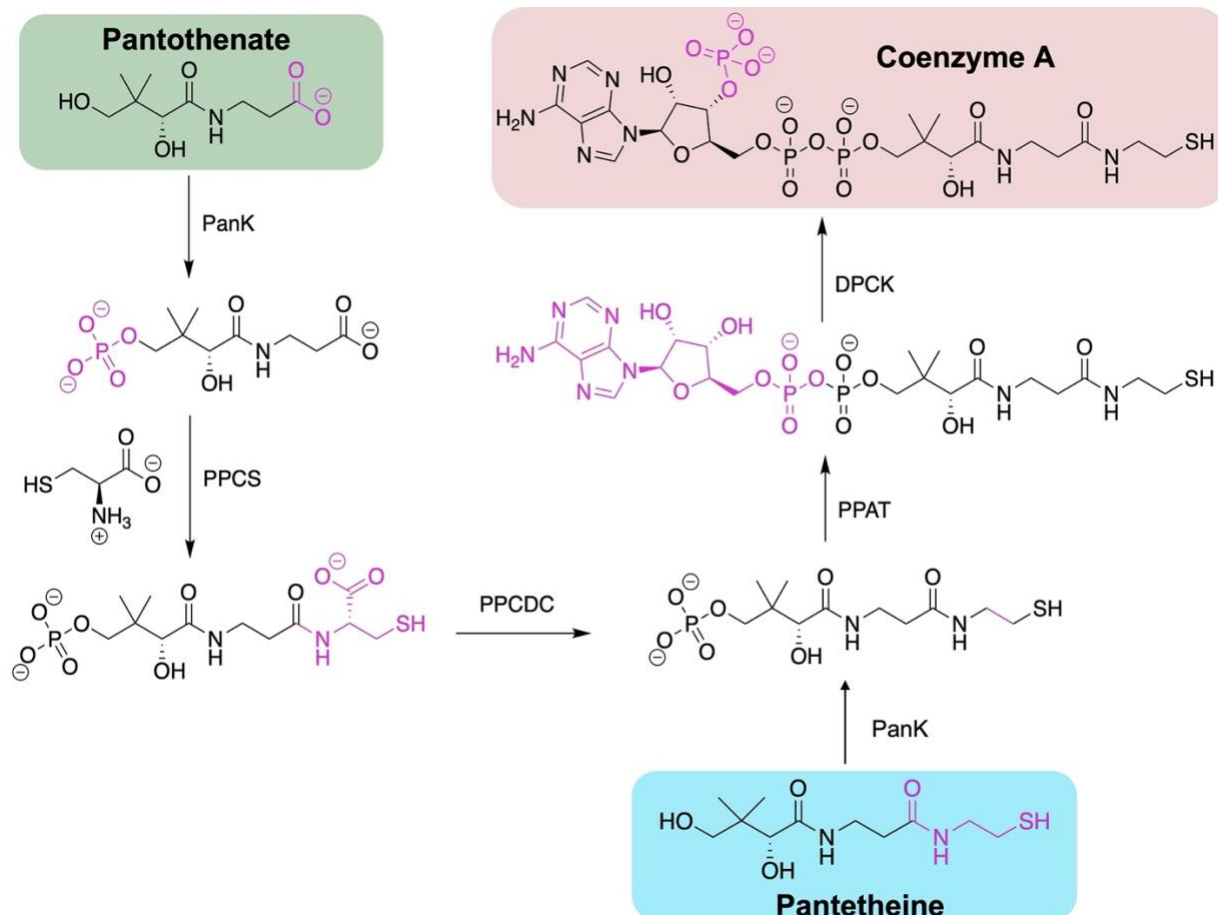
1.4. Coenzyme A Biosynthesis

Coenzyme A (CoA) is essential to life given the necessity of its production in several different species spanning animals, microorganisms, and plants.³⁶ About 9 % of all known enzymes require CoA as an important cofactor, making it a desirable target for drug development.^{36,37} Chemically, CoA acts as an acyl group carrier and carbonyl

activating group.³⁶ Fundamentally, there are substantial differences between prokaryotic and eukaryotic CoA biosynthetic enzymes, including low sequence homology, structural differences, and pathway regulation differences.^{36,37} These dissimilarities allow the possibility of selectively targeting the CoA biosynthetic pathway of disease-causing microorganisms over that of eukaryotes through small molecules.^{36,37}

Pantothenate (vitamin B₅) is a known precursor to CoA. Mammals rely on the uptake of pantothenate from the nutrients they consume; meanwhile, bacteria, fungi, and plants are able to transform β -alanine into pantothenate, and *Plasmodium* parasites can acquire pantothenate from their host and draw it into their intracellular space.³⁶

Once an organism has acquired pantothenate, it undergoes 5 enzymatic transformations into CoA (Scheme 1.1). To start, pantothenate kinase (PanK) catalyzes the phosphorylation of pantothenate to give 4'-phosphopantothenate. Then, cysteine is condensed onto 4'-phosphopantothenate, a reaction catalyzed by phosphopantothenoylcysteine synthase (PPCS). Next, phosphopantothenoylcysteine decarboxylase (PPCDC) catalyzes the decarboxylation of the cysteine residue to give 4'-phosphopantetheine. Phosphopantetheine adenylyltransferase (PPAT) then adds an adenylyl group to the molecule and lastly, phosphorylation at the 3' position of the ribose moiety is catalyzed by dephospho-CoA kinase (DPCK) to give CoA.



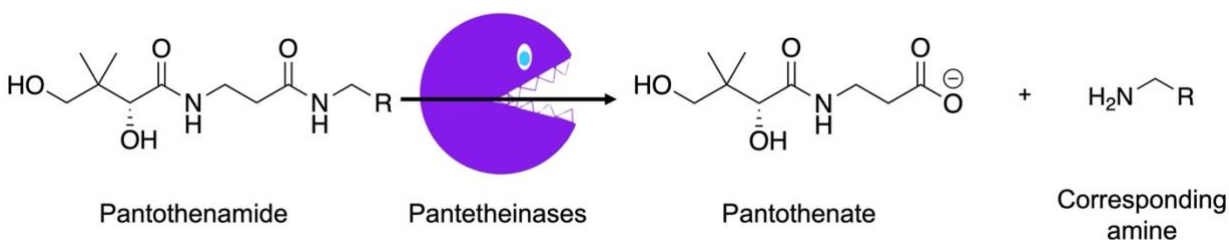
Scheme 1.1: The biosynthesis of CoA. The traditional pathway starts with pantothenate (highlighted in green). The CoA salvage pathway begins with pantetheine (highlighted in blue).

Some organisms are able to access CoA alternatively through the CoA salvage pathway (Scheme 1.1). In this pathway when pantothenate is scarce, the precursor, pantetheine, is directly phosphorylated by PanK to yield 4'-phosphopantetheine.³⁸ Bypassing the PPCS and PPCDC enzymatic steps completely, PPAT then catalyzes the transfer of an adenyl group onto 4'-phosphopantetheine which is then subject to phosphorylation at the 3' position of the ribose by DPCK to give CoA.³⁸

1.5. Pantothenamides

Pantothenamides are amide derivatives of pantothenate that have been shown to exhibit antibacterial,³⁹ antifungal,³⁹ and antiplasmodial activity.⁴⁰ The prototypical and

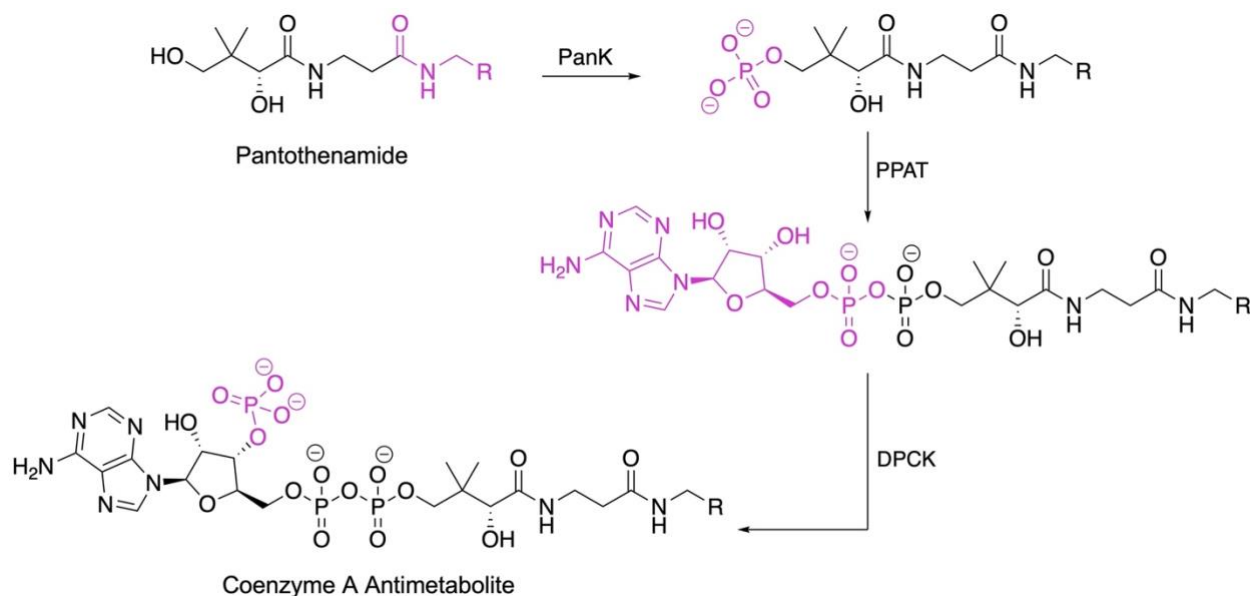
most studied pantothenamide for antibacterial activity is *N*-pentylpantothenamide (N5-pan) exhibiting a minimum inhibitory concentration (MIC) of $\sim 2\ \mu\text{M}$ against *E. coli* when cultured in a minimal medium^{39,41} and an MIC of $\sim 7\ \mu\text{M}$ against *S. aureus*.⁴² Meanwhile, one of the most potent antiplasmodial pantothenamides is *N*-phenethylpantothenamide with a half-maximal inhibitory concentration (IC_{50}) of $\sim 20\ \text{nM}$ against the intraerythrocytic stage of *P. falciparum* parasites.⁴⁰ Despite the low MIC and IC_{50} values for N5-pan and *N*-phenethylpantothenamide respectively, pantothenamides were never introduced into the clinics due to their susceptibility to hydrolysis by serum enzymes, called pantetheinases.⁴³ These enzymes belonging to the vanin family, rapidly hydrolyze pantothenamides into pantothenate and the corresponding amine, which render pantothenamides inactive *in vivo* (Scheme 1.2).⁴³



Scheme 1.2: Pantothenamide hydrolysis catalyzed by pantetheinases.

Due to the rapid increase in antimicrobial resistance today, pantothenamides are being reexplored with the goals of increasing their potency and stability in human serum.

In the absence of pantetheinases, pantothenamides were found to exhibit a new mechanism of action that is unseen in antimicrobials reported to date, taking advantage of CoA biosynthetic enzymes available in microorganisms to bioactive themselves into CoA antimetabolites (Scheme 1.3).⁴²



Scheme 1.3: Bioactivation of a generic pantothenamide into a CoA antimetabolite.

Pantothenamides are transformed by the CoA salvage pathway, starting by with phosphorylation by PanK to yield the corresponding 4'-phosphopantotheamides. Then, PPAT and DPCK transfer an adenylyl group and phosphorylate the 3' position of the ribose moiety, respectively, yielding a CoA antimetabolite. Since the CoA antimetabolite lacks the terminal thiol substituent of CoA (Figure 1.7), it has been shown to disrupt downstream CoA-utilizing processes such as fatty acid synthesis.^{44,45} In some organisms, pantothenamides have also been shown to interrupt the biosynthesis of CoA itself, causing cell death.⁵²

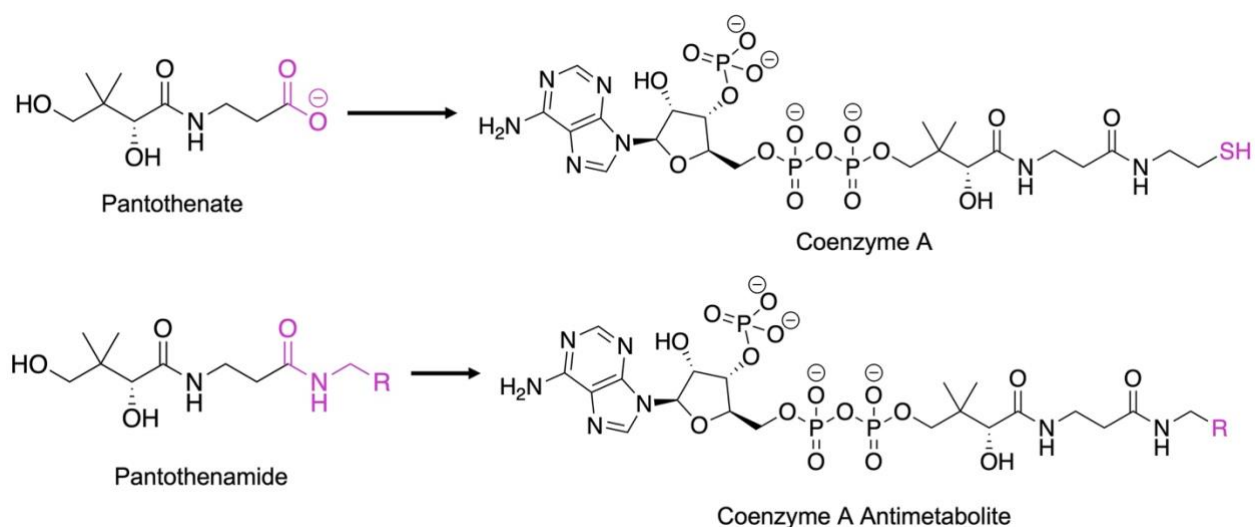


Figure 1.7: Comparison of CoA antimetabolites and CoA. CoA antimetabolites lack the terminal thiol group necessary for acyl group transfer.

To overcome pantetheinase-mediated degradation of pantothenamides, synthetic strategies have been employed using the pantothenamide backbone as a scaffold (Figure 1.8) to create pantothenamide mimicking compounds (PanMCs). These alterations include modifications at the geminal dimethyl group,^{42,45,46} the β -alanine moiety,^{43,47,49} and the labile amide.^{49,50,51}

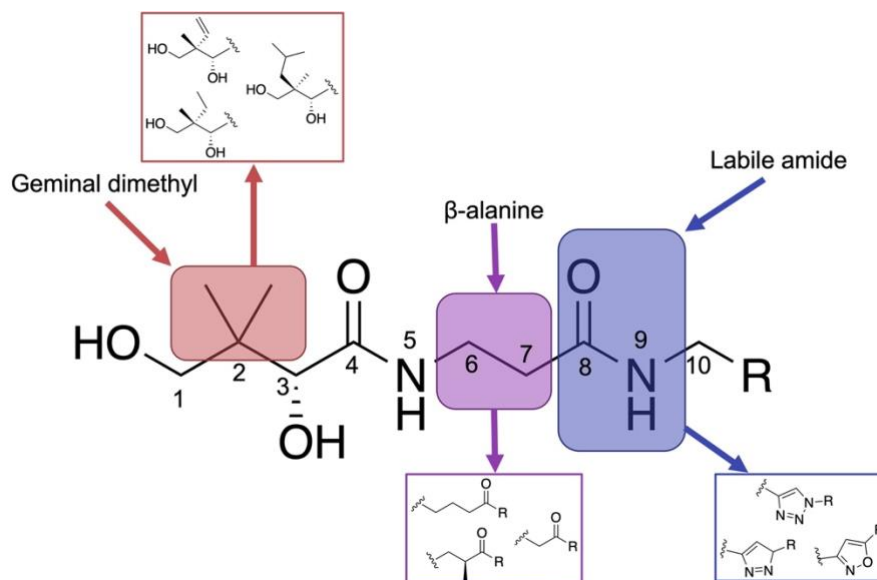
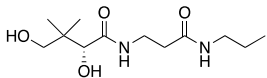
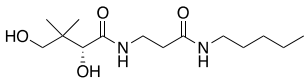
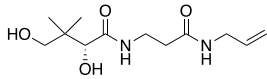
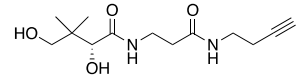
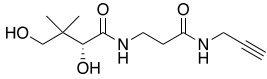


Figure 1.8: Different regions of synthetic modifications on the pantothenamide scaffold.

Structure activity relationships (SARs) have been reported for the activity of pantothenamides against *E. coli*,^{52–54} *S. aureus*,^{52,53} and *P. falciparum*,^{43,48,49} through investigation with several small compound libraries. The main motif that is recognized by most CoA biosynthetic enzymes is the pantoyl moiety; therefore, many synthetic strategies have kept this region intact and focused more on modifications of the β -alanine moiety, labile amide, or the *N*-substituents. Unfortunately, most pantothenamides lack antibacterial activity against Gram-negative bacteria. They are equipped with an additional outer cell membrane (Section 1.2, Bacteria and Antibiotics) that poses permeability challenges to antibiotics. Additionally, this outer cell membrane contains small proteins called TolC-dependent efflux pumps that can recognize and eject small molecules from the cell.⁵² Table 1.2 summarizes the known pantothenamides that are active against *E. coli*, followed by Figure 1.9 that summarizes the known SARs of PanMCs for *E. coli*.

Table 1.2: Pantothenamides active against *E. coli*. Compounds with an MIC less than 10 μM are shown.^{52–54}

Pantothenamides	MIC (μM)	Pantothenamides	MIC (μM)
	1		6
	3		7.5
	4		

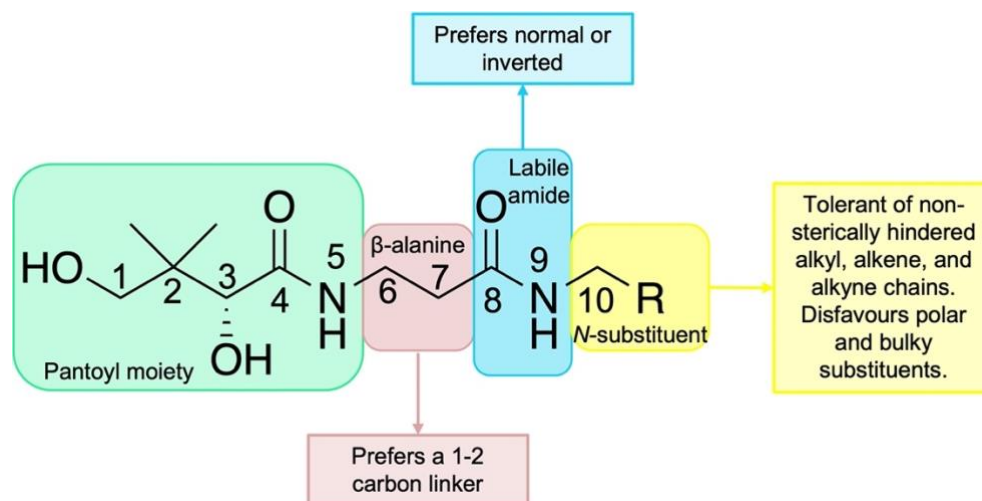
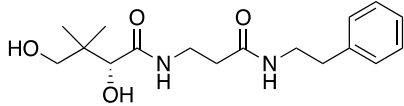
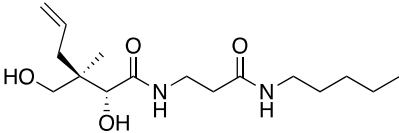
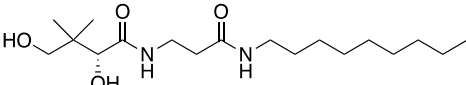
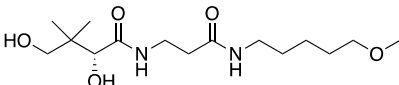
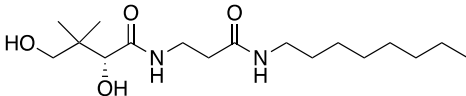
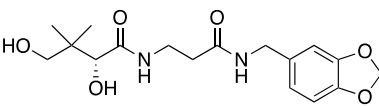
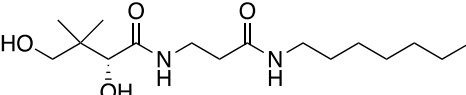
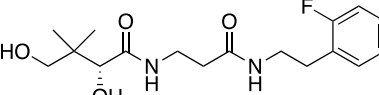
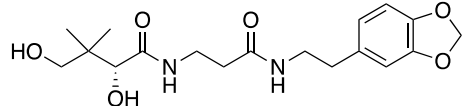
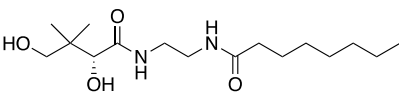
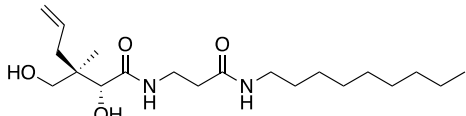
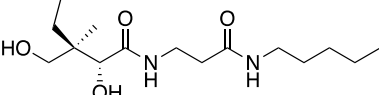
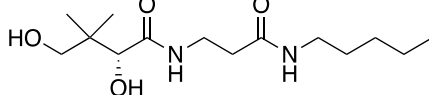
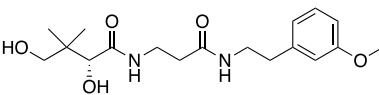
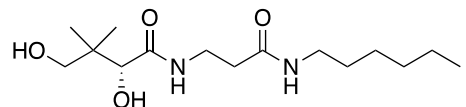


Figure 1.9: Summarized SARs for activity against *E. coli*.

In summary, the optimal linker length between N5 and C8 is one to two carbons.⁵² The C8 amide carbonyl must be conserved or inverted but should not be replaced with other bioisosteres.⁵² Lastly, the *N*-substituent is tolerant of non-sterically hindered alkyl, alkene, and alkyne chains.^{52,53}

S. aureus, a Gram-positive bacteria, is more susceptible to pantothenamides than *E. coli*, and can tolerate much more variety in the structure of its growth inhibitors. Table 1.3 captures the pantothenamides and PanMCs that are active against *S. aureus* with an MIC less than 10 μM , while Figure 1.10 depicts the corresponding SARs.^{52,53}

Table 1.3: Pantothenamides and PanMCs active against *S. aureus*. Compounds with an MIC less than 10 μM are shown.^{52,53}

Structure	MIC (μM)	Structure	MIC (μM)
	0.25		3.2
	0.4		4.0
	0.74		4
	0.77		5.9
	1		6.3
	1		7
	1.5		8.0
	3.14		

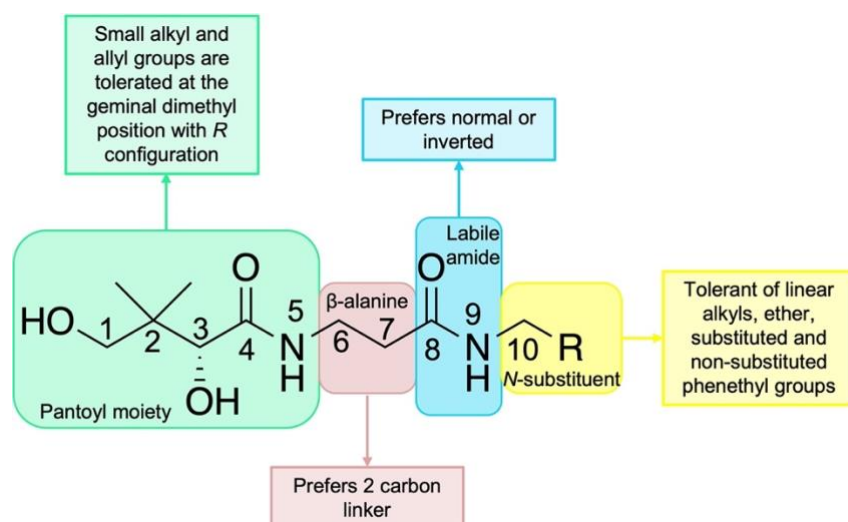
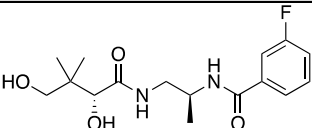
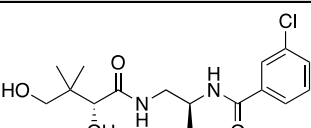
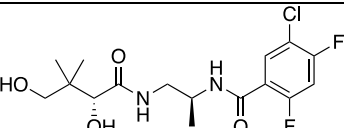
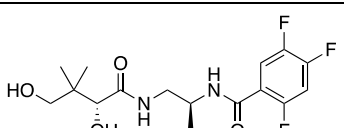
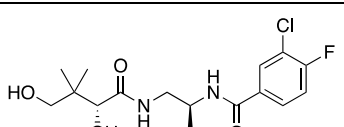
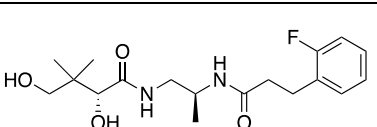
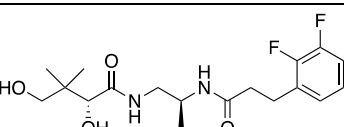
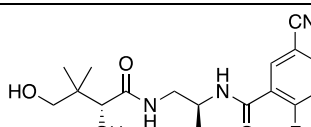
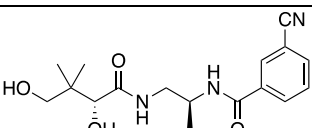
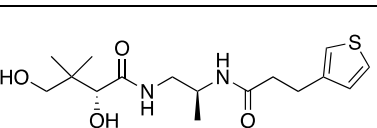
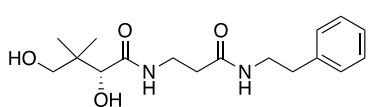
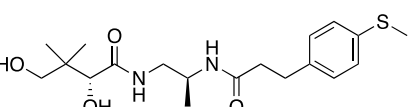
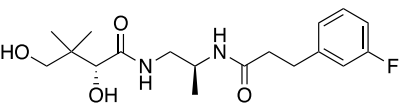
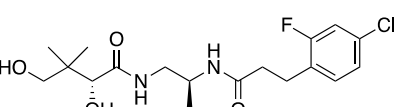
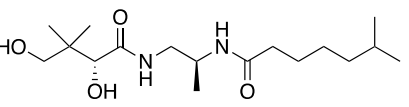
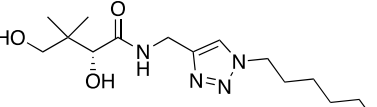
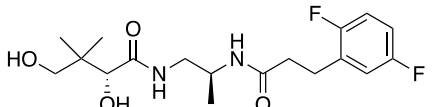
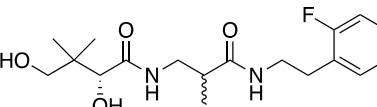
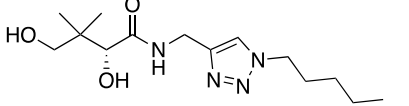
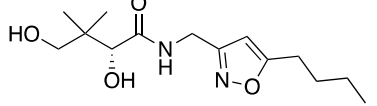


Figure 1.10: Summarized SARs for activity against *S. aureus*.

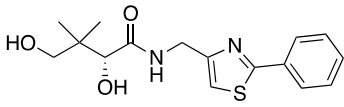
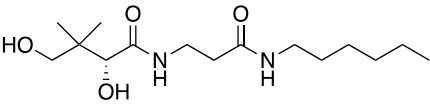
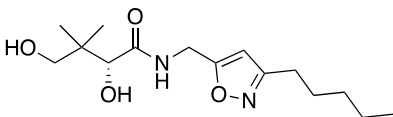
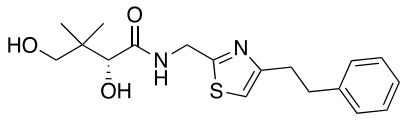
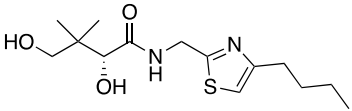
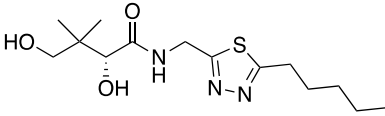
Interestingly, the optimal linker length between N5 and C8 is still two carbons, which is not significantly different from *E. coli*.^{42,46,50} At the C2 position, small alkyl substituents with an *R* configuration is preferred.^{42,46,53} The amide bond at C8 is tolerant of both a normal and inverted amide bond.⁵³ Preferred *N*-substituents include linear alkyls, thioethers, ethers, and substituted ethyl aromatics.⁵³ Additionally, non-polar *N*-substituents are preferred owing to their high cell permeability.⁵⁵

To date, an immense number of pantothenamides and PanMCs have displayed antiparasitic activity against *P. falciparum*. Table 1.4 depicts the quantity of PanMCs that have displayed potent activity *P. falciparum*, while Figure 1.11 visually depicts the SARs known to date.

Table 1.4: Pantothenamides and PanMCs active against *P. falciparum*. Compounds with an IC₅₀ less than 1 μ M are shown.^{43,48,49} The IC₅₀ values in red are from molecules tested in pantetheinase-inactivated media.^{40,49}

Structure	IC ₅₀ (μ M)	Structure	IC ₅₀ (μ M)
	0.019		0.0021
	0.0023		0.0024
	0.0034		0.005
	0.006		0.0062
	0.0074		0.017
	0.072 0.020		0.021
	0.028		0.037
	0.041		0.055
	0.053		0.070 0.024
	0.056		0.072

	0.071		0.107 0.027
	0.106 0.079		0.122
	0.294 0.159		0.147
	0.139		0.16
	0.156 0.058		0.19
	0.175		0.214 0.097
	0.21		0.235
	76 0.23		0.248 0.08
	0.24		44 0.067
	0.277 0.177		0.299
	0.50		0.54

	0.5474		0.55
	0.63		0.77
	0.78		0.96

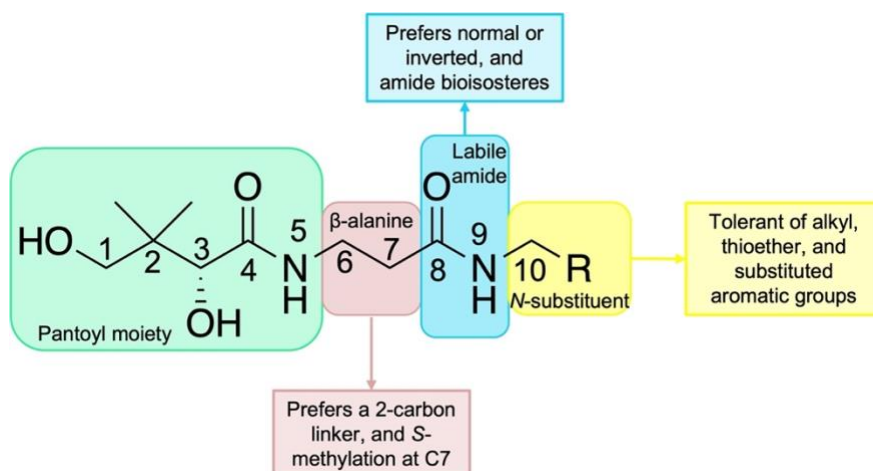


Figure 1.11: Summarized SARs for activity against *P. falciparum*.

Briefly, the same trend is observed here against *P. falciparum* with a two-carbon linker between N5 and C8 being preferred.⁴⁰ However, methylation at C7 with an *S* configuration,^{40,43} as well as inversion of the C8 amide bond,⁵⁶ and replacement of the C8 labile amide bond with bioisosteres^{42,47,57} have been shown to limit pantetheinase-mediated degradation while also enhancing the potency of many PanMCs.⁴⁹ Finally, tolerated *N*-substituents include: alkyl chains, thioesters, and non-sterically hindered aromatic groups.⁴³

Several serum stable PanMCs have been discovered with antiparasmodial activity in the nanomolar range, yet very few of them have been tested in animal models^{50,56} displaying little activity, and none have ever made it to clinical trials.⁴⁹ To overcome this

challenge, further SARs need to be uncovered through the discovery of novel PanMCs and screening.

Antimicrobial resistance is among the top 10 global public health threats facing humanity, along with air pollution and climate change.⁵⁸ There is a desperate need for new antimicrobials with a novel mechanism of action to combat this looming threat to public health. PanMCs have been shown to be easily accessible non-toxic synthetic targets that exhibit activity against both bacterial and parasitic species, and they have multiple new mode(s) of action. Therefore, more research in PanMCs is highly warranted.

1.6. Research Objective

The overarching goal of this thesis is to synthesize a small library of novel, blood stable, and more potent PanMCs that contain a 4,5-dihydroisoxazole ring in place of the labile amide bond, and thus add to the diversity of PanMCs made in the Auclair lab. Additionally, the antibacterial and antiplasmodial activity of the PanMCs synthesized in this thesis, as well as PanMCs synthesized by group members Chunling Blue Lan and Victoria Virgilio will be explored. Chapter 2 will present the synthetic design and strategy while chapter 3 will focus on the antibacterial activity. Chapter 4 will then consist of the antiplasmodial results obtained from collaborators in the Saliba lab at the Australian National University for the PanMCs synthesized in this thesis as well as for the PanMCs synthesized by previous group member Victoria Virgilio. Chapter 5 will summarize the contributions made and suggest future directions of this work. Finally, chapter 6 will constitute a detailed description of the experimental procedures and compound characterization.

Chapter 2

Synthetic Design and Strategy

2.1. Preface and Contributions

Previous members of the Auclair lab have previously synthesized many PanMCs containing various heteroaromatic rings to replace the labile amide group. These rings included: triazole, 1,2,4-triazole, thiazole, thiadiazole, pyrazole, thiophene, 1,3,4-oxadiazole, 1,2,4-oxadiazole, oxazole, and isoxazole. Of these various ring structures, the triazole-, thiadiazole-, and isoxazole-containing PanMCs were found to display antiparasmodial activity at nanomolar concentrations at the intraerythrocytic stage of *P. falciparum*. To further diversify the library of PanMCs, the Auclair lab recently shifted their sights on 5-membered, non-aromatic, heteroatom-containing rings. In this chapter, the synthetic design and strategy of 6 PanMCs containing a 4,5-dihydroisoxazole ring are depicted. All compounds reported in this chapter were prepared by the author of this thesis, using routes established for similar compounds by previous group member Victoria Virgilio and senior group member Chunling Blue Lan, and further optimized by the author.

2.2. Introduction

As aforementioned, antimicrobial resistance is a rising public health menace, which is rapidly nullifying the therapeutic effect of current antimicrobials on the market. As such, the need for novel antimicrobials exhibiting new mode(s) of action is dire.^{36,40,42–57} Pantothenamides have been identified as new potent antimicrobials with a unique mechanism of action,^{36,39,59,60} but due to their susceptibility to cleavage by pantetheinases in human serum, they are typically inactive *in vivo*.^{40,43,48} Synthetic techniques have been employed by the Auclair lab and others to limit pantetheinase-related degradation, such as: modifications to the geminal dimethyl,^{42,59} the β -alanine,^{43,56} and the labile amide moiety.^{43,50,57} Previously, the Auclair lab has extensively explored replacing the labile amide bond with diverse, 5-membered heteroaromatic rings, which was very fruitful in finding blood-stable, and highly potent antiparasmodial agents.^{50,57} However, the Auclair lab has recently been shifting their focus on substituting the labile amide bond with 5-membered, non-aromatic, heteroatom-containing rings.

Natural products have long served as inspiration for the development of various pharmaceuticals. In fact, more than 90 % of all small molecule drugs contain at least one ring system, many of which are derived from natural products.⁶¹ The ring system in small molecules often determines the structural orientation of substituents and the conformational flexibility of the molecule, hence delivering an impact in biological activity.⁶¹ Many pharmaceuticals exhibit 5-membered, non-aromatic rings in their chemical structure, including spirotryprostatin A, an anticancer drug, topiramate, used in the treatment of epilepsy, and nucleocidin, an antibiotic (Figure 2.1).

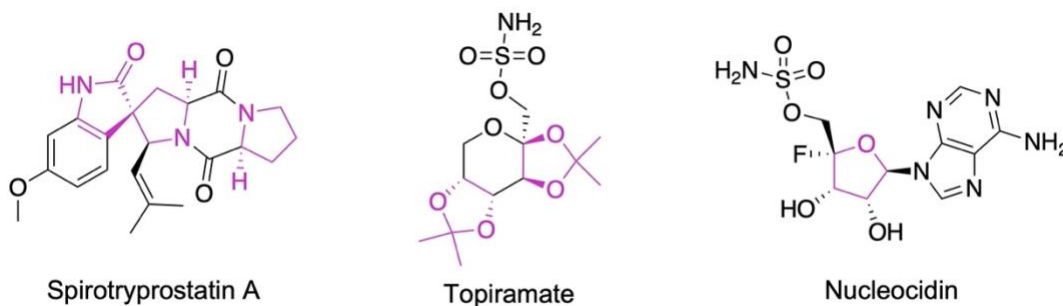


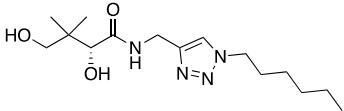
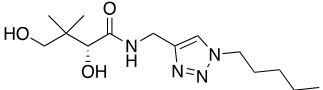
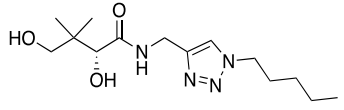
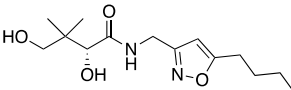
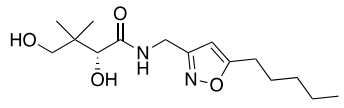
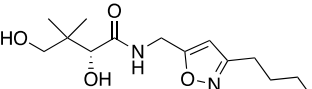
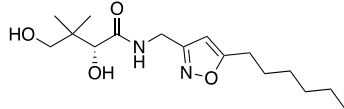
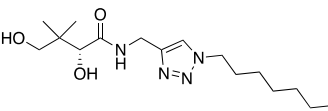
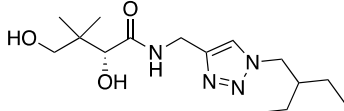
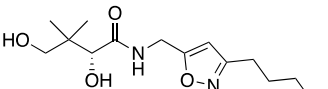
Figure 2.1: Examples of pharmaceuticals exhibiting a 5-membered, non-aromatic, heteroatom-containing rings. Said ring structures are highlighted in pink.

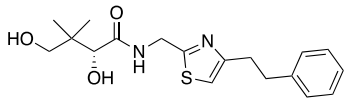
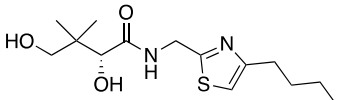
There are several advantages to exploring nonaromatic ring systems in the replacement of the labile amide group of PanMCs. Many of these advantages include fundamental structural differences. For example, aromatic rings are flat in nature, while non-aromatic rings introduce non-linear angles into the small molecule's structure and orientation.⁶² Additionally, the sp^3 character that non-aromatic rings exhibit, add 3D dimensionality to the molecule and allows it to occupy space differently than aromatic sp^2 hybridization in heteroaromatic ring systems.⁶² Also, the difference in hybridization allows for further diversification of a library of small molecules as it allows for one additional substituent per sp^3 carbon atom. Finally, introducing heteroatoms into non-aromatic ring systems is a clever strategy to achieve modification of solubility, hydrogen bonding capacity, lipophilicity, and polarity of biologically active compounds.^{62,63}

2.3. Synthetic Design of PanMCs Containing a 4,5-Dihydroisoxazole Moiety

Previously, the Auclair lab has reported many PanMCs with activity against *P. falciparum*, which exhibit diverse heteroaromatic rings in place of the labile amide group.^{50,57} Of all the heteroaromatics explored by the Auclair group, the triazole, thiazole, and isoxazole rings have produced the most potent antiplasmodial agents with activity in the nanomolar range towards intraerythrocytic *P. falciparum* (Table 2.1) as well as featuring low toxicity toward mammalian cells.⁵⁷

Table 2.1: The most potent PanMCs against *P. falciparum* featuring a triazole, thiazole, or isoxazole ring in place of the labile amide group. Only compounds with nanomolar activity are shown.

PanMC	IC ₅₀ (μM)	PanMC	IC ₅₀ (μM)
	0.055 ± 0.005 ⁵⁷		0.056 ± 0.005 ⁵⁷
	0.071 ± 0.003 ⁵⁷		0.072 ± 0.003 ⁵⁰
	0.16 ± 0.01 ⁵⁰		0.19 ± 0.03 ⁵⁰
	0.24 ± 0.05 ⁵⁰		0.50 ± 0.05 ⁵⁷
	0.5 ± 0.1 ⁵⁷		0.63 ± 0.07 ⁵⁰

	0.77 ± 0.09^{64}		0.8 ± 0.1^{64}
---	----------------------	--	--------------------

Given the potency of the isoxazole series, the 4,5-dihydroisoxazole ring was chosen for further exploration and derivatization of a small library of small molecules. As previously mentioned in Section 1.5, when designing PanMCs that have activity against *P. falciparum*, a 2-carbon linker with or without S-methylation between the pantoyl and labile amide moieties is preferred. Additionally, the non-pantoyl side chain is tolerant of various substituents, including substituted aromatic groups, alkyl chains, and thioesters.

Organofluorine compounds continue to emerge in several biomedical applications, highlighting the advantages of introducing fluorine atoms into small molecule drugs (Figure 2.2). For example, carbon-fluorine bonds introduce metabolic stability to small molecules as these bonds are among the strongest carbon containing bond (the C–F bond dissociation energy is 131 kcal mol⁻¹ compared to the bond dissociation energy of C–H of 104 kcal mol⁻¹), therefore these bonds have a low susceptibility to oxidative metabolism.^{65,66} Beyond the protective role that organofluorines introduce, they also allow for the engagement of various noncovalent interactions with the biological target and they affect the physicochemical properties of the molecule.^{65,66}

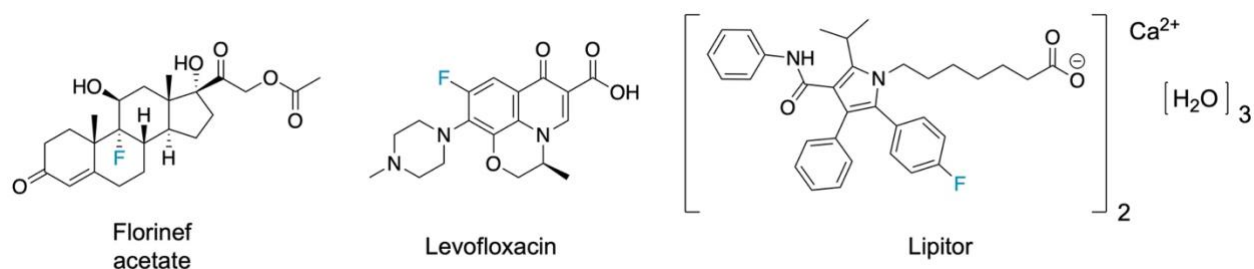


Figure 2.2: Examples of fluorinated pharmaceuticals. Florinef acetate is used in the treatment of adrenogenital syndrome, adrenal insufficiency, and postural hypotension.⁶⁶ Levofloxacin is an antibiotic, and Lipitor is a cholesterol-lowering agent. Fluorine atoms are highlighted in blue.

2.4. Objective

Colleague Chunling Blue Lan synthesized the first PanMC containing a 4,5-dihydroisoxazole ring (labelled **1a** in Figure 2.3) as a diastereomeric mixture, and previous group member Victoria Virgilio adapted the methodology to prepare 8 additional derivatives as diastereomeric mixtures, **2a–2h** (Figure 2.3).

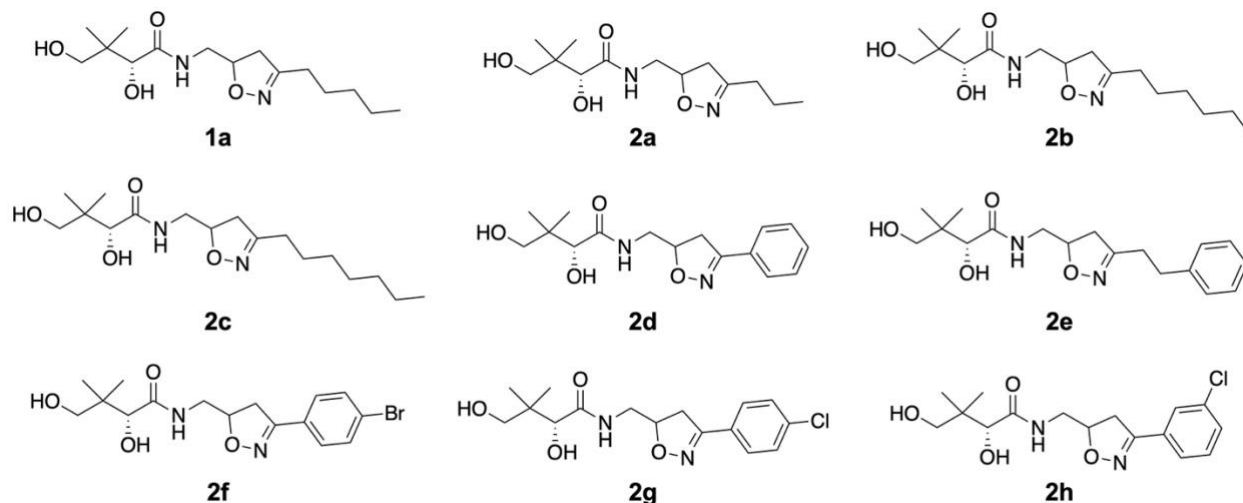


Figure 2.3: The current library of PanMCs featuring a 4,5-dihydroisoxazole ring synthesized by Chunling Blue Lan (**1a**) and Victoria Virgilio (**2a–2h**) as diastereomeric mixtures.

The objective of this thesis is to expand upon the existing library of PanMCs containing a 4,5-dihydroisoxazole ring in place of the labile amide bond, further diversifying the existing library (Figure 2.4). Another goal was to remake compound **2b**, originally synthesized by Victoria Virgilio⁶⁷, as it was not made in large enough quantity for biological testing (now named **3f**).

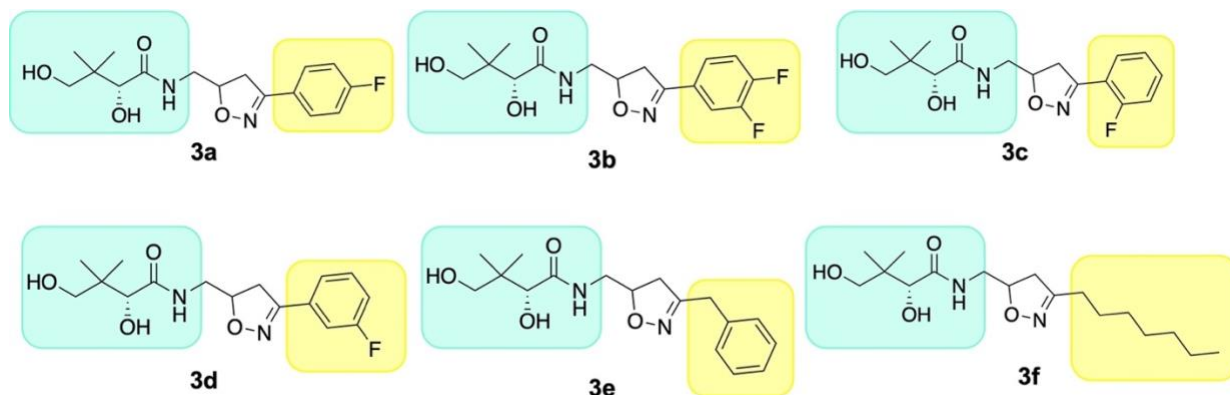


Figure 2.4: PanMCs synthesized by the author in this thesis as diastereomeric mixtures. **3f** was originally synthesized by Victoria Virgilio⁶⁷ but was remade for biological testing. The pantoyl moiety is highlighted in green and the side chain is highlighted in yellow.

2.5. Synthetic Results and Discussion

The common fragment in all the synthetic targets (shown in Figure 2.4 and Figure 2.5) is the pantoyl moiety. Therefore, to access these PanMCs a similar synthetic strategy was used (Figure 2.5), which included first the intermolecular cyclization of an oxime chloride and *tert*-butyl *N*-allylcarbamate to form the 4,5-dihydroisoxazole ring with the side chain in place. Deprotection of the amine would next enable the ring opening of the D-pantolactone to yield the final PanMCs.

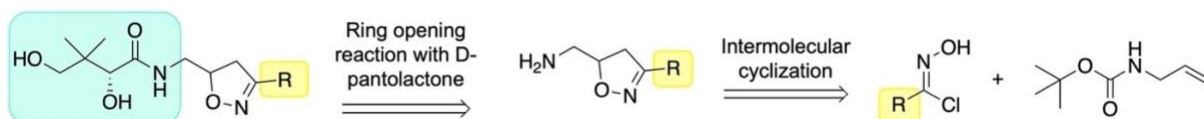
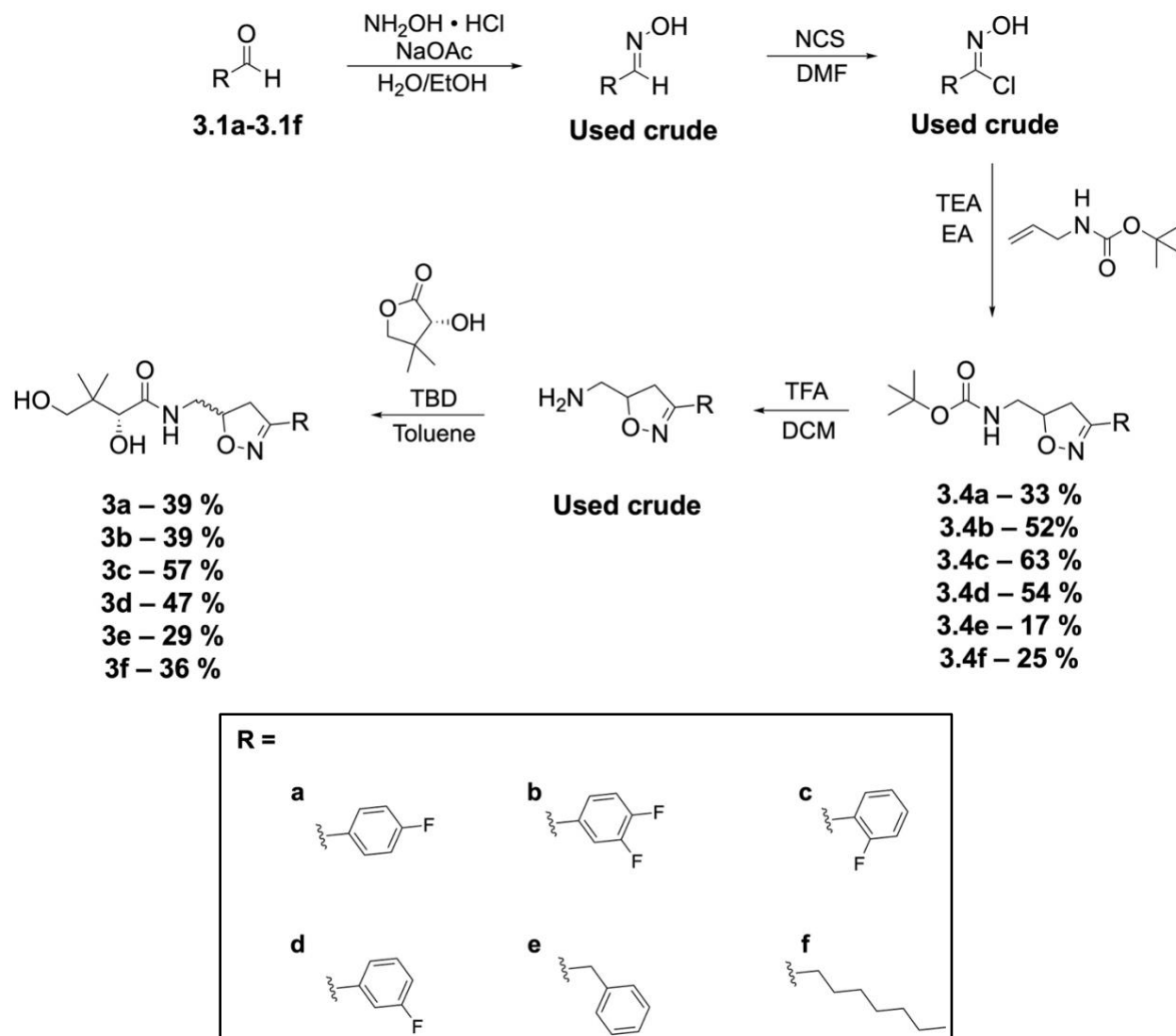


Figure 2.5: Retrosynthesis to accessing the PanMCs generated in this thesis. The common fragment, the pantoyl moiety is highlighted in green and the side chain is highlighted in yellow.

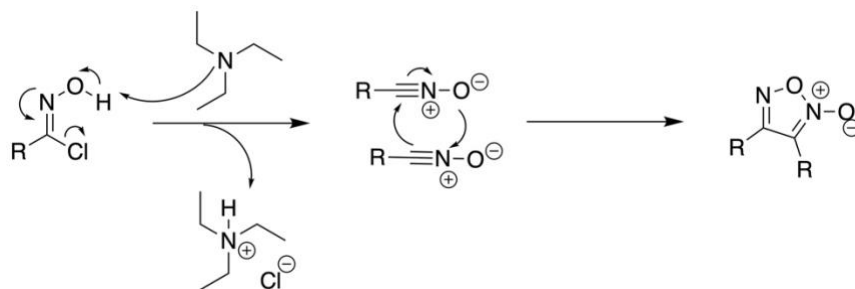
The following scheme (Scheme 2.1) depicts the synthetic route used to access the PanMCs shown in Figure 2.4 (**3a–3f**).



Scheme 2.1: The synthetic route used to access PanMCs **3a–3f**. NaOAc: sodium acetate, EtOH: ethanol, NCS: *N*-chlorosuccinimide, DMF: dimethylformamide, TEA: triethylamine, EA: ethyl acetate, TFA: trifluoroacetic acid, DCM: dichloromethane, TBD: triazabicyclodecene. Stepwise yields are given (i.e. from **3.1** to **3.4** and **3.4** to **3**) on steps involving purification.

To start, the aldehyde of choice (one of **3.1a–3.1f**) was transformed into the corresponding oxime (**3.2b–3.2f**) through the addition of hydroxylammonium chloride and sodium acetate in an ethanol-water mixture. The crude oxime was then reacted

with *N*-chlorosuccinimide to yield the corresponding oxime chloride (**3.3a–3.3f**). Previously, the transformation of the oxime chloride reacted overnight at room temperature. However, it was found in these reactions that full conversion to the oxime chloride was achieved in 3 hours at room temperature. Next, the crude oxime chloride underwent an intermolecular cyclization with *tert*-butyl *N*-allylcarbamate to generate the 4,5-dihydroisoxazole ring-containing intermediate (**3.4a–3.4f**). The yields of this intermediate are quite variable because a side product is often generated at this stage (Scheme 2.2). The addition of triethylamine to the oxime chloride can generate a nitrile oxide which can then undergo cyclization with itself to form the side product shown in Scheme 2.2. Then, this side product is removed through column chromatography, resulting in a loss of yield.



Scheme 2.2: Formation of a possible side product during the intermolecular cyclization (not characterized in thesis).

A Boc-deprotection reaction was next performed through the addition of trifluoroacetic acid to give the free amine intermediate (**3.5a–3.5f**). Finally, a D-pantolactone ring opening reaction was performed between this crude free amine intermediate and D-pantolactone in the presence of catalytic amounts of triazabicyclodecene to yield the final PanMCs (**3a–3f**) as diastereomeric mixtures (approximately 1:1). Separation of the diastereomers would only be envisaged if the PanMCs were sufficiently active biologically (displaying activity in the nanomolar or low micromolar range). The yields at the final product (starting from 3.4) also span 29 % to 57 % and this is largely due to left over, unreacted starting materials. The D-pantolactone ring opening reaction described here was optimized by group member Chunling Blue Lan.

2.6. Conclusion

This chapter entailed the synthetic design and strategy for accessing the 6 PanMCs synthesized by the author in five linear steps. Overall, the yields were acceptable and sufficient quantities of all PanMCs were synthesized for acquiring biological results. Robust synthetic pathways have been developed, which can find use for further expansion of the compound library. The next chapter will discuss the experiments performed to determine the antibacterial activity (against *Acinetobacter baumannii*, *Escherichia coli*, *Klebsiella pneumoniae*, *Pseudomonas aeruginosa*, *Staphylococcus aureus*, and *Salmonella enterica* serovar Typhimurium) of these PanMCs as well as five other PanMCs synthesized by group member Chunling Blue Lan.

Chapter 3

Antibacterial Results

3.1. Preface and Contributions

Antimicrobial resistance is a rising issue that threatens modern medicine and healthcare systems globally. In the previous chapter, one PanMC was remade⁶⁷ with the purpose of obtaining biological results and five novel PanMCs were synthesized (Figure 3.2). Herein, all six of these PanMCs, as well as five PanMCs synthesized by Auclair group member Chunling Blue Lan (Figure 3.3) were tested by the author of this thesis for antibacterial activity against *Acinetobacter baumannii*, *Escherichia coli*, *Klebsiella pneumoniae*, *Pseudomonas aeruginosa*, *Staphylococcus aureus*, and *Salmonella enterica* serovar Typhimurium.

3.2. Introduction

As mentioned in chapter 1, the rise of antimicrobial resistance and the lack of new antimicrobials in the pre-clinical pipeline⁶⁸ are making pathogenic bacteria more dangerous to human life. The World Health Organization (WHO) lists carbapenem-resistant *A. baumannii*, carbapenem-resistant *P. aeruginosa*, as well as carbapenem-resistant and extended spectrum β -lactamase producing *Enterobacteriaceae* to be critical pathogens for the research and discovery of new antibiotics.⁶⁸ Looking more closely at the bacteria being tested in the following experiments, all six of these pathogens can be found on the WHO's priority list of pathogens at various levels of priority.⁶⁷ Nevertheless every single one of these species can cause life-threatening disease in both humans and animals, as summarized in Figure 3.1. Not to mention, resistance mechanisms of these bacteria are increasing exponentially.^{69–75} It is crucial to find more antibiotics with a novel mechanism of action to combat drug-resistant bacterial infections.

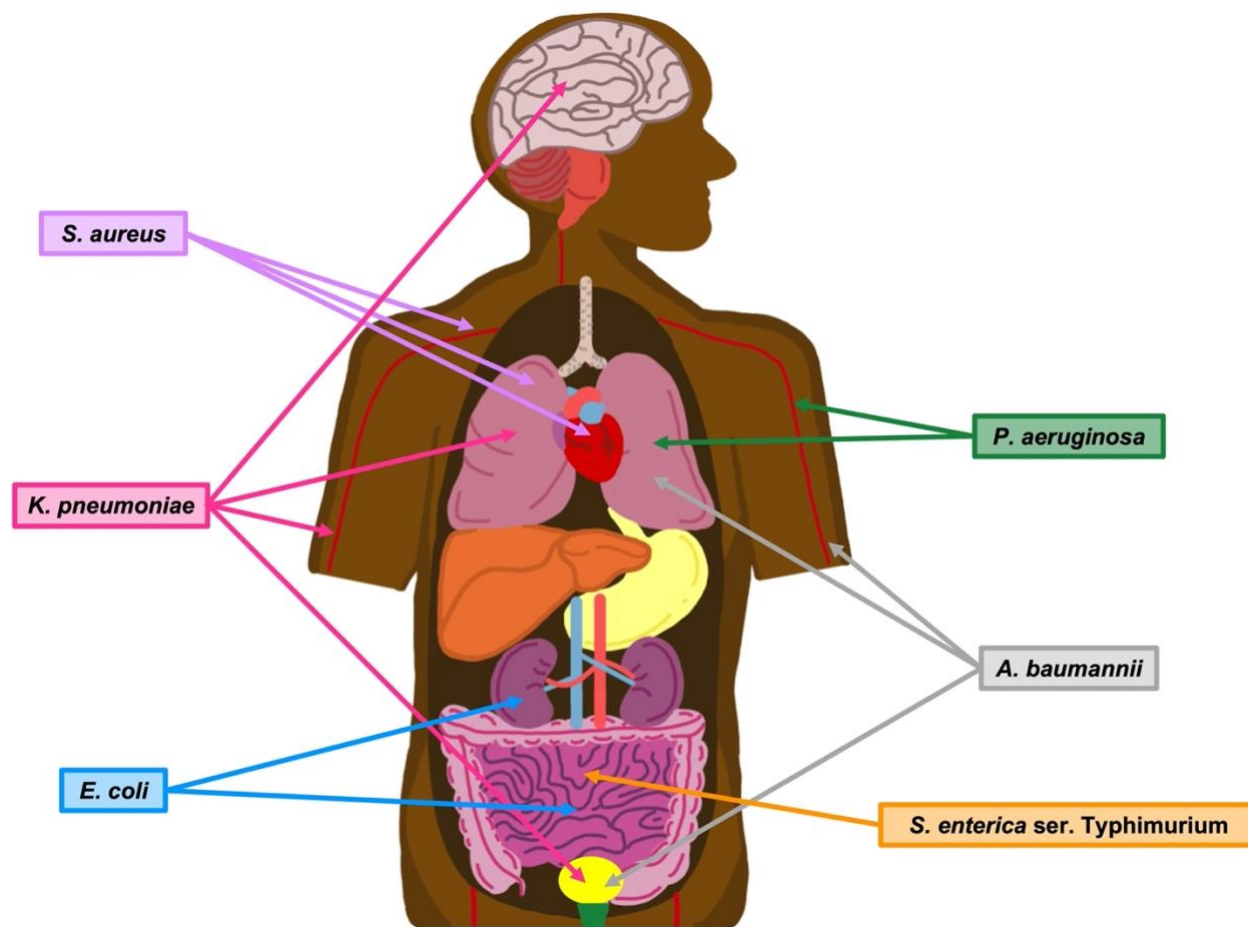


Figure 3.1: Examples of common sites of infection for the six bacterial species being explored.^{69–75}

Traditionally, it has been significantly more difficult to treat infections caused by Gram-negative bacteria (Section 1.2, Bacteria and Antibiotics) due to an extra outer cellular membrane that they possess. The TolC-dependent efflux pumps of Gram-negative bacteria pose an additional challenge in developing antibiotics as these pumps can rapidly recognize a variety of diverse, unrelated molecules and eject them from the cell.⁷⁶ As such, most of the WHO's top priority pathogens are Gram-negative.⁶⁹ *S. aureus* and *Enterococcus faecium* are the only two Gram-positive bacteria to make the list.⁶⁹

In the battle against antimicrobial resistance, herein lies antibacterial activity results of eleven PanMCs against six pathogenic bacteria: *A. baumannii*, *E. coli*, *K. pneumoniae*, *P. aeruginosa*, *S. aureus*, and *S. Typhimurium*.

3.3. Evaluation of Antibacterial Activity

Of the eleven PanMCs tested for antibacterial activity against *A. baumannii*, *E. coli*, *K. pneumoniae*, *P. aeruginosa*, *S. aureus*, and *S. Typhimurium*, six (Figure 3.2, **3a–3f**) were synthesized by the author of the thesis (see Chapter 2). The remaining five were synthesized by Chunling Blue Lan (Figure 3.3).

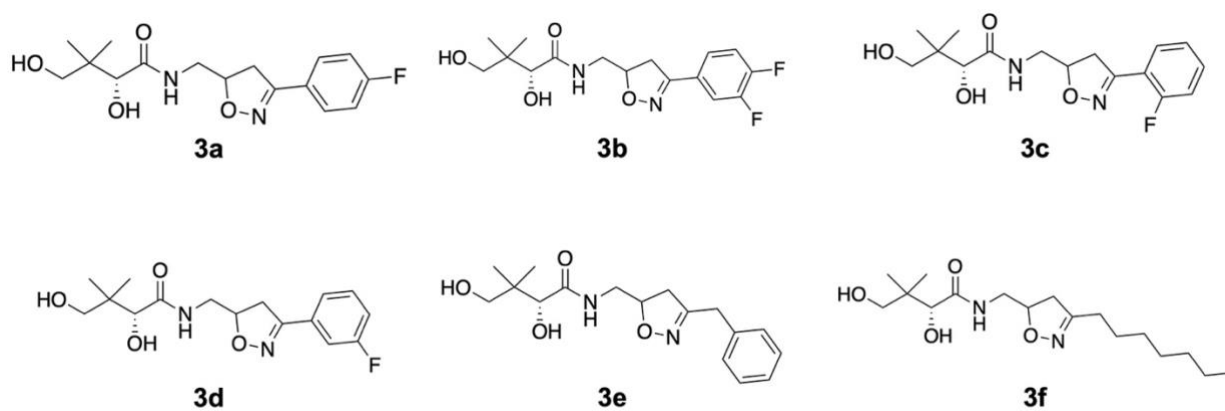


Figure 3.2: Structures of the PanMCs synthesized by the author. **3f** was originally synthesized by Victoria Virgilio⁶⁷ but was remade for biological testing.

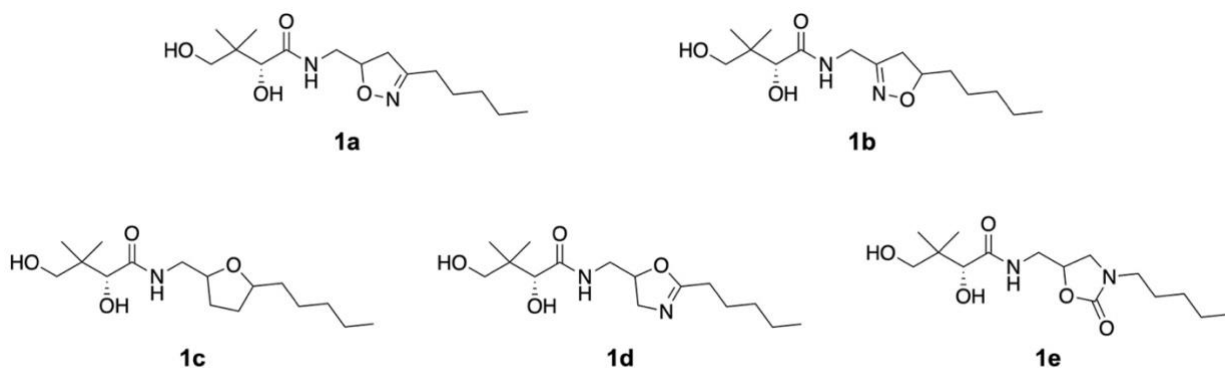


Figure 3.3: Structures of the PanMCs synthesized by group member Chunling Blue Lan that were tested here for antibacterial activity.

Commonly, the Clinical and Laboratory Standards Institute broth microdilution method is employed to measure antibacterial activity, as quantified by the minimum inhibitory concentration (MIC).⁷⁷ However, before determining the MIC for the PanMCs, a screen was performed at 50 μ M of compounds to look for inhibition of bacterial

growth. This concentration of compound is high enough that it allows to identify promising compounds. Compounds that show no bacterial growth inhibition activity at 50 μM are not potent enough to be pharmaceutically relevant, whereas those that show >50 % growth inhibition at this concentration are worth investigating further and determining their exact MIC value. In Figure 3.4, the percent bacterial growth inhibition observed for each PanMCs at 50 μM is shown.

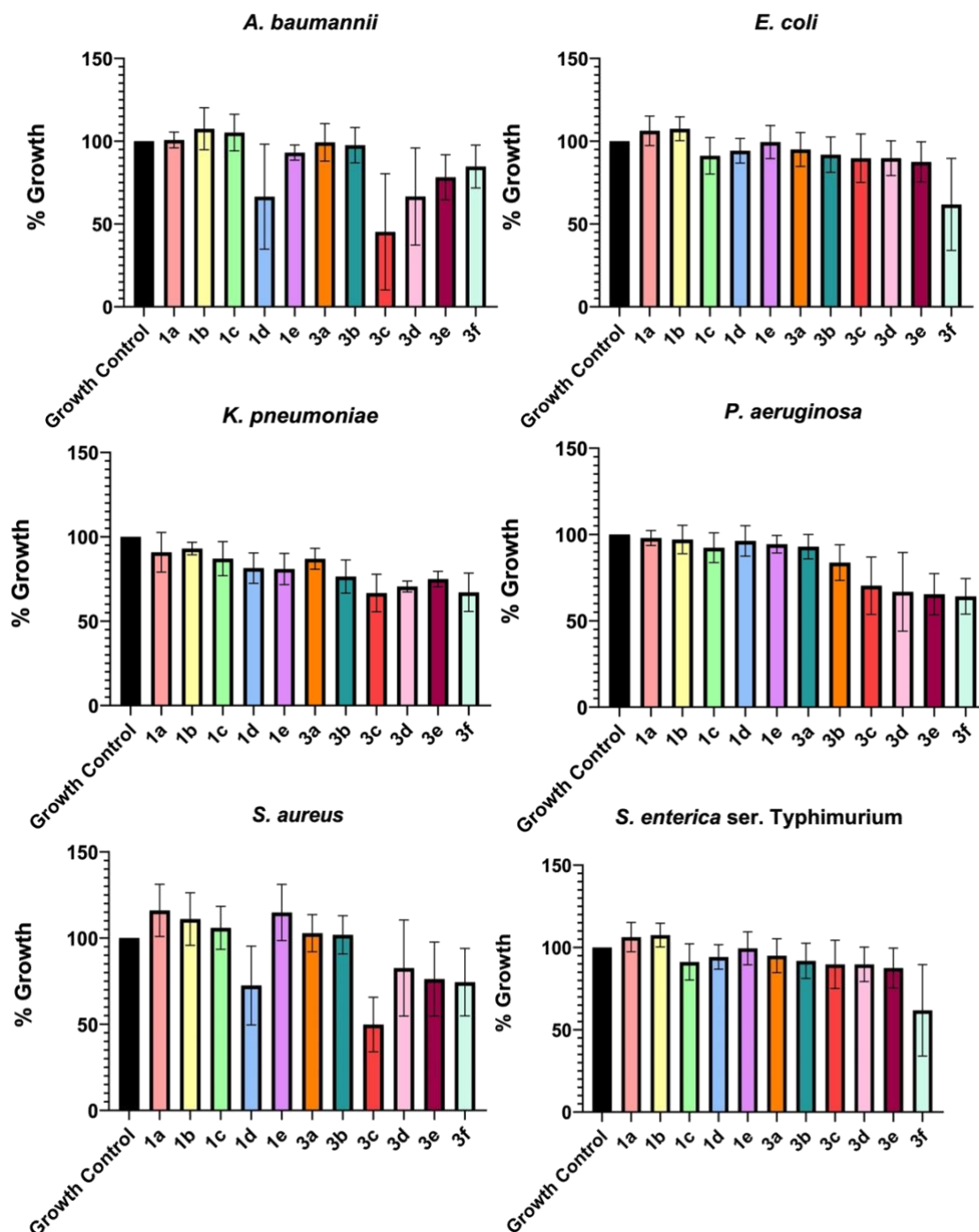


Figure 3.4: Percent growth inhibition of *A. baumannii*, *E. coli*, *K. pneumoniae*, *P. aeruginosa*, *S. aureus*, and *S. Typhimurium* in the presence of compound (50 μ M). The first lane is the control with no compound added and is adjusted to 100 % growth. All experiments were performed in triplicates. Standard error of mean was used to determine the error bars.

Although a few compounds reduced bacterial growth of the strains tested, none of them completely inhibited growth at 50 μM . Compounds **1d** and **3c** appeared to inhibit the growth of *S. aureus* and *A. baumannii* significantly. This is interesting because no pantothenamides or PanMCs have been reported to inhibit the growth of *A. baumannii*. MIC values were therefore measured for these 2 compounds against *S. aureus*, and *A. baumannii*.

The estimated MICs of the compounds **1d** and **3c** against *S. aureus*, appear to be >50 mM (Figure 3.5), which is too high to warrant further studies. Exact MIC values could not be determined with precision due to a lack of solubility of the compounds above 50 mM in water, indicating that the exact MIC value must be >50 mM.

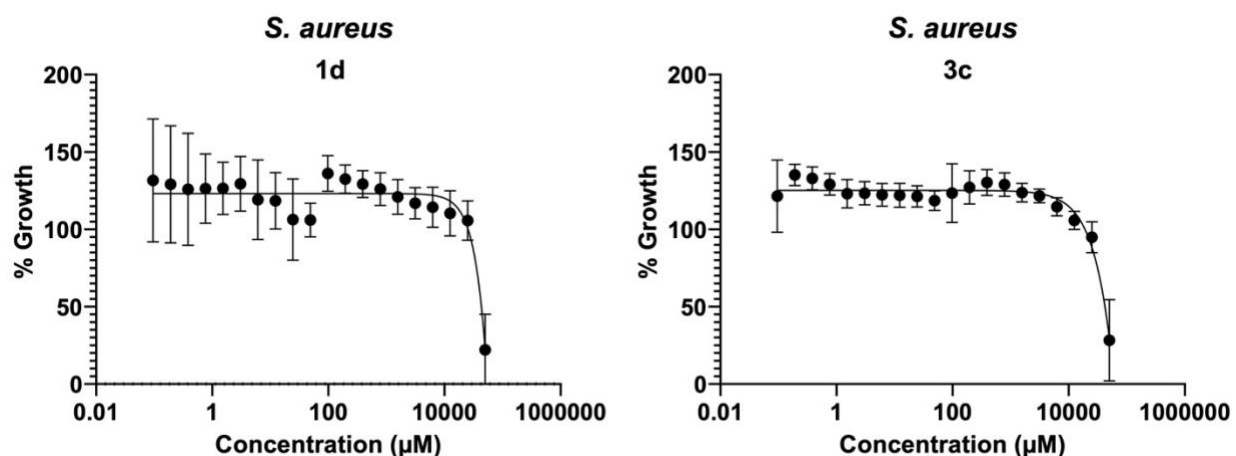


Figure 3.5: MIC curves of **1d** (left) and **3c** (right) for growth inhibition of *S. aureus*. The highest concentration of compound tested was 50 mM. All experiments were performed in triplicates. Standard error of mean was used to determine the error bars.

Similarly, the MICs of **1d** and **3c** against *A. baumannii* were well above 50 mM (Figure 3.6). It is important to note that the data presented on Figure 3.6 was collected from two separate experiments, one for compound concentration 0.1 – 50 μM and another one for concentrations 100 – 50,000 μM , which explains the two trends observed. Nevertheless, the data clearly shows that 100 % growth inhibition is not reached, even at the highest concentrations.

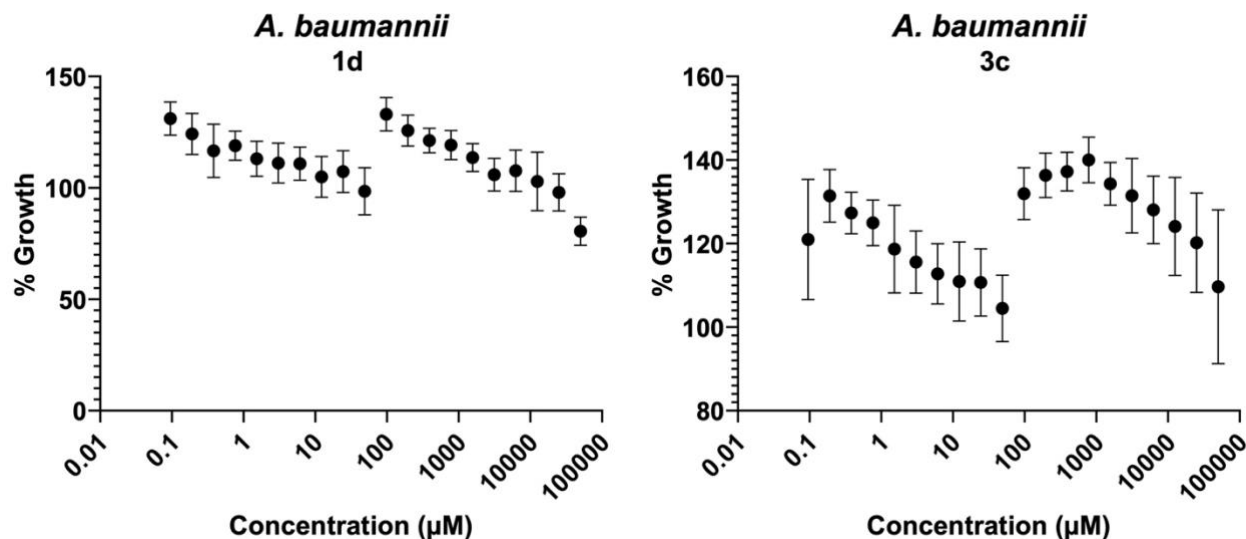


Figure 3.6: MIC curves of **1d** (left) and **3c** (right) for growth inhibition of *A. baumannii*. The highest concentration of compound tested was 50 mM. All experiments were performed in triplicates. Standard error of mean was used to determine the error bars.

Current antibiotics have MICs in the nanomolar or the low micromolar range, making the PanMCs presented here poor antibiotic candidates in comparison. For example, erythromycin has an MIC of ~680 nM and rifampin has an MIC of ~1.2 μM.⁷⁸ Despite the high MIC values of the PanMCs, these results provide some insight that the ring structures tested here in replacement of the labile amide group are poorly tolerated for antibacterial activity against Gram-negative bacteria. Against Gram-positive bacteria the MIC values were still >50 mM; however, growth was reduced to ca. 20% at 50 mM against *S. aureus* (Figure 3.3). This indicates that the ring structures present in **1d** and **3c** to replace the labile amide group are more tolerated in comparison to Gram-negative bacteria. Therefore, more investigation into further derivatization of the existing ring structures present in **1d** and **3c** in replacement of the labile amide group is warranted.

Additionally, a few compounds from the 50 μM antibacterial screen were found to increase the growth of the bacteria such as **1a** and **1b** against *S. aureus* and *S. Typhimurium*, or **1d** and **3c** against *A. baumannii*. Such a result suggests that the bacteria may be able to use these small molecules as a carbon source in their metabolism.

3.4. Conclusion

In this chapter, 10 novel PanMCs were tested against the following bacterial strains: *A. baumannii*, *E. coli*, *K. pneumoniae*, *P. aeruginosa*, *S. aureus*, and *S. Typhimurium*. The PanMC that was remade (**3f**) had previously been tested against *A. baumannii*, *E. coli*, *K. pneumoniae*, *P. aeruginosa*, and *S. aureus*,⁶⁶ but was tested here for the first time against *S. Typhimurium*. Unfortunately, none of the PanMCs tested exhibited sufficient activity to warrant further studies. In the next chapter, results from intraerythrocytic *Plasmodium falciparum* growth inhibition studies will be presented for some of these PanMCs and more.

Chapter 4

Antiplasmodial Results

4.1. Preface and Contributions

As discussed in chapter 1, there were approximately 241 million malaria cases in 2020, as well as 627 000 deaths.^{27,29} In chapter 3, eleven novel PanMCs (**1a–1e** and **3a–3e**) were tested against six different bacterial strains. In this chapter, growth inhibition results against intraerythrocytic *Plasmodium falciparum* for 10 PanMCs synthesized by group member Victoria Virgilio, and 6 PanMCs synthesized by the author are reported and discussed. Growth inhibition of intraerythrocytic *P. falciparum* was measured by Xiangning Christine Liu in the laboratory of Prof. Kevin Saliba at the Australian National University.

4.2. Introduction

Currently, malaria is the most fatal parasitic infection globally and resistance to all antimalarials is rampant.^{27,29} ACTs are the current benchmark treatments for malaria, but even these combination treatments are losing their efficacy at alarming rates.²⁹ Therefore, new antiplasmodial medicines are urgently needed to treat those infected with *Plasmodium* species, of which *P. falciparum* causes the most severe symptoms and the most deaths.²⁹

Pantothenamides and PanMCs exhibit a unique antiplasmodial mechanism of action, making them excellent candidates for the development of new antimicrobials (Section 1.5, Pantothenamides). Previous Auclair group members have discovered various blood-stable antiplasmodial PanMCs through replacing the labile amide bond with various heteroaromatic rings. This chapter will detail the antiplasmodial results of ten novel PanMCs synthesized by Victoria Virgilio (Figure 4.1), five novel PanMCs synthesized by the author, and 1 PanMC (**3f**) remade by the author for the purpose of acquiring biological data (Figure 4.2).

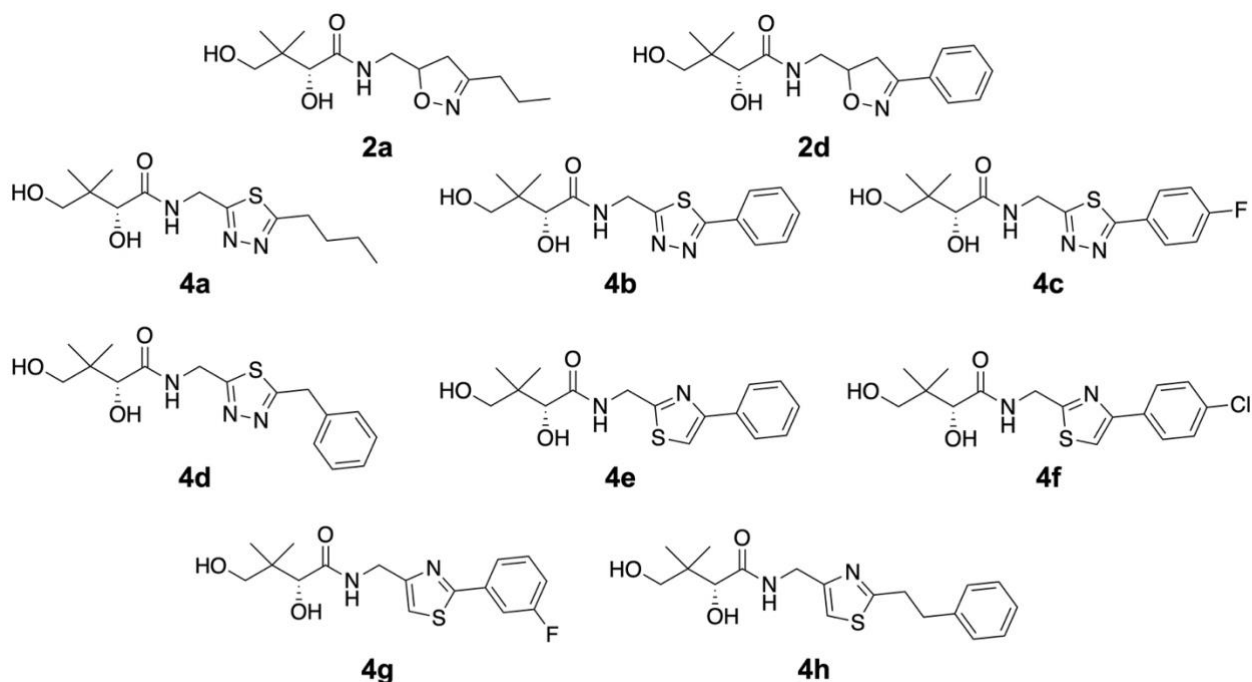


Figure 4.1: PanMCs synthesized by previous group member Victoria Virgilio.⁶⁷

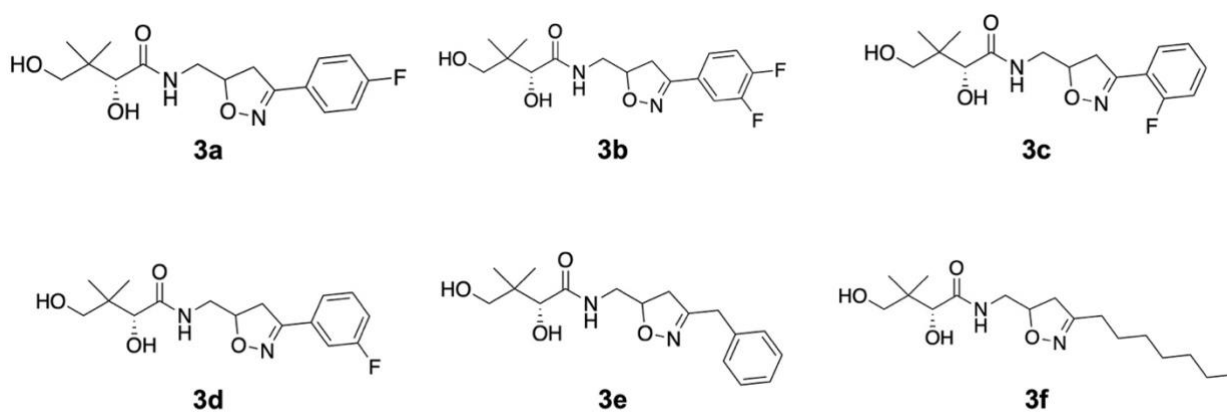


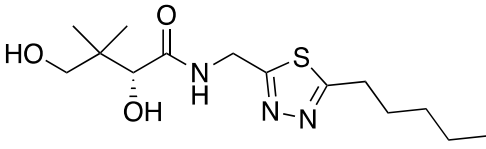
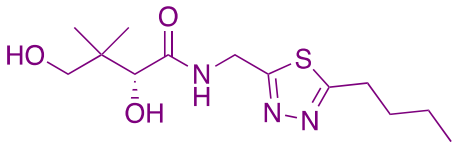
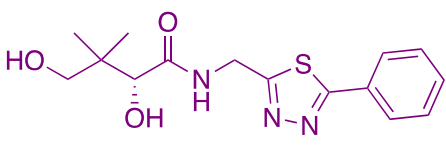
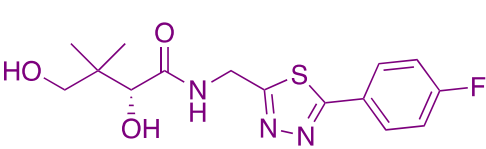
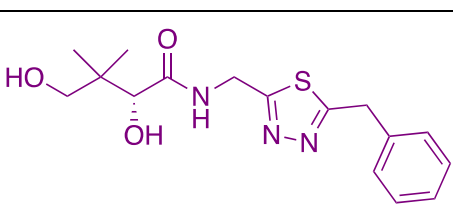
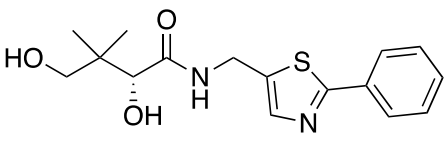
Figure 4.2: PanMCs synthesized by the author. **3f** was first synthesized by previous group member Victoria Virgilio and remade here.⁶⁷

4.3. Evaluation of Antiplasmodial Results

The biological assay used to determine the IC₅₀ values of the PanMCs listed above were determined at the intraerythrocytic stage of the *P. falciparum* lifecycle. Also, these experiments were performed at the Australian National University by Xiangning

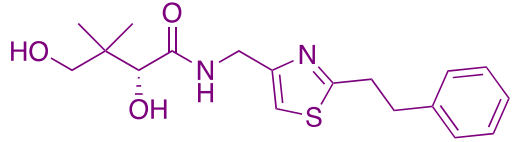
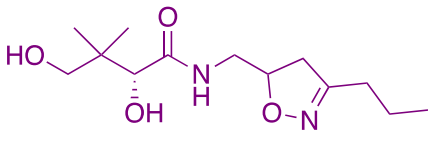
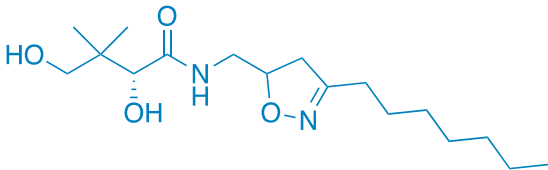
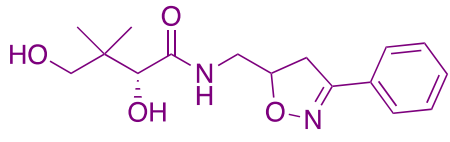
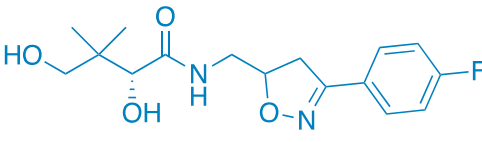
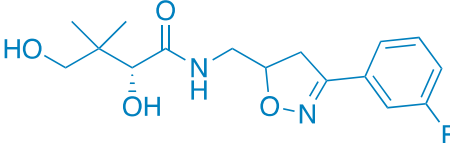
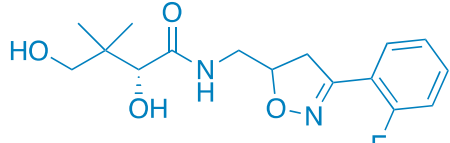
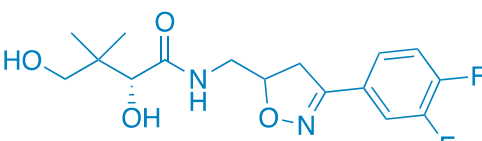
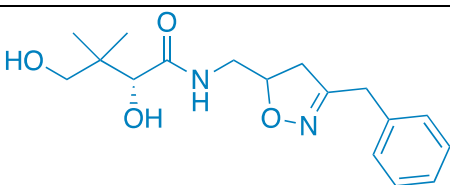
Christine Liu in the laboratory of Prof. Kevin Saliba's group. The results for each PanMC are tabulated in Table 4.1 and presented as concentrations that give 50% inhibition (IC_{50}).

Table 4.1: IC_{50} values for compounds **2a**, **2d**, **4a–4h**, and **3a–3f** against intraerythrocytic *P. falciparum* are highlighted in purple and blue, respectively. IC_{50} values for the previously reported PanMCs^{50,64} featuring the same rings in replacement of the labile amide group (**5a–5r**) are also shown in black for the purpose of establishing broader SARs. Standard error of the mean was used to calculate error. PanMCs with activity in the nanomolar range are highlighted in red.

Compound	PanMC	IC_{50} (μM)
5a		0.96 ± 0.05
2a		1.36 ± 0.08
2b		22 ± 3
2c		13 ± 2
2d		7 ± 1
5b		6.59

5c		9.79
5d		35.53
5e		35.05
5f		9.721
5g		2.3 ± 0.2
5h		4.3 ± 0.4
5i		0.8 ± 0.1
5j		2.9 ± 0.2
4e		1.1 ± 0.1
4f		4.8 ± 0.4

5k		5.980
5l		3.912
5m		0.5474
5n		2.533
5o		53.46
5p		22.18
4g		4.2 ± 0.2
5q		1.937
5r		6.588

4h		4.5 ± 0.5
2a		110 ± 20
3f		52.0 ± 0.7
2d		20 ± 1
3a		15.1 ± 0.6
3d		11.7 ± 0.4
3c		34 ± 2
3b		6.9 ± 0.4
3e		24.5 ± 0.7

Interestingly, several PanMCs synthesized by the author (blue) and by Victoria Virgilio (purple) inhibited the growth of *P. falciparum* at low micromolar concentrations

(**4a**, **4d–4h**, and **3b**). Additionally, the PanMCs containing a thiazole ring exhibit more activity than both the thiadiazole and 4,5-dihydroisoxazole rings (e.g. **4e** compared to **4b**), and the 4,5-dihydroisoxazole-containing compounds (e.g. **4e** compared to **2a**, **5q** compared to **3e**, and **4g** compared to **3d**).

The thiadiazole containing PanMCs (**5a**, **4a–4d**), appear to perform better when linear side chains are in place over phenyl and substituted phenyls (e.g. **5a** and **4a** compared to **4b–4d**). However, when a methylene linker between the thiadiazole ring and the phenyl substituent is present, the activity improves compared to when there is not (e.g. **4d** compared to **4a–4c**). Among the thiazole containing PanMCs (**4e–4h** and **5b–5r**), **5b–5f** generally perform worse than the other orientations of the thiazole ring (e.g. **5b** compared to **4e** and **5m**). A wide variety of different function groups at the side chain of the thiazole ring are well tolerated, affording activity in the low micromolar range (e.g. **5i**, **5j**, **4e**), with CF₃-substituted phenyl rings producing the worst results of this series (e.g. **5o** and **5p** compared to **5n** and **4g**).

Notably, the combination of a 4,5-dihydroisoxazole ring with a linear carbon chain is especially detrimental to antiplasmodial activity (e.g. see **2a** and **3f**). Even a benzyl substituent on the ring is decreasing the activity (**3e**). On the other hand, combining the 4,5-dihydroisoxazole ring with a phenyl ring directly attached to it (**2d**, **3a–3d**) seems to improve activity, compared to an alkyl chain (**2a** and **3f**).⁵¹ Interestingly, the position of the fluorine atom on the aromatic ring has a significant effect on activity, with *meta* (**3d**) affording the best activity, followed by *para* (**3a**), and finally *ortho* (**3c**) derivatives. The doubly fluorinated molecule (**3b**), with two fluorine atoms at both the *meta* and *para* positions, yields almost double the activity than just one or the other. These trends also apply to the thiazole series (**5e** and **5f**, **5o** and **5p**), although in this case, the linear alkyl substituent is superior (**5i**).

Attempting to derive target-based SARs from these IC₅₀ values only is challenging because PanMCs must first enter erythrocytes and then enter the parasite, before undergoing a multi-step bioactivation, and finally inhibiting one or more CoA-utilizing enzymes. Subtle structural differences can have a major impact at each step of this pathway. Identification of specific targets of PanMCs and measurements of membrane permeability may give a better understanding of SARs when combined with

IC₅₀ values. However, in light of the fact that the compounds reported here inhibit parasite growth only at concentrations ca. 1000-fold higher than current antimalarials (e.g. piperaquine 42 ± 10 nM, lumefantrine 24 ± 14 nM, and dihydroartemisin 2 ± 1 nM)⁷⁹ it was decided not to pursue further biological studies of our compounds.

4.4. Conclusion

The PanMCs explored in this chapter exhibited marginal activity against *P. falciparum*. However, the expedition into 5-membered, non-aromatic, heteroatom-containing rings in replacement of the labile amide group is valuable for determining SARs. The importance of the labile amide region of the pantothenamide backbone has been further confirmed here by the incredible change in activity with different ring structures. Therefore, further investigation into different ring structures in replacement of the labile amide group, as well as diversifying the 4,5-dihydroisoxazole ring series would be meaningful for the development of SARs.

Chapter 5

Contributions and Future Directions

5.1. Contributions

The looming threat of antimicrobial resistance warrants the need for novel antimicrobials. Pantothenamides and PanMCs have been shown to be potent growth inhibitors of both bacteria and malaria-causing parasites. These small molecules are excellent candidates for future research and development of antimicrobials due to their new and multiple mechanism(s) of action. However, due to the presence of pantetheinases in human serum that inactivate pantothenamides *in vivo*, their clinical utility is limited. This thesis details the synthesis of 5 novel pantetheinase-resistant PanMCs and the resynthesis of 1 PanMC previously made by Victoria Virgilio⁶⁷ that all exhibit a 4,5-dihydroisoxazole ring in place of the labile amide group.

All six of the PanMCs that were synthesized in this thesis, as well as an additional 5 novel PanMCs synthesized by Chunling Blue Lan displaying various 5-membered, non-aromatic rings were tested for antibacterial activity against *A. baumannii*, *E. coli*, *K. pneumoniae*, *P. aeruginosa*, *S. aureus*, and *S. Typhimurium*. None of the PanMCs tested here displayed sufficient activity to warrant further investigation.

Lastly, 10 novel PanMCs synthesized by Victoria Virgilio (containing either a 4,5-dihydroisoxazole ring, a thiazole, or thiadiazole ring) and all six PanMCs synthesized in this thesis were tested for growth inhibition of intraerythrocytic *P. falciparum*. The best of these compounds were active at micromolar concentrations. Analysis of these results enabled SARs to be determined for the 4,5-dihydroisoxazole series and provided a comparison with thiazoles and thiadiazoles.

5.2. Future Directions

SARs for PanMCs containing a 4,5-dihydroisoxazole ring instead of a labile amide are beginning to be established. The results from this thesis suggest that combining the 4,5-dihydroisoxazole ring with a phenyl substituent is favourable, and addition of a fluoro group at the *meta* position of this phenyl was even more beneficial. Exploring other substituted phenyl groups, especially those with functional groups at the *meta* position (Figure 5.1, **6a–6c**) would be promising given the results from this thesis. Additionally, since very few pantothenamides and PanMCs with branched alkyl chains

have been reported, it would be intriguing to compare the activity of a branched alkyl chain (Figure 5.1, **6d**) to that of a linear chain on the 4,5-dihydroisoxazole ring.

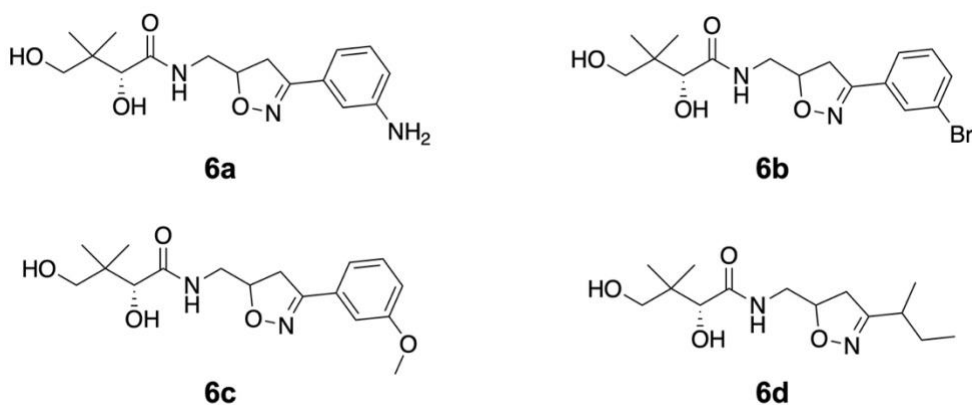


Figure 5.1: Potential PanMCs featuring a 4,5-dihydroisoxazole ring to add to the library.

In parallel, it would also be interesting to explore derivatives of the 4,5-dihydroisoxazole ring such that the 4,5-dihydroisoxazole ring is inverted (Figure 5.2, **7a–7c**).

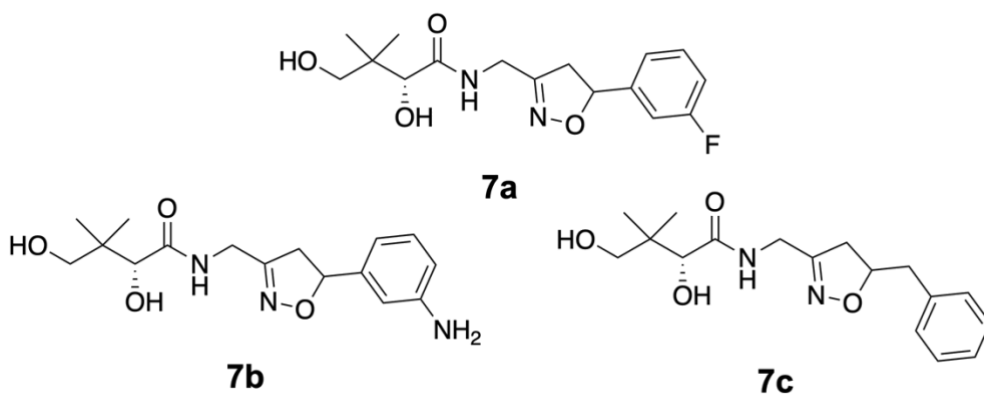


Figure 5.2: Potential PanMCs featuring a 4,5-dihydroisoxazole ring in a different orientation.

Importantly, once more potent PanMCs are identified, further mechanistic studies will be warranted to compare their mechanism to those of the corresponding pantothenamides.

Chapter 6

Experimental Protocols

6.1. Chemistry

6.1.1. Materials and Instruments

All reagents and solvents were purchased from Sigma-Aldrich Canada, Fisher Scientific, or Chem Impex International Inc. All aldehydes were further purified via vacuum distillation before usage. Solvents and triethylamine were dried following the protocols found in the Purification of Laboratory Chemicals (Armarego and Chai 2013)⁸⁰ before usage in all experiments. All water used was first purified using the milli-Q water purification system to a specific resistance of 18.2 MΩ cm at 25 °C. Thin-layer chromatography (TLC) involved using silica plates coated with the fluorescent indicator F254, and having an overall thickness of 200 μm. A UVGL-55 UV lamp was used to visualize UV-absorbing compounds on TLC at 254 or 365 nm. To visualize non-UV-absorbing compounds, a potassium permanganate, ninhydrin, or cerium molybdate stain were used instead. Flash chromatography was performed on a Biotage® Isolera™ Systems instrument using Sfar Silica D – Duo 60 μm chromatography columns. All compounds synthesized are novel, unless otherwise stated. NMR (¹H, ¹³C, ¹⁹F) spectra were obtained on a Bruker AVIIIHD 500 instrument. Chemical shifts were referenced to CDCl₃, d₆-DMSO, or MeOD solvent peaks at 7.26, 2.50, and 3.31 ppm respectively, and are reported in parts per million (ppm). Coupling constants are given in hertz (Hz). The NMR signal multiplicity is reported as: singlet (s), broad singlet (bs), doublet (d), doublet of doublet (dd), doublet of doublet of doublet (ddd), doublet of doublet of doublet of doublet (dddd), doublet of triplet (dt), triplet (t), triplet of triplet (tt), triplet of doublet (td), pentet (p), or multiplet (m). High resolution mass spectrometry (HRMS) spectra were obtained using a Thermo Fisher Scientific EXACTIVE™ Plus Orbitrap Mass Spectrometer or a Bruker MaXis Impact HD Mass Spectrometer at the McGill University Mass Spectral Facility. Purity traces were acquired using both Methods A and B (described in Table 6.1) for all compounds that do not contain a free amine functional group, on an Agilent 1100 series high performance liquid chromatography (HPLC) system equipped with a G1314A variable wavelength detector that uses a deuterium lamp. For all compounds containing a free amine functional group, purity traces were acquired using both Methods C and D (described in Table 6.2) on the same HPLC instrument.

Table 6.1: HPLC methods for purity measurements of non-free amine containing compounds.

Method A

Flow Rate: 1 mL/min; detector wavelength: 214 nm.

Column: LUNA 5 μ m C18(2) 250 x 4.6 mm from Phenomenex.

Time (min)	Water (%)	Acetonitrile (%)
0.00	99.0	1.0
5.00	99.0	1.0
15.00	50.0	50.0
20.00	50.0	50.0
25.00	1.0	99.0
30.00	1.0	99.0
32.00	99.0	1.0
35.00	99.0	1.0

Method B

Flow Rate: 1 mL/min; detector wavelength: 214 nm.

Column: LUNA 5 μ m C18(2) 250 x 4.6 mm from Phenomenex.

Time (min)	Water (%)	Acetonitrile (%)
0.00	99.0	1.0
10.00	1.0	99.0
20.00	1.0	99.0
22.00	99.0	1.0
25.00	99.0	1.0

Table 6.2: HPLC methods for purity measurements of free amine-containing compounds.

Method C

Flow Rate: 1 mL/min; detector wavelength: 214 nm.

Column: ZORBAX NH2 5 μ m 4.6 x 150 nm from Agilent.

Time (min)	Water (%)	Acetonitrile (%)
0.00	1.0	99.0
3.00	1.0	99.0
5.00	10.0	90.0
10.00	15.0	85.0
13.00	30.0	70.0
26.00	30.0	70.0
29.00	100.0	0.0
31.00	100.0	0.0
34.00	1.0	99.0
36.00	1.0	99.0

Method D

Flow Rate: 1 mL/min; detector wavelength: 214 nm.

Column: ZORBAX NH2 5 μ m 4.6 x 150 nm from Agilent.

Time (min)	Water (%)	Acetonitrile (%)
0.00	1.0	99.0
1.00	1.0	99.0
8.00	40.0	60.0
10.00	40.0	60.0
15.00	100.0	0.0
25.00	100.0	0.0
28.00	1.0	99.0
30.00	1.0	99.0

6.1.1. Compound Synthesis

6.1.1.1. General Protocol 1 for the Synthesis of 3.2a–3.2f

The synthesis of compounds **3.2a–3.2f** followed a known procedure with modifications.⁸¹ The analogous aldehyde (10.0 – 15.0 mmol, 1 eq) was mixed with hydroxylammonium chloride (20.0 – 30 mmol, 2 eq) in an ethanol and water (2:1) solution at room temperature. The mixture was then cooled to 0 °C in an ice bath. Then, sodium acetate (30 – 45 mmol, 3 eq) was added slowly. The resulting mixture then stirred overnight. Next, the ethanol was removed *in vacuo* and the leftover solution was then diluted in water (20 mL). The oxime product was then extracted in ethyl acetate (3 x 30 mL) and saturated aqueous sodium bicarbonate (2 x 20 mL). Then, the organic layers were combined and dried over sodium sulfate, filtered, and then concentrated *in vacuo* to yield the crude oximes **3.2a–3.2f**.

6.1.1.2. General Protocol 2 for the Synthesis of 3.3a–3.3f

The synthesis of compounds **3.3a–3.3f** followed a known procedure with modifications.⁸¹ The corresponding oxime (10.0 – 14.0 mmol, 1 eq) was dissolved in dimethylformamide (18 – 22 mL) before slow addition of *N*-chlorosuccinimide (13.0 – 18.2 mmol, 1.3 eq). The resulting solution was stirred for 3 hours at room temperature. Next, the reaction mixture was washed with water (3 x 20 mL) and brine (3 x 20 mL). The organic layers were then combined and dried over sodium sulfate, filtered, and then concentrated *in vacuo* to yield the crude oxime chloride **3.3a–3.3f**.

6.1.1.3. General Protocol 3 for the Synthesis of 3.4a–3.4f

The synthesis of compounds **3.4a–3.4f** followed a known procedure with modifications.⁸¹ The analogous oxime chloride **3.3a–3.3f** (8.0 – 12.0 mmol, 1 eq) was mixed with *tert*-butyl *N*-allylcarbamate (8.0 – 12.0 mmol, 1 eq) in ethyl acetate (34 – 45 mL). This solution was cooled to 0 °C in an ice bath. In parallel, triethylamine (9.6 – 14.4 mmol, 1.2 eq) was first diluted in ethyl acetate (5 – 10 mL) and then added dropwise to the solution containing the oxime chloride and *tert*-butyl *N*-allylcarbamate. The resulting solution was stirred at room temperature overnight. Then, the reaction mixture was diluted in ethyl acetate (20 mL) and washed with saturated aqueous sodium bicarbonate (2 x 20 mL), and brine (2 x 20 mL). The organic layers were combined and then dried over sodium sulfate, filtered, and concentrated *in vacuo*. The final product **3.4a–3.4f** was purified by flash chromatography (eluted with ethyl acetate-hexanes, 05:95 to 15:85).

6.1.1.4. General Protocol 4 for the Synthesis of 3.5a–3.5f

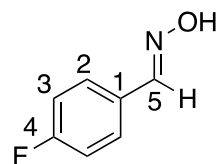
The synthesis of compounds **3.5a–3.5f** followed a procedure developed by Auclair group member, Chunling Blue Lan. First, **3.4a–3.4f** (1.0 – 4.0 mmol, 1 eq) was dissolved in dichloromethane (2 – 10 mL) before addition of trifluoroacetic acid (10 – 40 mmol, 10 eq). The resulting solution was stirred at room temperature for 2 hours. Afterwards, an aqueous solution of sodium hydroxide (15 % w/v) was added dropwise to the reaction mixture until a pH of ~14 was reached. Then, the free amine product was extracted in ethyl acetate (3 x 10 mL). The combined organic layers were dried over

sodium sulfate, filtered, and concentrated *in vacuo* to yield the crude free amine **3.5a–3.5f**. The product was used in the next step within 24 hours of synthesizing it.

6.1.1.5. General Protocol 5 for the Synthesis of **3a–3f**

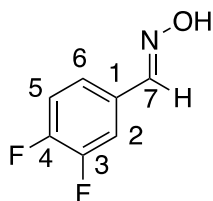
The synthesis of compounds **3a–3f** followed a procedure developed by Auclair group member, Chunling Blue Lan. The free amine **3.5a–3.5f** (0.8 – 3.2 mmol, 1 eq), D-pantolactone (1.6 – 6.4 mmol, 2 eq), and triazabicyclodecene (0.08 – 0.32 mmol, 0.1 eq) were dissolved in toluene (1.0 – 3.0 mL). The resulting solution was stirred at room temperature overnight. Then, the reaction mixture was concentrated *in vacuo*, and the final product **3a–3f** was purified by flash chromatography (eluted with ethyl acetate-hexanes 20:80 to remove impurities, followed by methanol-dichloromethane 05:95).

4-Fluorobenzaldehyde Oxime (**3.2a**)



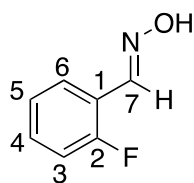
This known compound⁸² was prepared from 4-fluorobenzaldehyde (15.0 mmol, 1.0 eq), hydroxylammonium chloride (30.0 mmol, 2.0 eq), and sodium acetate (45.0 mmol, 3.0 eq) using General Protocol 1 to give the product as a white, fluffy powder. Crude yield: 2.13 g. R_f = 0.66 (30% EtOAc in hexanes). The compound characterization agreed with previously reported literature.⁸² ^1H NMR (500 MHz, CDCl_3): δ 8.13 (s, H-5), 7.57 (dd, J = 8.3, 5.1 Hz, 2H, H-2), 7.08 (t, J = 8.7 Hz, 2H, H-3). ^{13}C NMR (125 MHz, CDCl_3): δ 163.9 (d, $J_{\text{C-F}}$ = 250.4 Hz), 149.4, 129.0 (d, $J_{\text{C-F}}$ = 8.5 Hz), 128.3 (d, $J_{\text{C-F}}$ = 3.4 Hz), 116.1 (d, $J_{\text{C-F}}$ = 22.0 Hz). ^{19}F NMR (471 MHz, CDCl_3): δ -110.05 (tt, J = 8.5, 5.1 Hz). HRMS for $\text{C}_7\text{H}_7\text{FNO}$ $[\text{M}+\text{H}]^+$ calcd: 140.0506 found: 140.0507.

3,4-Difluorobenzaldehyde Oxime (3.2b)



This known compound⁸³ was prepared from 3,4-difluorobenzaldehyde (15.0 mmol, 1.0 eq), hydroxylammonium chloride (30.0 mmol, 2.0 eq), and sodium acetate (45.0 mmol, 3.0 eq) using General Protocol 1 to give the product as a white powder. Crude yield: 2.97 g. R_f = 0.66 (30% EtOAc in hexanes). The compound characterization agreed with previously reported literature.⁸³ ^1H NMR (500 MHz, CDCl_3): δ 8.08 (bs, 1H, O-H), 7.45 (ddd, J = 11.0, 7.7, 2.1 Hz, 1H, H-2), 7.27 (m, 1H, H-6), 7.18 (m, 1H, H-5). ^{13}C NMR (125 MHz, CDCl_3): δ 152.2 (dd, $J_{\text{C-F}}$ = 252.6, 12.9 Hz), 150.2 (dd, $J_{\text{C-F}}$ = 249.4, 13.2 Hz), 148.6, 129.3 (dd, $J_{\text{C-F}}$ = 6.6, 3.5 Hz), 123.9 (dd, $J_{\text{C-F}}$ = 7.6, 3.8 Hz), 117.8 (d, $J_{\text{C-F}}$ = 17.9 Hz), 115.5 (d, $J_{\text{C-F}}$ = 18.6 Hz). ^{19}F NMR (471 MHz, CDCl_3): δ -134.74 (m), -136.63 (m). HRMS for $\text{C}_7\text{H}_4\text{F}_2\text{NO}$ $[\text{M-H}]^-$ calcd: 156.0266 found: 156.0258.

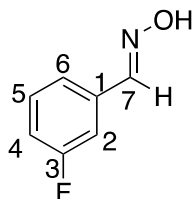
2-Fluorobenzaldehyde Oxime (3.2c)



This compound was prepared from 2-fluorobenzaldehyde (10.0 mmol, 1.0 eq), hydroxylammonium chloride (20.0 mmol, 2.0 eq), and sodium acetate (30.0 mmol, 3.0 eq) using General Protocol 1 to give the product as a white powder. Crude yield: 1.52 g. R_f = 0.79 (50% EtOAc in hexanes). Purity was 96 % based on HPLC, R_t = 19.0 minutes with Method A and R_t = 9.8 minutes with Method B (Table 6.1). ^1H NMR (500 MHz, CDCl_3): δ 8.93 (bs, 1H, O-H), 8.39 (s, 1H, H-7), 7.72 (td, J = 7.6, 1.8 Hz, 1H, H-5), 7.37 (m, 1H, H-4), 7.17 (td, J = 7.7, 1.6 Hz, 1H, H-3), 7.10 (m, 1H, H-6). ^{13}C NMR (125 MHz, CDCl_3): δ 161.0 (d, $J_{\text{C-F}}$ = 252.6 Hz), 144.6 (d, $J_{\text{C-F}}$ = 3.2 Hz), 131.7 (d, $J_{\text{C-F}}$ = 8.6 Hz), 127.3 (d, $J_{\text{C-F}}$ = 2.7 Hz), 124.6 (d, $J_{\text{C-F}}$ = 3.6 Hz), 119.9 (d, $J_{\text{C-F}}$ = 10.9 Hz), 116.2 (d, $J_{\text{C-F}}$

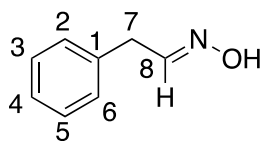
= 21.1 Hz). ^{19}F NMR (471 MHz, CDCl_3): δ -118.35 (m). HRMS for $\text{C}_7\text{H}_7\text{FNO}$ $[\text{M}+\text{H}]^+$ calcd. 140.0506, found 140.0502.

3-Fluorobenzaldehyde Oxime (3.2d)



This compound was prepared from 3-fluorobenzaldehyde (15.0 mmol, 1.0 eq), hydroxylammonium chloride (30.0 mmol, 2.0 eq), and sodium acetate (45.0 mmol, 3.0 eq) using General Protocol 1 to give the product as a beige powder. Crude yield: 2.12 g. R_f = 0.63 (30% EtOAc in hexanes). Purity was 86 % based on HPLC, R_t = 19.6 minutes with Method A and R_t = 10.0 minutes with Method B (Table 6.1). ^1H NMR (500 MHz, CDCl_3): δ 8.66 (bs, 1H, O-H), 8.14 (s, 1H, H-7), 7.38-7.31 (m, 3H, H-2, H-5 and H-6), 7.09 (m, 1H, H-4). ^{13}C NMR (125 MHz, CDCl_3): δ 163.1 (d, $J_{\text{C-F}}$ = 246.7 Hz), 149.5 (d, $J_{\text{C-F}}$ = 3.1 Hz), 134.2 (d, $J_{\text{C-F}}$ = 8.2 Hz), 130.5 (d, $J_{\text{C-F}}$ = 8.2 Hz), 123.3 (d, $J_{\text{C-F}}$ = 2.9 Hz), 117.2 (d, $J_{\text{C-F}}$ = 21.5 Hz), 113.5 (d, $J_{\text{C-F}}$ = 22.9 Hz). ^{19}F NMR (471 MHz, CDCl_3): δ -112.32 (m). HRMS for $\text{C}_7\text{H}_7\text{FNO}$ $[\text{M}+\text{H}]^+$ calcd. 140.0506, found 140.0502.

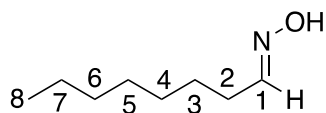
2-Phenylacetaldehyde Oxime (3.2e)



This known compound⁸⁴ was prepared from phenylacetaldehyde (15.0 mmol, 1.0 eq), hydroxylammonium chloride (30.0 mmol, 2.0 eq), and sodium acetate (45.0 mmol, 3.0 eq) using General Protocol 1 to give the product as a white powder. Crude yield: 1.55 g. R_f = 0.56 (30% EtOAc in hexanes). The compound characterization agreed with previously reported literature.⁸⁴ ^1H NMR (500 MHz, CDCl_3): δ 9.20 (bs, 1H, OH), 7.33 (m, 2H, H-2 and H-6), 7.27 (m, 3H, H-3 and H-4 and H-5), 6.93 (t, J = 5.3 Hz, 1H, H-8), 3.77 (d, J = 5.3 Hz, 2H, H-7). ^{13}C NMR (125 MHz, CDCl_3): δ 151.0, 136.8, 128.9, 128.9, 126.8, 31.8.

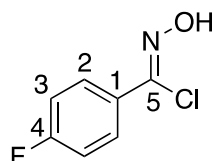
HRMS for C₈H₉FNONa [M+Na]⁺ calcd. 158.0576, found 158.0576.

Octanal Oxime (3.2f)



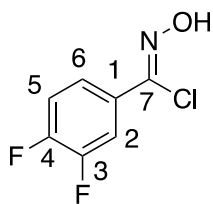
This known compound⁸⁵ was prepared from octanal (10.0 mmol, 1.0 eq), hydroxylammonium chloride (20.0 mmol, 2.0 eq), and sodium acetate (30.0 mmol, 3.0 eq) using General Protocol 1 to give the product as a white powder. Crude yield: 1.68 g. *R*_f = 0.83 (30% EtOAc in hexanes). The compound characterization agreed with previously reported literature.⁸⁵ ¹H NMR (500 MHz, CDCl₃): δ 7.42 (t, *J* = 6.1 Hz, H-1), 2.34 (bs, 1H, OH), 1.49 (m, 2H, H-2), 1.35-1.23 (m, 10H, H-3, H-4, H-5, H-6, and H-7), 0.87 (t, *J* = 7.2 Hz, H-8). ¹³C NMR (125 MHz, CDCl₃): δ 152.5, 31.9, 29.6, 29.2, 26.7, 26.1, 22.7, 14.2. HRMS for C₈H₁₈NO [M+H]⁺ calcd. 144.1383, found 144.1382.

4-Fluoro-*N*-Hydroxybenzimidoyl Chloride (3.3a)



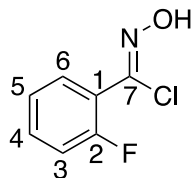
This known compound⁸⁶ was prepared from **3.2a** (13.0 mmol, 1.0 eq) and *N*-chlorosuccinimide (16.9 mmol, 1.3 eq) using General Protocol 2 to give the product as a transparent yellow oil. Crude yield: 2.57 g. *R*_f = 0.78 (30% EtOAc in hexanes). The compound characterization agreed with previously reported literature.⁸⁶ ¹H NMR (500 MHz, CDCl₃): δ 9.50 (bs, OH), 7.81 (dd, *J* = 8.3, 5.2 Hz, 2H, H-2), 7.05 (t, *J* = 8.7 Hz, 2H, H-3). ¹³C NMR (125 MHz, CDCl₃): δ 164.2 (d, *J*_{C-F} = 251.3 Hz), 138.3, 129.3 (d, *J*_{C-F} = 8.4 Hz), 129.0 (d, *J*_{C-F} = 3.3 Hz), 115.6 (d, *J*_{C-F} = 22.2 Hz). ¹⁹F NMR (471 MHz, CDCl₃): δ -109.86 (tt, *J* = 8.5, 5.2 Hz).

3,4-Difluoro-*N*-Hydroxybenzimidoyl Chloride (3.3b)



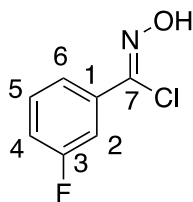
This known compound⁸⁷ was prepared from **3.2b** (13.0 mmol, 1.0 eq) and *N*-chlorosuccinimide (16.9 mmol, 1.3 eq) using General Protocol 2 to give the product as a white powder. Crude yield: 3.01 g. R_f = 0.81 (30% EtOAc in hexanes). The compound characterization agreed with previously reported literature.⁸⁷ ^1H NMR (500 MHz, CDCl_3): δ 7.68 (ddd, J = 11.3, 7.6, 2.3 Hz, 1H, H-2), 7.61 (m, 1H, H-6), 7.20 (m, 1H, H-5). ^{13}C NMR (125 MHz, CDCl_3): δ 152.2 (dd, $J_{\text{C-F}}$ = 254.0, 12.8 Hz), 150.2 (dd, $J_{\text{C-F}}$ = 249.4, 13.2 Hz), 138.3 (d, $J_{\text{C-F}}$ = 2.6 Hz), 129.5 (dd, $J_{\text{C-F}}$ = 6.4, 3.7 Hz), 123.8 (dd, $J_{\text{C-F}}$ = 6.8, 3.7 Hz), 117.6 (d, $J_{\text{C-F}}$ = 18.1 Hz), 116.6 (d, $J_{\text{C-F}}$ = 19.8 Hz). ^{19}F NMR (471 MHz, CDCl_3): δ -133.62 (m), -136.33 (m).

2-Fluoro-*N*-Hydroxybenzimidoyl Chloride (3.3c)



This compound was prepared from **3.2c** (10.0 mmol, 1.0 eq) and *N*-chlorosuccinimide (13.0 mmol, 1.3 eq) using General Protocol 2 to give the product as a white crystalline powder. Crude yield: 1.43 g. R_f = 0.67 (30% EtOAc in hexanes). Purity was 78 % based on HPLC, R_t = 22.2 minutes with Method A and R_t = 10.8 minutes with Method B (Table 6.1). ^1H NMR (500 MHz, CDCl_3): δ 9.11 (s, 1H, O-H), 7.68 (td, J = 7.6, 1.8 Hz, 1H, H-5), 7.44 (m, 1H, H-4), 7.23 (td, J = 7.7, 1.7 Hz, 1H, H-3), 7.16 (m, 1H, H-6). ^{13}C NMR (125 MHz, CDCl_3): δ 160.0 (d, $J_{\text{C-F}}$ = 255.6 Hz), 135.5 (d, $J_{\text{C-F}}$ = 4.5 Hz), 132.4 (d, $J_{\text{C-F}}$ = 8.7 Hz), 130.9 (d, $J_{\text{C-F}}$ = 1.3 Hz), 124.5 (d, $J_{\text{C-F}}$ = 3.8 Hz), 121.1 (d, $J_{\text{C-F}}$ = 11.0 Hz), 116.8 (d, $J_{\text{C-F}}$ = 22.3 Hz). ^{19}F NMR (471 MHz, CDCl_3): δ -111.91 (m). HRMS for $\text{C}_7\text{H}_6\text{ClFNO}$ $[\text{M}+\text{H}]^+$ calcd. 174.0116, found 174.0110.

3-Fluoro-*N*-Hydroxybenzimidoyl Chloride (3.3d)



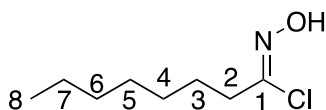
This known compound⁸⁸ was prepared from **3.2d** (14.0 mmol, 1.0 eq) and *N*-chlorosuccinimide (18.2 mmol, 1.3 eq) using General Protocol 2 to give the product as a yellow oil. Crude yield: 3.09 g. R_f = 0.77 (30% EtOAc in hexanes). The compound characterization agreed with previously reported literature.⁸⁸ ^1H NMR (500 MHz, CDCl_3): δ 8.66 (bs, 1H, O-H), 8.14 (s, 1H, H-7), 7.38-7.31 (m, 3H, H-2, H-5 and H-6), 7.09 (m, 1H, H-4). ^{13}C NMR (125 MHz, CDCl_3): δ 163.1 (d, $J_{\text{C-F}}$ = 246.7 Hz), 149.5 (d, $J_{\text{C-F}}$ = 3.1 Hz), 134.2 (d, $J_{\text{C-F}}$ = 8.2 Hz), 130.5 (d, $J_{\text{C-F}}$ = 8.2 Hz), 123.3 (d, $J_{\text{C-F}}$ = 2.9 Hz), 117.2 (d, $J_{\text{C-F}}$ = 21.5 Hz), 113.5 (d, $J_{\text{C-F}}$ = 22.9 Hz). ^{19}F NMR (471 MHz, CDCl_3): δ -112.32 (m).

N-Hydroxy-2-phenylacetimidoyl Chloride (3.3e)



This known compound⁸⁹ was prepared from **3.2e** (10.0 mmol, 1.0 eq) and *N*-chlorosuccinimide (13.0 mmol, 1.3 eq) using General Protocol 2 to give the product as a yellow solid. Crude yield: 1.72 g. Used directly in next step.

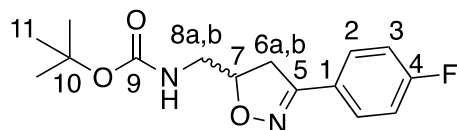
N-Hydroxyoctanimidoyl Chloride (3.3f)



This known compound⁹⁰ was prepared from **3.2f** (10.0 mmol, 1.0 eq) and *N*-chlorosuccinimide (13.0 mmol, 1.3 eq) using General Protocol 2 to give the product as a blue solid. Crude yield: 1.91 g. R_f = 0.62 (30% EtOAc in hexanes). The compound characterization agreed with previously reported literature.⁹⁰ ^1H NMR (500 MHz, CDCl_3): δ 9.16 (bs, 1H, O-H), 2.47 (t, J = 7.5 Hz, 2H, H-2), 1.61 (p, J = 7.7 Hz, H-3), 1.25 (m, 8H, H-4, H-5, H-6 and H-7), 0.84 (t, J = 7.1 Hz, 3H, H-8). ^{13}C NMR (125 MHz, CDCl_3): δ

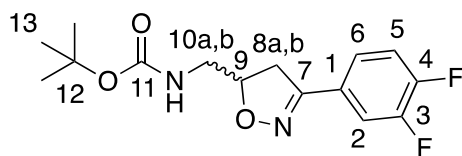
142.6, 36.6, 31.7, 28.9, 28.5, 26.3, 22.6, 14.1. HRMS for C₈H₁₇ClNO [M+H]⁺ calcd. 178.0993, found 178.0991.

***tert*-Butyl((3-(4-Fluorophenyl)-4,5-Dihydroisoxazol-5-yl)methyl)carbamate (3.4a)**



This compound was prepared from **3.3a** (10.0 mmol, 1.0 eq), *tert*-butyl *N*-allylcarbamate (10.0 mmol, 1.0 eq), and triethylamine (12.0 mmol, 1.2 eq) using General Protocol 3 to give the product as a white, faintly pink powder. Yield: 33 %, 0.98 g. *R*_f = 0.30 (30% EtOAc in hexanes). Purity was 99 % based on HPLC, *R*_t = 25.2 minutes with Method A and *R*_t = 11.5 minutes with Method B (Table 6.1). ¹H NMR (500 MHz, CDCl₃): δ 7.64 (dd, *J* = 8.3, 5.2 Hz, 2H, H-2), 7.08 (t, *J* = 8.7 Hz, 2H, H-3), 4.95 (bs, 1H, NH), 4.84 (m, 1H, H-7), 3.45 (m, 1H, H-8a), 3.38 (dd, *J* = 16.9, 7.7 Hz, 2H, H-8b and H-6a), 3.13 (dd, *J* = 16.8, 7.4 Hz, 1H, H-6b), 1.39 (s, 9H, H-11). ¹³C NMR (125 MHz, CDCl₃): δ 163.9 (d, *J*_{C-F} = 251.0 Hz), 156.4, 156.1, 128.8 (d, *J*_{C-F} = 8.6 Hz), 125.7 (d, *J*_{C-F} = 3.3 Hz), 116.0 (d, *J*_{C-F} = 22.0 Hz), 80.4, 79.9, 43.7, 37.6, 28.4. ¹⁹F NMR (471 MHz, CDCl₃): δ -109.75 (m). HRMS for C₁₅H₁₉FN₂O₃Na [M+Na]⁺ calcd. 317.1272, found 317.1273.

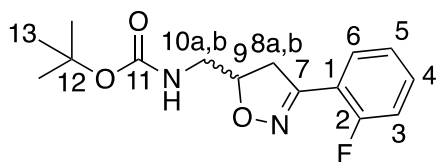
***tert*-Butyl((3-(3,4-difluorophenyl)-4,5-dihydroisoxazol-5-yl)methyl)carbamate (3.4b)**



This compound was prepared from **3.3b** (8.0 mmol, 1.0 eq), *tert*-butyl *N*-allylcarbamate (8.0 mmol, 1.0 eq), and triethylamine (9.6 mmol, 1.2 eq) using General Protocol 3 to give the product as a white, faintly pink powder. Yield: 52 %, 1.31 g. *R*_f = 0.40 (30% EtOAc in hexanes). Purity was 98 % based on HPLC, *R*_t = 25.8 minutes with Method A and *R*_t = 11.7 minutes with Method B (Table 6.1). ¹H NMR (500 MHz, CDCl₃): δ 7.54 (ddd, *J* = 11.1, 7.6, 2.1 Hz, 1H, H-2), 7.34 (m, 1H, H-6), 7.19 (m, 1H, H-5), 4.93 (bs, 1H, N-H), 4.87 (m, 1H, H-9), 3.43 (m, 2H, H-8a and H-8b), 3.33 (dd, *J* = 16.7, 10.6 Hz, 1H, H-10a), 3.12 (dd, *J* = 16.8, 7.5 Hz, 1H, H-10b), 1.39 (s, 9H, H-13). ¹³C NMR (125 MHz,

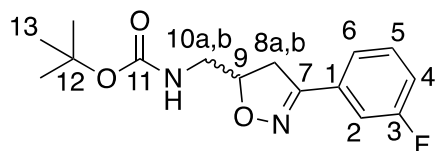
CDCl₃): δ 156.4, 155.5, 151.6 (dd, J_{C-F} = 253.2, 12.9 Hz), 150.6 (dd, J_{C-F} = 249.9, 13.2 Hz), 126.6 (dd, J_{C-F} = 6.4, 4.0 Hz), 123.3 (dd, J_{C-F} = 6.6, 3.8 Hz), 117.8 (d, J_{C-F} = 17.8 Hz), 115.8 (d, J_{C-F} = 18.9 Hz), 80.8, 79.9, 43.7, 37.3, 28.4. ¹⁹F NMR (471 MHz, CDCl₃): δ -134.27 (m), -136.31 (m). HRMS for C₁₅H₁₈F₂N₂O₃Na [M+Na]⁺ calcd. 335.1178, found 335.1168.

***tert*-Butyl((3-(2-fluorophenyl)-4,5-dihydroisoxazol-5-yl)methyl)carbamate (3.4c)**



This compound was prepared from **3.3c** (8.0 mmol, 1.0 eq), *tert*-butyl *N*-allylcarbamate (8.0 mmol, 1.0 eq), and triethylamine (9.6 mmol, 1.2 eq) using General Protocol 3 to give the product as a light yellow solid. Yield: 63 %, 1.49 g. R_f = 0.47 (30% EtOAc in hexanes). Purity was 98 % based on HPLC, R_t = 25.0 minutes with Method A and R_t = 11.4 minutes with Method B (Table 6.1). ¹H NMR (500 MHz, CDCl₃): δ 7.80 (td, J = 7.7, 1.7 Hz, 1H, H-5), 7.38 (m, 1H, H-4), 7.17 (m, 1H, H-6), 7.10 (m, 1H, H-3), 4.95 (t, J = 6.3 Hz, 1H, N-H), 4.84 (m, 1H, H-9), 3.49-3.43 (m, 2H, H-8a and H-8b), 3.36 (m, 1H, H-10a), 3.21, (ddd, J = 17.5, 7.5, 2.4 Hz, 1H, H-10b), 1.40 (s, 9H, H-13). ¹³C NMR (125 MHz, CDCl₃): δ 160.5 (d, J_{C-F} = 252.8), 156.3, 153.9, 132.0 (d, J_{C-F} = 8.5 Hz), 129.1 (d, J_{C-F} = 3.1 Hz), 124.6 (d, J_{C-F} = 3.5 Hz), 117.6 (d, J_{C-F} = 11.7 Hz), 116.6 (d, J_{C-F} = 22.1 Hz), 80.4, 79.8, 43.7, 39.3, 28.4. ¹⁹F NMR (471 MHz, CDCl₃): δ -112.20 (m). HRMS for C₁₅H₁₉FN₂NaO₃ [M+Na]⁺ calcd. 317.1272, found 317.1267.

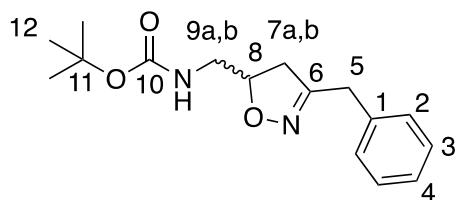
***tert*-Butyl((3-(3-fluorophenyl)-4,5-dihydroisoxazol-5-yl)methyl)carbamate (3.4d)**



This compound was prepared from **3.3d** (12.0 mmol, 1.0 eq), *tert*-butyl *N*-allylcarbamate (12.0 mmol, 1.0 eq), and triethylamine (14.4 mmol, 1.2 eq) using General Protocol 3 to give the product as a light yellow solid. Yield: 54 %, 1.92 g. R_f = 0.41 (30% EtOAc in

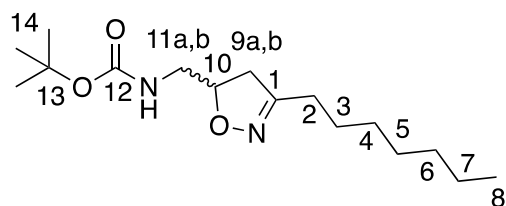
hexanes). Purity was 93 % based on HPLC, R_t = 25.8 minutes with Method A and R_t = 11.8 minutes with Method B (Table 6.1). ^1H NMR (500 MHz, CDCl_3): δ 7.41-7.33 (m, 3H, H-2, H-5 and H-6), 7.10 (m, 1H, H-4), 4.95 (bs, 1H, N-H), 4.87 (m, 1H, H-9), 3.46 (m, 1H, H-10a), 3.40 (m, 1H, H-10b), 3.34 (dd, J = 16.9, 10.7 Hz, 1H, H-8a), 3.13 (dd, J = 16.9, 7.5 Hz, 1H, H-8b), 1.39 (s, 9H, H-13). ^{13}C NMR (125 MHz, CDCl_3): δ 162.9 (d, $J_{\text{C-F}}$ = 246.6 Hz), 156.4, 156.3, 131.6 (d, $J_{\text{C-F}}$ = 8.1 Hz), 130.5 (d, $J_{\text{C-F}}$ = 8.3 Hz), 122.6 (d, $J_{\text{C-F}}$ = 2.9 Hz), 117.3 (d, $J_{\text{C-F}}$ = 21.3 Hz), 113.6 (d, $J_{\text{C-F}}$ = 23.1 Hz), 80.6, 79.9, 43.7, 37.2, 28.4. ^{19}F NMR (471 MHz, CDCl_3): δ -112.12 (m). HRMS for $\text{C}_{15}\text{H}_{19}\text{FN}_2\text{NaO}_3$ $[\text{M}+\text{Na}]^+$ calcd. 317.1272, found 317.1267.

***tert*-Butyl ((3-benzyl-4,5-dihydroisoxazol-5-yl)methyl)carbamate (3.4e)**



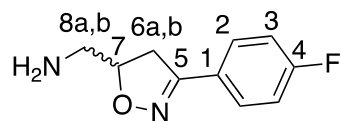
This compound was prepared from **3.3e** (8.0 mmol, 1.0 eq), *tert*-butyl *N*-allylcarbamate (8.0 mmol, 1.0 eq), and triethylamine (9.6 mmol, 1.2 eq) using General Protocol 3 to give the product as a light yellow solid. Yield: 17 %, 0.39 g. R_f = 0.32 (30% EtOAc in hexanes). Purity was 96 % based on HPLC, R_t = 24.8 minutes with Method A and R_t = 11.3 minutes with Method B (Table 6.1). ^1H NMR (500 MHz, CDCl_3): δ 7.33-7.19 (m, 5H, H-2, H-3 and H-4), 4.98 (s, 1H, N-H), 4.63 (m, 1H, H-8), 3.66 (s, 2H, H-5), 3.33 (m, 1H, 7a), 3.19 (m, 1H, H-7b), 2.86 (dd, J = 17.3, 10.6 Hz, 1H, H-9a), 2.56 (dd, J = 17.3, 7.4 Hz, 1H, H-9b), 1.41 (s, 9H, H-12). ^{13}C NMR (125 MHz, CDCl_3): δ 158.4, 156.3, 135.6, 129.0, 128.9, 127.3, 79.7, 79.3, 43.6, 39.0, 34.2, 28.4. HRMS for $\text{C}_{16}\text{H}_{22}\text{N}_2\text{O}_3\text{Na}$ $[\text{M}+\text{Na}]^+$ calcd. 313.1523, found 313.1527.

***tert*-Butyl((3-heptyl-4,5-dihydroisoxazol-5-yl)methyl)carbamate (3.4f)**



This known compound⁶⁷ was prepared from **3.3f** (9.0 mmol, 1.0 eq), *tert*-butyl *N*-allylcarbamate (9.0 mmol, 1.0 eq), and triethylamine (10.8 mmol, 1.2 eq) using General Protocol 3 to give the product as a light yellow oil. Yield: 25 %, 0.67 g. R_f = 0.34 (30% EtOAc in hexanes). Purity was 90 % based on HPLC, R_t = 28.1 minutes with Method A and R_t = 13.4 minutes with Method B (Table 6.1). The compound characterization agreed with previously reported literature.⁶⁷ ^1H NMR (500 MHz, CDCl_3): δ 4.90 (bs, 1H, N-H), 4.62 (m, 1H, H-10), 3.34 (m, 1H, H-11a), 3.23 (dt, J = 14.2, 6.1 Hz, 1H, H-11b), 2.95 (dd, J = 17.2, 10.5 Hz, 1H, H-9a), 2.67 (dd, J = 17.2, 7.2 Hz, 1H, H-9b), 2.30 (t, J = 7.7 Hz, 2H, H-2), 1.52 (p, J = 7.5 Hz, 2H, H-3), 1.42 (s, 9H, H-14), 1.31-1.24 (m, 8H, H-4, H-5, H-6 and H-7), 0.86 (t, J = 7.1 Hz, H-8). ^{13}C NMR (125 MHz, CDCl_3): δ 159.6, 156.4, 79.7, 78.8, 43.7, 39.6, 31.8, 29.3, 29.0, 28.4, 27.7, 26.5, 22.7, 14.2. HRMS for $\text{C}_{16}\text{H}_{30}\text{N}_2\text{O}_3\text{Na}$ $[\text{M}+\text{Na}]^+$ calcd. 321.2149, found 321.2143.

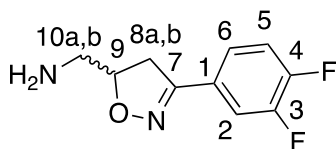
(3-(4-Fluorophenyl)-4,5-dihydroisoxazol-5-yl)methanamine (3.5a)



This compound was prepared from **3.4a** (3.0 mmol, 1.0 eq), and trifluoroacetic acid (30.0 mmol, 10.0 eq) using General Protocol 4 to give the product as a light orange semi-solid. Crude yield: 0.72 g. R_f = 0.04 (100 % EtOAc). Purity was 97 % based on HPLC, R_t = 8.5 minutes with Method C and R_t = 6.4 minutes with Method D (Table 6.2). ^1H NMR (500 MHz, MeOD): δ 7.73 (dd, J = 8.3, 5.2 Hz, 2H, H-2), 7.17 (t, J = 8.8 Hz, 2H, H-3), 4.77 (dddd, J = 10.6, 7.5, 6.4, 4.7 Hz, 1H, H-7), 3.47 (dd, J = 17.0, 10.6 Hz, 1H, H-8a), 3.19 (dd, J = 17.1, 7.6 Hz, 1H, H-6a), 2.84 (m, 2H, H-6b and H-8b). ^{13}C NMR (125 MHz, d_6 -DMSO): δ 162.9 (d, $J_{\text{C-F}}$ = 247.6 Hz), 155.7, 128.8 (d, $J_{\text{C-F}}$ = 8.6 Hz), 126.3 (d, $J_{\text{C-F}}$ = 3.2 Hz), 115.8 (d, $J_{\text{C-F}}$ = 21.7 Hz), 82.6, 44.9, 36.9. ^{19}F NMR (471 MHz,

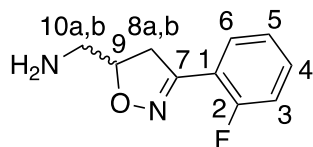
MeOD): δ -112.40 (tt, J = 8.6, 5.6 Hz). HRMS for $C_{10}H_{12}FN_2O$ $[M+H]^+$ calcd. 195.0928, found 195.0931.

(3-(3,4-Difluorophenyl)-4,5-dihydroisoxazol-5-yl)methanamine (3.5b)



This compound was prepared from **3.4b** (3.0 mmol, 1.0 eq), and trifluoroacetic acid (30.0 mmol, 10.0 eq) using General Protocol 4 to give the product as a dark orange semi-solid. Crude yield: 0.93 g. R_f = 0.07 (100 % EtOAc). Purity was 99 % based on HPLC, R_t = 8.4 minutes with Method C and R_t = 6.4 minutes with Method D (Table 6.2). 1H NMR (500 MHz, d_6 -DMSO): δ 7.85 (ddd, J = 11.9, 7.8, 2.0 Hz, 1H, H-2), 7.65-7.74 (m, 2H, H-5 and H-6), 4.85 (ddt, J = 10.6, 7.6, 5.2 Hz, 1H, H-9), 3.54 (m, 2H, H-8a and H-8b), 3.38 (m, 2H, H-10a and H-10b), 2.87 (bs, 2H, N-H). ^{13}C NMR (125 MHz, d_6 -DMSO): δ 155.3, 150.9 (dd, J_{C-F} = 249.4, 12.8 Hz), 148.9 (dd, J_{C-F} = 246.2, 13.2 Hz), 127.4 (dd, J_{C-F} = 6.5, 3.7 Hz), 123.8 (dd, J_{C-F} = 6.9, 3.6 Hz), 118.1 (d, J_{C-F} = 17.7 Hz), 115.5 (d, J_{C-F} = 18.4 Hz), 83.1, 44.8, 36.7. ^{19}F NMR (471 MHz, d_6 -DMSO): δ -136.36 (m), -137.80 (m). HRMS for $C_{10}H_{11}F_2N_2O$ $[M+H]^+$ calcd. 213.0834, found 213.0830.

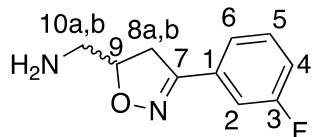
(3-(2-Fluorophenyl)-4,5-dihydroisoxazol-5-yl)methanamine (3.5c)



This compound was prepared from **3.4c** (4.0 mmol, 1.0 eq), and trifluoroacetic acid (40.0 mmol, 10.0 eq) using General Protocol 4 to give the product as a dark orange oil. Crude yield: 0.58 g. R_f = 0.36 (10 % methanol in DCM). Purity was 94 % based on HPLC, R_t = 8.3 minutes with Method C and R_t = 6.4 minutes with Method D (Table 6.2). 1H NMR (500 MHz, $CDCl_3$): δ 7.82 (td, J = 7.7, 1.8 Hz, 1H, H-5), 7.37 (dddd, J = 8.4, 7.8, 5.2, 1.8 Hz, 1H, H-4), 7.16 (m, 1H, H-6), 7.09 (ddd, J = 11.4, 8.3, 1.6 Hz, 1H, H-3), 4.78 (m, 1H, H-9), 3.46 (ddd, J = 17.3, 10.6, 2.4, 1H, H-10a), 3.21 (ddd, J = 17.4, 7.7, 2.5 Hz, 1H, H-10a), 2.96-2.89 (m, 2H, H-8b and H-10b), 1.40 (bs, 2H, N-H). ^{13}C NMR

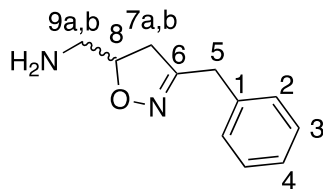
(125 MHz, CDCl₃): δ 160.5 (d, J = 252.3 Hz), 153.6 (d, J = 2.8 Hz), 131.8 (d, J = 8.7 Hz), 129.1 (d, J = 3.1 Hz), 124.6 (d, J = 3.3 Hz), 117.8 (d, J = 11.6 Hz), 116.5 (d, J = 22.2 Hz), 82.8, 45.7, 39.3. ¹⁹F NMR (471 MHz, CDCl₃): δ -112.60 (m). HRMS for C₁₀H₁₂FN₂O [M+H]⁺ calcd. 195.0928, found 195.0931.

(3-(3-Fluorophenyl)-4,5-dihydroisoxazol-5-yl)methanamine (3.5d)



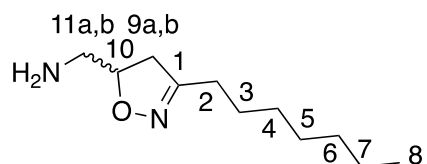
This compound was prepared from **3.4d** (4.0 mmol, 1.0 eq), and trifluoroacetic acid (40.0 mmol, 10.0 eq) using General Protocol 4 to give the product as a light orange oil. Crude yield: 1.11 g. R_f = 0.32 (10 % methanol in DCM). Purity was 50 % based on HPLC, R_t = 8.3 minutes with Method C and R_t = 6.3 minutes with Method D (Table 6.2). ¹H NMR (500 MHz, CDCl₃): δ 7.43-7.34 (m, 3H, H-2, H-5 and H-6), 7.09 (m, 1H, H-4), 4.81 (m, 1H, H-9), 3.35 (dd, J = 16.6, 10.7, 1H, H-8a) 3.13 (dd, J = 16.6, 7.7 Hz, 1H, H-8b), 3.01 (m, 1H, H-10a), 2.89 (m, 1H, H-10b), 1.32 (bs, 2H, N-H). ¹³C NMR (125 MHz, CDCl₃): δ 162.9 (d, J_{C-F} = 246.7 Hz), 156.0 (d, J_{C-F} = 2.9 Hz), 131.8 (d, J_{C-F} = 8.2 Hz), 130.4 (d, J_{C-F} = 8.3 Hz), 122.5 (d, J_{C-F} = 3.1 Hz), 117.1 (d, J_{C-F} = 21.4 Hz), 113.6 (d, J_{C-F} = 23.0 Hz), 82.9, 45.6, 37.3. ¹⁹F NMR (471 MHz, CDCl₃): δ -112.25 (m). HRMS for C₁₀H₁₂FN₂O [M+H]⁺ calcd. 195.0928, found 195.0921.

(3-Benzyl-4,5-dihydroisoxazol-5-yl)methanamine (3.5e)



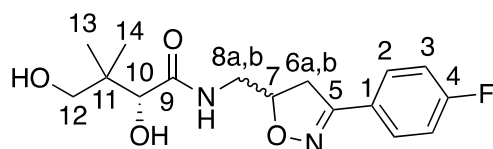
This compound was prepared from **3.4e** (1.0 mmol, 1.0 eq), and trifluoroacetic acid (10.0 mmol, 10.0 eq) using General Protocol 4 to give the product as a light orange oil. Crude yield: 0.44 g. It was used directly in the next step.

(3-Heptyl-4,5-dihydroisoxazol-5-yl)methanamine (3.5f)



This compound was prepared from **3.4f** (1.5 mmol, 1.0 eq), and trifluoroacetic acid (15.0 mmol, 10.0 eq) using General Protocol 4 to give the product as an orange oil. Crude yield: 0.41 g. It was used directly in the next step.

(2R)-N-((3-(4-Fluorophenyl)-4,5-dihydroisoxazol-5-yl)methyl)-2,4-dihydroxy-3,3-dimethylbutanamide (3a)

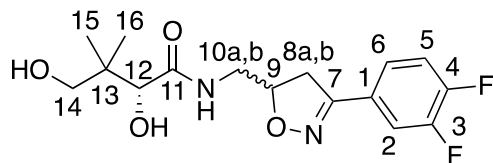


This compound was prepared from **3.5a** (2.8 mmol, 1.0 eq), D-pantolactone (5.5 mmol, 2.0 eq), and triazabicyclodecene (0.3 mmol, 0.1 eq) using General Protocol 4 to give the product as a dark yellow oil. Yield: 39 %, 0.34 g. R_f = 0.59 (10 % methanol in DCM).

Purity was 99 % based on HPLC, R_t = 17.5 minutes with Method A and R_t = 8.7 minutes with Method B (Table 6.1). ^1H NMR (500 MHz, CDCl_3) Diastereomer 1: δ 7.61 (dd, J = 8.7, 5.4 Hz, 2H, H-2), 7.31 (bs, 1H, NH), 7.07 (t, J = 8.6 Hz, 2H, H-3), 4.88 (m, 1H, H-7), 4.13 (bs, 1H, OH), 4.06 (s, 1H, H-10), 3.60 (m, 2H, H-12), 3.47 (m, 2H, H-8a and H-8b), 3.42 (dd, J = 8.7, 6.1 Hz, 1H, H-6a), 3.10 (dd, J = 7.4, 5.3 Hz, 1H, H-6b), 0.95 (s, 3H, H-13), 0.86 (s, 3H, H-14). ^1H NMR (500 MHz, CDCl_3) Diastereomer 2: δ 7.61 (dd, J = 8.7, 5.4 Hz, 2H, H-2), 7.31 (bs, 1H, NH), 7.07 (t, J = 8.6 Hz, 2H, H-3), 4.88 (m, 1H, H-7), 4.13 (bs, 1H, OH), 4.04 (s, 1H, H-10), 3.60 (m, 2H, H-12), 3.47 (m, 2H, H-8a and H-8b), 3.39 (dd, J = 10.6, 7.9 Hz, 1H, H-6a), 3.07 (dd, J = 7.4, 5.3 Hz, 1H, H-6b), 0.95 (s, 3H, H-13), 0.86 (s, 3H, H-14). ^{13}C NMR (125 MHz, CDCl_3) Diastereomer 1: δ 174.2, 164.0 (d, $J_{\text{C-F}}$ = 251.4), 156.2, 128.8 (d, $J_{\text{C-F}}$ = 3.3 Hz), 125.4 (t, $J_{\text{C-F}}$ = 3.3 Hz), 116.2 (d, $J_{\text{C-F}}$ = 2.7 Hz), 79.9, 77.7, 71.3, 42.3, 39.4, 38.1, 21.3, 20.5. ^{13}C NMR (125 MHz, CDCl_3) Diastereomer 2: δ 174.0, 164.0 (d, $J_{\text{C-F}}$ = 251.3), 156.1, 128.8 (d, $J_{\text{C-F}}$ = 3.5 Hz), 125.4 (t, $J_{\text{C-F}}$ = 3.3 Hz), 116.0 (d, $J_{\text{C-F}}$ = 2.7 Hz), 79.9, 77.7, 71.3, 42.2, 39.3, 38.0, 21.3, 20.3. ^{19}F NMR (471 MHz, CDCl_3) Diastereomer 1: δ -109.27 (tt, J = 8.7, 5.3 Hz). ^{19}F NMR (471

MHz, CDCl₃) Diastereomer 2: δ –109.33 (tt, J = 8.5, 5.1 Hz). HRMS for C₁₆H₂₁FN₂O₄Na [M+Na]⁺ calcd. 347.1378, found 347.1389.

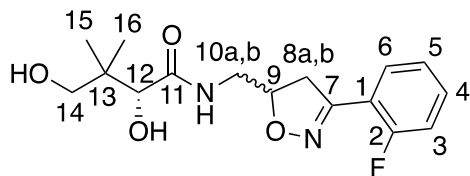
(2*R*)-*N*-((3-(3,4-Difluorophenyl)-4,5-dihydroisoxazol-5-yl)methyl)-2,4-dihydroxy-3,3-dimethylbutanamide (3b)



This compound was prepared from **3.5b** (2.8 mmol, 1.0 eq), D-pantolactone (5.5 mmol, 2.0 eq), and triazabicyclodecene (0.3 mmol, 0.1 eq) using General Protocol 4 to give the product as a yellow semi-solid. Yield: 39 %, 0.37 g. R_f = 0.66 (10 % methanol in DCM). Purity was 98 % based on HPLC, R_t = 18.2 minutes with Method A and R_t = 9.1 minutes with Method B (Table 6.2). ¹H NMR (500 MHz, CDCl₃) Diastereomer 1: δ 7.51 (ddd, J = 11.0, 7.5, 2.1 Hz, 1H, H-2), 7.31 (m, 1H, H-6), 7.25 (bs, 1H, O-H), 7.19 (m, 1H, H-5), 4.91 (m, 1H, H-9), 4.06 (s, 1H, H-12), 3.99 (bs, 1H, N-H), 3.68 (m, 1H, H-10a), 3.58 (m, 1H, H-10b), 3.49 (m, 2H, H-14), 3.40 (dd, J = 10.9, 6.8 Hz, 1H, H-8a), 3.09 (dd, J = 10.8, 6.1 Hz, 1H, H-8b), 1.00 (s, 3H, H-15), 0.91 (s, 3H, H-16). ¹H NMR (500 MHz, CDCl₃) Diastereomer 2: δ 7.51 (ddd, J = 11.0, 7.5, 2.1 Hz, 1H, H-2), 7.31 (m, 1H, H-6), 7.25 (bs, 1H, O-H), 7.19 (m, 1H, H-5), 4.91 (m, 1H, H-9), 4.04 (s, 1H, H-12), 3.99 (bs, 1H, N-H), 3.65 (m, 1H, H-10a), 3.58 (m, 1H, H-10b), 3.49 (m, 2H, H-14), 3.37 (dd, J = 10.7, 6.6 Hz, 1H, H-8a), 3.06 (dd, J = 10.8, 6.0 Hz, 1H, H-8b), 0.92 (s, 3H, H-15), 0.83 (s, 3H, H-16). ¹³C NMR (125 MHz, CDCl₃) Diastereomer 1: δ 174.0, 155.5, 152.2 (dd, J_{C-F} = 251.8, 3.6 Hz), 150.6 (dd, J_{C-F} = 247.8, 1.3 Hz), 126.4 (dd, J_{C-F} = 3.5, 2.2 Hz), 123.4 (dd, J_{C-F} = 3.6, 2.2 Hz), 117.9 (d, J_{C-F} = 2.7 Hz), 115.9 (d, J_{C-F} = 6.2 Hz), 80.3, 77.9, 71.4, 42.2, 39.4, 37.8, 21.3, 20.5. ¹³C NMR (125 MHz, CDCl₃) Diastereomer 2: δ 173.9, 155.4, 151.6 (dd, J_{C-F} = 252.0, 3.5 Hz), 150.5 (dd, J_{C-F} = 248.6, 1.3 Hz), 126.3 (dd, J_{C-F} = 3.7, 2.7 Hz), 123.3 (dd, J_{C-F} = 3.3, 2.4 Hz), 117.9 (d, J_{C-F} = 2.7 Hz), 115.7 (d, J_{C-F} = 6.3 Hz), 80.2, 77.9, 71.4, 42.2, 39.3, 37.7, 21.2, 20.3. ¹⁹F NMR (471 MHz, CDCl₃): δ –133.85 (m), –136.01 (m).

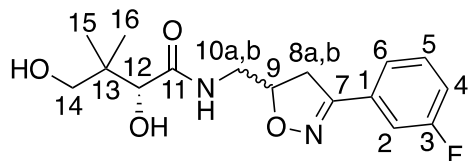
HRMS for C₁₆H₂₀F₂N₂O₄Na [M+Na]⁺ calcd. 365.1283, found 365.1270.

(2*R*)-*N*-((3-(2-Fluorophenyl)-4,5-dihydroisoxazol-5-yl)methyl)-2,4-dihydroxy-3,3-dimethylbutanamide (3c)



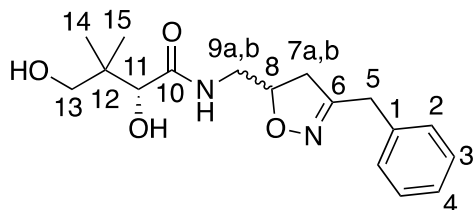
This compound was prepared from **3.5c** (2.4 mmol, 1.0 eq), D-pantolactone (4.8 mmol, 2.0 eq), and triazabicyclodecene (0.2 mmol, 0.1 eq) using General Protocol 4 to give the product as a viscous, amber-coloured oil. Yield: 57 %, 0.44 g. R_f = 0.76 (10 % methanol in DCM). Purity was 98 % based on HPLC, R_t = 17.4 minutes with Method A and R_t = 8.7 minutes with Method B (Table 6.1). ^1H NMR (500 MHz, CDCl_3) Diastereomer 1: δ 7.76 (m, 1H, H-5), 7.39 (m, 1H, H-4), 7.29 (bs, 1H, O-H), 7.16 (m, 1H, H-3), 7.10 (dd, J = 11.4, 1.1 Hz, 1H, H-6), 4.88 (m, 1H, H-9), 4.07 (m, 1H, H-12), 3.65 (m, 1H, H-8a), 3.54 (m, 1H, H-10a), 3.48 (m, 2H, H-14), 3.45 (m, 1H, H-10b), 3.40 (s, 1H, O-H), 3.20 (m, 1H, H-8b), 1.01 (s, 3H, H-15), 0.92 (s, 3H, H-16). ^1H NMR (500 MHz, CDCl_3) Diastereomer 2: δ 7.76 (m, 1H, H-5), 7.39 (m, 1H, H-4), 7.29 (bs, 1H, O-H), 7.16 (m, 1H, H-3), 7.10 (dd, J = 11.4, 1.1 Hz, 1H, H-6), 4.88 (m, 1H, H-9), 4.07 (m, 1H, H-12), 3.65 (m, 1H, H-10a), 3.54 (m, 1H, H-8a), 3.48 (m, 2H, H-14), 3.45 (m, 1H, H-10b), 3.40 (s, 1H, O-H), 3.16 (m, 1H, H-8b), 0.95 (s, 3H, H-15), 0.85 (s, 3H, H-16). ^{13}C NMR (125 MHz, CDCl_3) Diastereomer 1: δ 174.0, 160.5 (d, $J_{\text{C-F}}$ = 253.0 Hz), 153.9 (d, $J_{\text{C-F}}$ = 3.0 Hz), 132.1 (d, $J_{\text{C-F}}$ = 8.6 Hz), 129.1 (d, $J_{\text{C-F}}$ = 3.5 Hz), 124.7 (d, $J_{\text{C-F}}$ = 3.2 Hz), 117.3 (d, $J_{\text{C-F}}$ = 1.5 Hz), 116.7, 77.9, 77.8, 71.3, 42.2, 39.7, 39.4, 21.4, 20.5. ^{13}C NMR (125 MHz, CDCl_3) Diastereomer 2: δ 173.9, 160.5 (d, $J_{\text{C-F}}$ = 253.0 Hz), 153.9 (d, $J_{\text{C-F}}$ = 3.2 Hz), 132.1 (d, $J_{\text{C-F}}$ = 8.6 Hz), 129.0 (d, $J_{\text{C-F}}$ = 3.3 Hz), 124.6 (d, $J_{\text{C-F}}$ = 3.3 Hz), 117.2 (d, $J_{\text{C-F}}$ = 1.0 Hz), 116.5, 77.8, 77.7, 71.3, 42.1, 39.6, 39.3, 21.4, 20.3. ^{19}F NMR (471 MHz, CDCl_3) Diastereomer 1: δ -111.91 (m). ^{19}F NMR (471 MHz, CDCl_3) Diastereomer 2: δ -111.98 (m). HRMS for $\text{C}_{16}\text{H}_{21}\text{FN}_2\text{O}_4\text{Na}$ $[\text{M}+\text{Na}]^+$ calcd. 347.1378, found 347.1370.

(2*R*)-*N*-((3-(3-Fluorophenyl)-4,5-dihydroisoxazol-5-yl)methyl)-2,4-dihydroxy-3,3-dimethylbutanamide (3d)



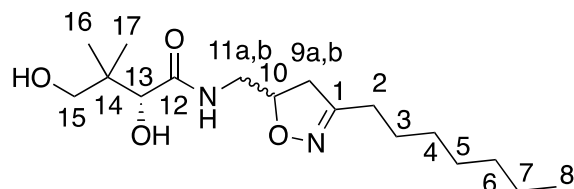
This compound was prepared from **3.5d** (3.2 mmol, 1.0 eq), D-pantolactone (6.4 mmol, 2.0 eq), and triazabicyclodecene (0.3 mmol, 0.1 eq) using General Protocol 4 to give the product as an off-white semi-solid. Yield: 47 %, 0.48 g. R_f = 0.62 (10 % methanol in DCM). Purity was 98 % based on HPLC, R_t = 17.9 minutes with Method A and R_t = 9.0 minutes with Method B (Table 6.1). ^1H NMR (500 MHz, CDCl_3) Diastereomer 1: δ 7.37-7.34 (m, 3H, H-2 and H-5 and H-6), 7.30 (bs, 1H, O-H), 7.11 (m, 1H, H-4), 4.91 (m, 1H, H-9), 4.13 (d, J = 5.0 Hz, 1H, N-H), 4.06 (d, J = 4.6 Hz, 1H, H-12), 3.61 (m, 1H, H-10a), 3.54 (m, 1H, H-10b), 3.46 (m, 2H, H-14), 3.43-3.37 (m, 2H, H-8a and O-H), 3.10 (dd, J = 12.5, 5.0 Hz, 1H, H-8b), 1.00 (s, 3H, H-15), 0.90 (s, 3H, H-16). ^1H NMR (500 MHz, CDCl_3) Diastereomer 2: δ 7.37-7.34 (m, 3H, H-2 and H-5 and H-6), 7.30 (bs, 1H, O-H), 7.11 (m, 1H, H-4), 4.91 (m, 1H, H-9), 4.09 (d, J = 5.0 Hz, 1H, N-H), 4.04 (d, J = 4.6 Hz, 1H, H-12), 3.61 (m, 1H, H-10a), 3.54 (m, 1H, H-10b), 3.46 (m, 2H, H-14), 3.43-3.37 (m, 2H, H-8a and O-H), 3.07 (dd, J = 11.9, 4.9 Hz, 1H, H-8b), 0.92 (s, 3H, H-15), 0.83 (s, 3H, H-16). ^{13}C NMR (125 MHz, CDCl_3) Diastereomer 1: δ 174.1, 162.9 (d, $J_{\text{C-F}}$ = 246.4 Hz), 156.3 (d, $J_{\text{C-F}}$ = 3.0 Hz), 131.3 (d, $J_{\text{C-F}}$ = 2.8 Hz), 130.6 (d, $J_{\text{C-F}}$ = 2.8 Hz), 122.6 (d, $J_{\text{C-F}}$ = 2.7 Hz), 117.6 (d, $J_{\text{C-F}}$ = 21.4 Hz), 113.7 (d, $J_{\text{C-F}}$ = 23.1 Hz), 80.1, 77.8, 71.3, 42.2, 39.4, 37.8, 21.3, 20.5. ^{13}C NMR (125 MHz, CDCl_3) Diastereomer 2: δ 174.0, 162.9 (d, $J_{\text{C-F}}$ = 246.4 Hz), 156.2 (d, $J_{\text{C-F}}$ = 2.9 Hz), 131.2 (d, $J_{\text{C-F}}$ = 2.9 Hz), 130.5 (d, $J_{\text{C-F}}$ = 2.8 Hz), 122.6 (d, $J_{\text{C-F}}$ = 2.7 Hz), 117.4 (d, $J_{\text{C-F}}$ = 21.4 Hz), 113.5 (d, $J_{\text{C-F}}$ = 23.1 Hz), 80.0, 77.8, 71.3, 42.2, 39.3, 37.8, 21.3, 20.3. ^{19}F NMR (471 MHz, CDCl_3) Diastereomer 1: δ -111.83 (m). ^{19}F NMR (471 MHz, CDCl_3) Diastereomer 2: δ -111.90 (m). HRMS for $\text{C}_{16}\text{H}_{21}\text{FN}_2\text{O}_4\text{Na}$ $[\text{M}+\text{Na}]^+$ calcd. 347.1378, found 347.1380.

(2*R*)-*N*-((3-Benzyl-4,5-dihydroisoxazol-5-yl)methyl)-2,4-dihydroxy-3,3-dimethylbutanamide (3e)



This compound was prepared from **3.5e** (0.8 mmol, 1.0 eq), D-pantolactone (1.6 mmol, 2.0 eq), and triazabicyclodecene (0.08 mmol, 0.1 eq) using General Protocol 4 to give the product as a yellow semi-solid. Yield: 29 %, 0.07 g. R_f = 0.48 (10 % methanol in DCM). Purity was 99 % based on HPLC, R_t = 17.2 minutes with Method A and R_t = 8.5 minutes with Method B (Table 6.1). ^1H NMR (500 MHz, CDCl_3) Diastereomer 1: δ 7.32 (m, 2H, H-2), 7.27 (m, 1H, H-4), 7.21 (tt, J = 7.6, 1.6 Hz, 2H, H-3), 4.66 (m, 1H, H-8), 4.03 (s, 1H, H-11), 3.65 (m, 2H, H-5), 3.51 (m, 1H, H-9a), 3.47 (m, 2H, H-13), 3.34 (m, 1H, H-9b), 2.93 (dd, J = 10.6, 8.0 Hz, H-7a), 2.57 (m, H-7b), 0.99 (s, 3H, H-14), 0.89 (s, 3H, H-15). ^1H NMR (500 MHz, CDCl_3) Diastereomer 2: δ 7.32 (m, 2H, H-2), 7.27 (m, 1H, H-4), 7.21 (t, J = 7.6, 1.6 Hz, 2H, H-3), 4.66 (m, 1H, H-8), 3.92 (s, 1H, H-11), 3.64 (m, 2H, H-5), 3.51 (m, 1H, H-9a), 3.47 (m, 2H, H-13), 3.31 (m, 1H, H-9b), 2.91 (dd, J = 10.5, 7.8 Hz, H-7a), 2.55 (m, 1H, H-7b), 0.98 (s, 3H, H-14), 0.87 (s, 3H, H-15). ^{13}C NMR (125 MHz, CDCl_3) Diastereomer 1: δ 173.9, 158.7, 135.5, 129.1, 128.9, 127.4, 79.0, 77.8, 77.4, 71.3, 42.1, 39.4, 34.2, 21.6, 20.4. ^{13}C NMR (125 MHz, CDCl_3) Diastereomer 2: δ 173.8, 158.7, 135.4, 129.1, 128.9, 127.4, 78.9, 77.5, 77.4, 71.2, 42.0, 39.4, 34.2, 21.5, 20.3. HRMS for $\text{C}_{17}\text{H}_{24}\text{N}_2\text{O}_4\text{Na}$ $[\text{M}+\text{Na}]^+$ calcd. 343.1628, found 343.1629.

(2*R*)-*N*-((3-Heptyl-4,5-dihydroisoxazol-5-yl)methyl)-2,4-dihydroxy-3,3-dimethylbutanamide (3f)



This known compound⁶⁶ was prepared from **3.5f** (1.5 mmol, 1.0 eq), D-pantolactone (3.0 mmol, 2.0 eq), and triazabicyclodecene (0.2 mmol, 0.1 eq) using General Protocol 4 to give the product as a yellow semi-solid. Yield: 36 %, 0.18 g. R_f = 0.59 (10 % methanol in DCM). Purity was 95 % based on HPLC, R_t = 22.1 minutes with Method A and R_t = 10.5 minutes with Method B (Table 6.1). The compound characterization agreed with previously reported literature.⁶⁶ ¹H NMR (500 MHz, CDCl₃) Diastereomer 1: δ 7.29 (t, J = 6.2 Hz, 1H, N-H), 4.65 (dddd, J = 18.2, 10.7, 6.9, 3.4 Hz, 1H, H-10), 4.38 (bs, 1H, O-H), 4.04 (d, J = 5.4 Hz, 1H, H-13), 3.74 (bs, 1H, O-H), 3.55 (m, 1H, H-11a), 3.47 (s, 2H, H-15), 3.34 (m, 1H, H-11b), 3.02 (dd, J = 10.6, 1.7 Hz, 1H, H-9a), 2.66 (m, 1H, H-9b), 2.28 (m, 2H, H-2), 1.52 (p, J = 7.4 Hz, 2H, H-3), 1.28 (m, 8H, H-4, H-5, H-6 and H-7), 0.99 (s, 3H, H-16), 0.91 (s, 3H, H-17), 0.86 (t, J = 7.1 Hz, 3H, H-8). ¹H NMR (500 MHz, CDCl₃) Diastereomer 2: δ 7.29 (t, J = 6.2 Hz, 1H, N-H), 4.65 (dddd, J = 18.2, 10.7, 6.9, 3.4 Hz, 1H, H-10), 4.38 (bs, 1H, O-H), 4.03 (d, J = 5.2 Hz, 1H, H-13), 3.74 (bs, 1H, O-H), 3.55 (m, 1H, H-11a), 3.47 (s, 2H, H-15), 3.19 (m, 1H, H-11b), 3.00 (dd, J = 10.6, 1.5 Hz, 1H, H-9a), 2.62 (m, 1H, H-9b), 2.28 (m, 2H, H-2), 1.52 (p, J = 7.4 Hz, 2H, H-3), 1.28 (m, 8H, H-4, H-5, H-6 and H-7), 0.98 (s, 3H, H-16), 0.89 (s, 3H, H-17), 0.86 (t, J = 7.1 Hz, 3H, H-8). ¹³C NMR (125 MHz, CDCl₃) Diastereomer 1: δ 174.2, 159.9, 78.4, 77.4, 71.2, 42.3, 40.2, 39.4, 31.7, 29.3, 29.0, 27.8, 26.4, 22.7, 21.5, 20.6, 14.2. ¹³C NMR (125 MHz, CDCl₃) Diastereomer 2: δ 174.0, 159.8, 78.2, 77.4, 71.1, 42.1, 40.2, 39.3, 31.7, 29.3, 29.0, 27.7, 26.4, 22.7, 21.3, 20.3, 14.2. HRMS for C₁₇H₃₂N₂O₄Na [M+Na]⁺ calcd. 351.2254, found 351.2248.

6.2. Biology

6.2.1. Materials

Bacterial strains included *Acinetobacter baumannii* (ATCC 19606), *Escherichia coli* (ATCC 25922), *Klebsiella pneumoniae* (ATCC 13883), *Pseudomonas aeruginosa* (ATCC 27853), *Staphylococcus aureus* (ATCC 29213), and *Salmonella enterica* ser. Typhimurium (ATCC 14028) and were all purchased from Cedarlane. *A. baumannii*, *E. coli*, and *K. pneumoniae* were grown on Difco™ Nutrient Agar and cultured in Difco™ Nutrient Broth. *P. aeruginosa*, *S. aureus*, and *S. Typhimurium* were grown on Difco™ Nutrient Agar and cultured in Fischer BioReagents™ LB Broth. Cation-adjusted Mueller Hinton Broth (CAMHB) was prepared accordingly to the protocol found in the Clinical and Laboratory Standards Institute (CLSI).⁹⁰ CAMHB is the standard medium used to perform susceptibility tests and is used in the experiments performed in this thesis.⁹¹ A Molecular Devices Spectra i3x multi-mode microtiter plate reader was used to measure the absorbance at 600 nm (OD₆₀₀).

6.2.2. Antimicrobial Susceptibility Test

The CLSI's M07 broth microdilution method⁹¹ was used at one concentration (50 µm) to determine the susceptibility of different bacteria to the compounds included in this thesis. To determine the concentration of bacteria from OD₆₀₀, a calibration curve was prepared. The calibration curve is expressed as a linear relationship such that $OD_{600} = mx + b$ where x is the concentration of bacteria (CFU/mL) and OD₆₀₀ is the optical density of bacteria at 600 nm (Table 6.3).

Table 6.3: Linear equations for each bacterial strain used to determine bacteria concentration.

Bacteria	Linear Calibration Equation
<i>A. baumannii</i>	$OD_{600} = 7 \times 10^{-10}x + 0.1$
<i>E. coli</i>	$OD_{600} = 3 \times 10^{-9}x + 0.3$
<i>K. pneumonia</i>	$OD_{600} = 4 \times 10^{-9}x + 0.1$
<i>P. aeruginosa</i>	$OD_{600} = 7 \times 10^{-10}x + 0.2$
<i>S. aureus</i>	$OD_{600} = 2 \times 10^{-9}x + 0.1$
<i>S. enterica</i> ser. Typhimurium	$OD_{600} = 2 \times 10^{-9}x$

To perform the antimicrobial susceptibility tests for each compound, bacteria strains were first allowed to grow on their corresponding agar medium at 37 °C for 18 hours. Then, 5 colonies from the agar culture were added to 5 mL of the appropriate media listed above and allowed to grow to stationary phase at 37 °C, 250 rpm over the course of 18 hours. Next, 60 µL of the bacteria grown to stationary phase was then added to 6 mL of CAMHB before incubation at 37 °C, 250 rpm until a bacterial concentration of 1×10^8 CFU/mL was achieved. In a 96-well plate, 50 µL containing the compound of interest (100 µM) in CAMHB were added to each well. Erythromycin and chloramphenicol (100 µM) were used as positive controls in place of the compound of interest. A PanMC (100 µM) that has been previously shown to have no activity against any strain of bacteria was used as a negative control (Figure 6.1).⁶⁷

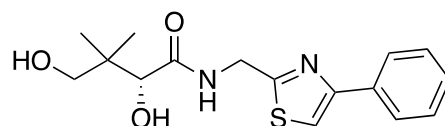


Figure 6.1: The structure of the PanMC used as a negative control.⁶⁷

Once the bacterial cultures had reached an OD_{600} that correlated to 1×10^8 CFU/mL, the culture was diluted to 1×10^6 CFU/mL in CAMHB. From here, 50 µL of the diluted

culture was then added to all wells in the 96-well plate, such that the final concentration of bacteria in each well of the 96-well plate is 5×10^5 CFU/mL and the final concentration of compound is 50 μ M. The 96-well plate was then incubated at 37 °C, 250 rpm for 18 hours. The OD₆₀₀ was next measured to quantify growth.

To compute the percentage of bacterial growth in the presence of compound, the blank (containing only CAMHB and DMSO) was subtracted from all the data gained from wells containing the compound of interest. The resulting data from the compound of interest was averaged, and then divided by the average of the growth control (containing bacteria, CAMHB, and DMSO) and finally multiplied by 100. All experiments were performed in biological triplicate.

6.2.3. MIC Antibacterial Susceptibility Tests

The CLSI's M07 broth microdilution method⁹¹ was used to determine the susceptibility of *A. baumannii* and *S. aureus* to two PanMCs explored in this thesis. *A. baumannii* and *S. aureus* were allowed to grow on their corresponding agar medium at 37 °C for 18 hours. Then, 5 colonies from the agar mediums were submerged in 5 mL of the appropriate liquid media and allowed to grow to stationary phase at 37 °C, 250 rpm over 18 hours. Next, 60 μ L of the bacteria grown to stationary phase was then added to 6 mL of CAMHB before incubation at 37 °C, 250 rpm until a bacterial concentration of 1×10^8 CFU/mL was achieved.

In a 96-well plate, 100 μ L containing the compound of interest (100 mM) in CAMHB were added to 6 wells (3 wells per compound). All other wells were filled with 50 μ L of CAMHB. The compounds of interest were then serially diluted in the 96-well plate by transferring 50 μ L from the wells containing the compound of interest and depositing it the next column of wells over. This process was continued until all remaining wells in the 96-well plate contained diluted compound, and the 50 μ L from the last dilution was discarded, such that each well only contained 50 μ L of volume. Erythromycin and chloramphenicol (100 μ M) were used as positive controls in place of the compound of interest. A PanMC (100 μ M) that has been previously shown to have no activity against any strain of bacteria was used as a negative control (Figure 6.1).⁶⁷

Once the bacterial cultures had reached an OD₆₀₀ that correlated to 1×10^8 CFU/mL, the culture was diluted to 1×10^6 CFU/mL in CAMHB. From here, 50 μ L of the diluted culture was then added to all wells in the 96-well plate, such that the final concentration of bacteria in each well of the 96-well plate is 5×10^5 CFU/mL and the final concentration of compound is half of what it was to begin with (50 mM being the most concentrated). The 96-well plate was then incubated at 37 °C, 250 rpm for 18 hours. The OD₆₀₀ was next measured to quantify growth.

To compute the percentage bacterial growth in the presence of compound, the blank (containing only CAMHB and DMSO) was subtracted from all the data gained from wells containing the compound of interest. The resulting data from the compound of interest was averaged, and then divided by the average of the growth control (containing bacteria, CAMHB, and DMSO) and finally multiplied by 100. All experiments were performed in biological triplicate.

6.2.4. Antiplasmodial Activity

The antiplasmodial activity assays were performed by Xiangning Christine Liu under the supervision of Prof. Kevin Saliba at the Australian National University. These experiments entailed using a modified version of the malaria SYBR Green I-based fluorescence assay and testing the PanMCs at the intraerythrocytic stage of *P. falciparum* in pantetheinase active media.^{40,92}

References

1. van Seventer, J. M.; Hochberg, N. S. Principles of Infectious Diseases: Transmission, Diagnosis, Prevention, and Control. *International Encyclopedia of Public Health* **2017**, 22–39.
2. Zumla, A.; Memish, Z. A.; Maeurer, M.; Bates, M.; Mwaba, P.; Al-Tawfiq, J. A.; Denning, D. W.; Hayden, F. G.; Hui, D. S. Emerging Novel and Antimicrobial-Resistant Respiratory Tract Infections: New Drug Development and Therapeutic Options. *Lancet. Infect. Dis.* **2014**, 14 (11), 1136–1149.
3. Lee, B.-K.; Ryu, S.; Oh, S.-K.; Ahn, H.-J.; Jeon, S.-Y.; Jeong, W.-J.; Cho, Y.-C.; Park, J.-S.; You, Y.-H.; Kang, C.-S. Lactate Dehydrogenase to Albumin Ratio as a Prognostic Factor in Lower Respiratory Tract Infection Patients. *The American Journal of Emergency Medicine* **2021**, 52, 54–58.
4. Kyu, H. H.; Vongpradith, A.; Sirota, S. B.; Novotney, A.; Troeger, C. E.; Doxey, M. C.; Bender, R. G.; Ledesma, J. R.; Biehl, M. H.; Albertson, S. B.; Frostad, J. J.; Burkart, K.; Bennitt, F. B.; Zhao, J. T.; Gardner, W. M.; Hagins, H.; Bryazka, D.; Dominguez, R.-M. V.; Abate, S. M.; Abdelmasseh, M.; Abdoli, A.; Abdoli, G.; Abedi, A.; Abedi, V.; Abegaz, T. M.; Abidi, H.; Aboagye, R. G.; Abolhassani, H.; Abtew, Y. D.; Abubaker Ali, H.; Abu-Gharbieh, E.; Abu-Zaid, A.; Adamu, K.; Addo, I. Y.; Adegboye, O. A.; Adnan, M.; Adnani, Q. E. S.; Afzal, M. S.; Afzal, S.; Ahinkorah, B. O.; Ahmad, A.; Ahmad, A. R.; Ahmad, S.; Ahmadi, A.; Ahmadi, S.; Ahmed, H.; Ahmed, J. Q.; Ahmed Rashid, T.; Akbarzadeh-Khiavi, M.; Al Hamad, H.; Albano, L.; Aldeyab, M. A.; Alemu, B. M.; Alene, K. A.; Algammal, A. M.; Alhalaiqa, F. A. N.; Alhassan, R. K.; Ali, B. A.; Ali, L.; Ali, M. M.; Ali, S. S.; Alimohamadi, Y.; Alipour, V.; Al-Jumaily, A.; Aljunid, S. M.; Almustanyir, S.; Al-Raddadi, R. M.; Al-Rifai, R. H. H.; Alryalat, S. A. S.; Alvis-Guzman, N.; Alvis-Zakzuk, N. J.; Ameyaw, E. K.; Aminian Dehkordi, J. J.; Amuasi, J. H.; Amugsi, D. A.; Anbesu, E. W.; Ansar, A.; Anyasodor, A. E.; Arabloo, J.; Areda, D.; Argaw, A. M.; Argaw, Z. G.; Arulappan, J.; Aruleba, R. T.; Asemahagn, M. A.; Athari, S. S.; Atlaw, D.; Attia, E. F.; Attia, S.; Aujayeb, A.; Awoke, T.; Ayana, T. M.; Ayanore, M. A.; Azadnajafabad, S.; Azangou-Khyavy, M.; Azari, S.; Azari Jafari, A.; Badar, M.; Badiye, A. D.; Baghcheghi, N.; Bagherieh, S.; Baig, A. A.; Banach, M.; Banerjee, I.; Bardhan, M.; Barone-Adesi, F.; Barqawi, H. J.; Barrow, A.; Bashiri,

A.; Bassat, Q.; Batiha, A.-M. M.; Belachew, A. B.; Belete, M. A.; Belgaumi, U. I.;
 Bhagavathula, A. S.; Bhardwaj, N.; Bhardwaj, P.; Bhatt, P.; Bhojaraja, V. S.;
 Bhutta, Z. A.; Bhuyan, S. S.; Bijani, A.; Bitaraf, S.; Bodicha, B. B. A.; Briko, N. I.;
 Buonsenso, D.; Butt, M. H.; Cai, J.; Camargos, P.; Cámara, L. A.; Chakraborty,
 P. A.; Chanie, M. G.; Charan, J.; Chattu, V. K.; Ching, P. R.; Choi, S.; Chong, Y.
 Y.; Choudhari, S. G.; Chowdhury, E. K.; Christopher, D. J.; Chu, D.-T.; Cobb, N.
 L.; Cohen, A. J.; Cruz-Martins, N.; Dadras, O.; Dagnaw, F. T.; Dai, X.; Dandona,
 L.; Dandona, R.; Dao, A. T. M.; Debela, S. A.; Demisse, B.; Demisse, F. W.;
 Demissie, S.; Dereje, D.; Desai, H. D.; Desta, A. A.; Desye, B.; Dhingra, S.; Diao,
 N.; Diaz, D.; Digesa, L. E.; Doan, L. P.; Dodangeh, M.; Dongarwar, D.; Dorostkar,
 F.; Dos Santos, W. M.; Dsouza, H. L.; Dubljanin, E.; Durojaiye, O. C.; Edinur, H.
 A.; Ehsani-Chimeh, E.; Eini, E.; Ekholuenetale, M.; Ekundayo, T. C.; El Desouky,
 E. D.; El Sayed, I.; El Sayed Zaki, M.; Elhadi, M.; Elkhapery, A. M. R.; Emami, A.;
 Engelbert Bain, L.; Erkhembayar, R.; Etaee, F.; Ezati Asar, M.; Fagbamigbe, A.
 F.; Falahi, S.; Fallahzadeh, A.; Faraj, A.; Faraon, E. J. A.; Fatehizadeh, A.;
 Ferrara, P.; Ferrari, A. A.; Fetensa, G.; Fischer, F.; Flavel, J.; Foroutan, M.; Gaal,
 P. A.; Gaidhane, A. M.; Gaihre, S.; Galehdar, N.; Garcia-Basteiro, A. L.; Garg, T.;
 Gebrehiwot, M. D.; Gebremichael, M. A.; Gela, Y. Y.; Gemed, B. N. B.;
 Gessner, B. D.; Getachew, M.; Getie, A.; Ghamari, S.-H.; Ghasemi Nour, M.;
 Ghashghaee, A.; Gholamrezanezhad, A.; Gholizadeh, A.; Ghosh, R.; Ghozy, S.;
 Goleij, P.; Golitaleb, M.; Gorini, G.; Goulart, A. C.; Goyomsa, G. G.; Guadie, H.
 A.; Gudisa, Z.; Guled, R. A.; Gupta, S.; Gupta, V. B.; Gupta, V. K.; Guta, A.;
 Habibzadeh, P.; Haj-Mirzaian, A.; Halwani, R.; Hamidi, S.; Hannan, M. A.;
 Harorani, M.; Hasaballah, A. I.; Hasani, H.; Hassan, A. M.; Hassani, S.;
 Hassanian-Moghaddam, H.; Hassankhani, H.; Hayat, K.; Heibati, B.; Heidari, M.;
 Heyi, D. Z.; Hezam, K.; Holla, R.; Hong, S. H.; Horita, N.; Hosseini, M.-S.;
 Hosseinzadeh, M.; Hostiuc, M.; Househ, M.; Hoveidamanesh, S.; Huang, J.;
 Hussein, N. R.; Iavicoli, I.; Ibitoye, S. E.; Ikuta, K. S.; Ilesanmi, O. S.; Ilic, I. M.;
 Ilic, M. D.; Immurana, M.; Ismail, N. E.; Iwagami, M.; Jaafari, J.; Jamshidi, E.;
 Jang, S.-I.; Javadi Mamaghani, A.; Javaheri, T.; Javanmardi, F.; Javidnia, J.;
 Jayapal, S. K.; Jayarajah, U.; Jayaram, S.; Jema, A. T.; Jeong, W.; Jonas, J. B.;

Joseph, N.; Joukar, F.; Jozwiak, J. J.; K, V.; Kabir, Z.; Kacimi, S. E. O.; Kadashetti, V.; Kalankesh, L. R.; Kalhor, R.; Kamath, A.; Kamble, B. D.; Kandel, H.; Kanko, T. K.; Karaye, I. M.; Karch, A.; Karkhah, S.; Kassa, B. G.; Katoto, P. D.; Kaur, H.; Kaur, R. J.; Keikavoosi-Arani, L.; Keykhaei, M.; Khader, Y. S.; Khajuria, H.; Khan, E. A.; Khan, G.; Khan, I. A.; Khan, M.; Khan, M. N.; Khan, M. A.; Khan, Y. H.; Khatatbeh, M. M.; Khosravifar, M.; Khubchandani, J.; Kim, M. S.; Kimokoti, R. W.; Kisa, A.; Kisa, S.; Kisooson, N.; Knibbs, L. D.; Kochhar, S.; Kompani, F.; Koohestani, H. R.; Korshunov, V. A.; Kosen, S.; Koul, P. A.; Koyanagi, A.; Krishan, K.; Kuate Defo, B.; Kumar, G. A.; Kurmi, O. P.; Kuttikkattu, A.; Lal, D. K.; Lám, J.; Landires, I.; Ledda, C.; Lee, S.-W.; Levi, M.; Lewycka, S.; Liu, G.; Liu, W.; Lodha, R.; Lorenzovici, L.; Lotfi, M.; Loureiro, J. A.; Madadizadeh, F.; Mahmoodpoor, A.; Mahmoudi, R.; Mahmoudimanesh, M.; Majidpoor, J.; Makki, A.; Malakan Rad, E.; Malik, A. A.; Mallhi, T. H.; Manla, Y.; Matei, C. N.; Mathioudakis, A. G.; Maude, R. J.; Mehrabi Nasab, E.; Melese, A.; Memish, Z. A.; Mendoza-Cano, O.; Mentis, A.-F. A.; Meretoja, T. J.; Merid, M. W.; Mestrovic, T.; Micheletti Gomide Nogueira De Sá, A. C.; Mijena, G. F. W.; Minh, L. H. N.; Mir, S. A.; Mirfakhraie, R.; Mirmoeeni, S.; Mirza, A. Z.; Mirza, M.; Mirza-Aghazadeh-Attari, M.; Misganaw, A. S.; Misganaw, A. T.; Mohammadi, E.; Mohammadi, M.; Mohammed, A.; Mohammed, S.; Mohan, S.; Mohseni, M.; Moka, N.; Mokdad, A. H.; Momtazmanesh, S.; Monasta, L.; Moniruzzaman, M.; Montazeri, F.; Moore, C. E.; Moradi, A.; Morawska, L.; Mosser, J. F.; Mostafavi, E.; Motaghinejad, M.; Mousavi Isfahani, H.; Mousavi-Aghdas, S. A.; Mubarik, S.; Murillo-Zamora, E.; Mustafa, G.; Nair, S.; Nair, T. S.; Najafi, H.; Naqvi, A. A.; Narasimha Swamy, S.; Natto, Z. S.; Nayak, B. P.; Nejadghaderi, S. A.; Nguyen, H. V. N.; Niazi, R. K.; Nogueira De Sá, A. T.; Nouraei, H.; Nowroozi, A.; Nuñez-Samudio, V.; Nzoputam, C. I.; Nzoputam, O. J.; Oancea, B.; Ochir, C.; Odukoya, O. O.; Okati-Aliabad, H.; Okekunle, A. P.; Okonji, O. C.; Olagunju, A. T.; Olufadewa, I. I.; Omar Bali, A.; Omer, E.; Oren, E.; Ota, E.; Otstavnov, N.; Oulhaj, A.; P A, M.; Padubidri, J. R.; Pakshir, K.; Pakzad, R.; Palicz, T.; Pandey, A.; Pant, S.; Pardhan, S.; Park, E.-C.; Park, E.-K.; Pashazadeh Kan, F.; Paudel, R.; Pawar, S.; Peng, M.; Pereira, G.; Perna, S.; Perumalsamy, N.; Petcu, I.-R.;

Pigott, D. M.; Piracha, Z. Z.; Podder, V.; Polibin, R. V.; Postma, M. J.; Pourasghari, H.; Pourtaheri, N.; Qadir, M. M. F.; Raad, M.; Rabiee, M.; Rabiee, N.; Raeghi, S.; Rafiei, A.; Rahim, F.; Rahimi, M.; Rahimi-Movaghar, V.; Rahman, A.; Rahman, M. O.; Rahman, M.; Rahman, M. A.; Rahmani, A. M.; Rahmanian, V.; Ram, P.; Ramezanzadeh, K.; Rana, J.; Ranasinghe, P.; Rani, U.; Rao, S. J.; Rashedi, S.; Rashidi, M.-M.; Rasul, A.; Ratan, Z. A.; Rawaf, D. L.; Rawaf, S.; Rawassizadeh, R.; Razeghinia, M. S.; Redwan, E. M. M.; Reitsma, M. B.; Renzaho, A. M. N.; Rezaeian, M.; Riad, A.; Rikhtegar, R.; Rodriguez, J. A. B.; Rogowski, E. L. B.; Ronfani, L.; Rudd, K. E.; Saddik, B.; Sadeghi, E.; Saeed, U.; Safary, A.; Safi, S. Z.; Sahebazzamani, M.; Sahebkar, A.; Sakhamuri, S.; Salehi, S.; Salman, M.; Samadi Kafil, H.; Samy, A. M.; Santric-Milicevic, M. M.; Sao Jose, B. P.; Sarkhosh, M.; Sathian, B.; Sawhney, M.; Saya, G. K.; Seidu, A.-A.; Seylani, A.; Shaheen, A. A.; Shaikh, M. A.; Shaker, E.; Shamshad, H.; Sharew, M. M.; Sharhani, A.; Sharifi, A.; Sharma, P.; Sheidaei, A.; Shenoy, S. M.; Shetty, J. K.; Shiferaw, D. S.; Shigematsu, M.; Shin, J. I.; Shirzad-Aski, H.; Shivakumar, K. M.; Shivalli, S.; Shobeiri, P.; Simegn, W.; Simpson, C. R.; Singh, H.; Singh, J. A.; Singh, P.; Siwal, S. S.; Skryabin, V. Y.; Skryabina, A. A.; Soltani-Zangbar, M. S.; Song, S.; Song, Y.; Sood, P.; Sreeramareddy, C. T.; Steiropoulos, P.; Suleman, M.; Tabatabaeizadeh, S.-A.; Tahamtan, A.; Taheri, M.; Taheri Soodejani, M.; Taki, E.; Talaat, I. M.; Tampa, M.; Tandukar, S.; Tat, N. Y.; Tat, V. Y.; Tefera, Y. M.; Temesgen, G.; Temsah, M.-H.; Tesfaye, A.; Tesfaye, D. G.; Tessema, B.; Thapar, R.; Ticoalu, J. H. V.; Tiyyuri, A.; Tleyjeh, I. I.; Togtmol, M.; Tovani-Palone, M. R.; Tufa, D. G.; Ullah, I.; Upadhyay, E.; Valadan Tahbaz, S.; Valdez, P. R.; Valizadeh, R.; Vardavas, C.; Vasankari, T. J.; Vo, B.; Vu, L. G.; Wagaye, B.; Waheed, Y.; Wang, Y.; Waris, A.; West, T. E.; Wickramasinghe, N. D.; Xu, X.; Yaghoubi, S.; Yahya, G. A. T.; Yahyazadeh Jabbari, S. H.; Yon, D. K.; Yonemoto, N.; Zaman, B. A.; Zandifar, A.; Zangiabadian, M.; Zar, H. J.; Zare, I.; Zareshahrabadi, Z.; Zarrintan, A.; Zastrozhin, M. S.; Zeng, W.; Zhang, M.; Zhang, Z.-J.; Zhong, C.; Zoladl, M.; Zumla, A.; Lim, S. S.; Vos, T.; Naghavi, M.; Brauer, M.; Hay, S. I.; Murray, C. J. L.. Age–sex Differences in the Global Burden of Lower Respiratory Infections and Risk Factors, 1990–2019: Results from the

- Global Burden of Disease Study 2019. *The Lancet Infectious Diseases* **2022**, 22 (11), 1626–1647. [https://doi.org/10.1016/s1473-3099\(22\)00510-2](https://doi.org/10.1016/s1473-3099(22)00510-2).
5. Bottery, M. J.; Pitchford, J. W.; Friman, V.-P.. Ecology and Evolution of Antimicrobial Resistance in Bacterial Communities. *The ISME Journal* **2021**, 15 (4), 939–948. <https://doi.org/10.1038/s41396-020-00832-7>.
 6. Lee, B.-K.; Ryu, S.; Oh, S.-K.; Ahn, H.-J.; Jeon, S.-Y.; Jeong, W.-J.; Cho, Y.-C.; Park, J.-S.; You, Y.-H.; Kang, C.-S. Lactate Dehydrogenase to Albumin Ratio as a Prognostic Factor in Lower Respiratory Tract Infection Patients. *The American Journal of Emergency Medicine* **2021**, 52, 54–58.
 7. Hwang, A. Y.; Gums, J. G. The Emergence and Evolution of Antimicrobial Resistance: Impact on a Global Scale. *Bioorganic & Medicinal Chemistry* **2016**, 24 (24), 6440–6445.
 8. Aminov, R. I. A Brief History of the Antibiotic Era: Lessons Learned and Challenges for the Future. *Frontiers in Microbiology* **2010**, 1.
 9. Alrebish, S. A.; Yusufoglu, H. S.; Alotibi, R. F.; Abdulkhalik, N. S.; Ahmed, N. J.; Khan, A. H.. Epidemiology of Healthcare-associated Infections and Adherence to the HAI Prevention Strategies. *Healthcare* **2022**, 11 (1), 63. <https://doi.org/10.3390/healthcare11010063>.
 10. Shinu, P.; Mouslem, A. K. A.; Nair, A. B.; Venugopala, K. N.; Attimarad, M.; Singh, V. A.; Nagaraja, S.; Alotaibi, G.; Deb, P. K.. Progress Report: Antimicrobial Drug Discovery in the Resistance Era. *Pharmaceuticals* **2022**, 15 (4), 413. <https://doi.org/10.3390/ph15040413>.
 11. Livermore, D. M.. The Need for New Antibiotics. *Clinical Microbiology and Infection* **2004**, 10, 1–9. <https://doi.org/10.1111/j.1465-0691.2004.1004.x>.
 12. Linciano, P.; Cavalloro, V.; Martino, E.; Kirchmair, J.; Listro, R.; Rossi, D.; Collina, S.. Tackling Antimicrobial Resistance with Small Molecules Targeting Lsrk: Challenges and Opportunities. *Journal of Medicinal Chemistry* **2020**, 63 (24), 15243–15257. <https://doi.org/10.1021/acs.jmedchem.0c01282>.

13. C Reygaert, W. An Overview of the Antimicrobial Resistance Mechanisms of Bacteria. *AIMS Microbiology* **2018**, 4 (3), 482–501.
14. Levin, P. A.; Angert, E. R.. Small but Mighty: Cell Size and Bacteria. *Cold Spring Harbor Perspectives in Biology* **2015**, 7 (7), a019216.
<https://doi.org/10.1101/cshperspect.a019216>.
15. Doron, S.; Gorbach, S. L. Bacterial Infections: Overview. *International Encyclopedia of Public Health* **2008**, 273–282.
16. Murray, C. J. L.; Ikuta, K. S.; Sharara, F.; Swetschinski, L.; Robles Aguilar, G.; Gray, A.; Han, C.; Bisignano, C.; Rao, P.; Wool, E.; Johnson, S. C.; Browne, A. J.; Chipeta, M. G.; Fell, F.; Hackett, S.; Haines-Woodhouse, G.; Kashef Hamadani, B. H.; Kumaran, E. A. P.; Mcmanigal, B.; Achalapong, S.; Agarwal, R.; Akech, S.; Albertson, S.; Amuasi, J.; Andrews, J.; Aravkin, A.; Ashley, E.; Babin, F.-X.; Bailey, F.; Baker, S.; Basnyat, B.; Bekker, A.; Bender, R.; Berkley, J. A.; Bethou, A.; Bielicki, J.; Boonkasidecha, S.; Bukosia, J.; Carneiro, C.; Castañeda-Orjuela, C.; Chansamouth, V.; Chaurasia, S.; Chiurchiù, S.; Chowdhury, F.; Clotaire Donatien, R.; Cook, A. J.; Cooper, B.; Cressey, T. R.; Criollo-Mora, E.; Cunningham, M.; Darboe, S.; Day, N. P. J.; De Luca, M.; Dokova, K.; Dramowski, A.; Dunachie, S. J.; Duong Bich, T.; Eckmanns, T.; Eibach, D.; Emami, A.; Feasey, N.; Fisher-Pearson, N.; Forrest, K.; Garcia, C.; Garrett, D.; Gastmeier, P.; Giref, A. Z.; Greer, R. C.; Gupta, V.; Haller, S.; Haselbeck, A.; Hay, S. I.; Holm, M.; Hopkins, S.; Hsia, Y.; Iregbu, K. C.; Jacobs, J.; Jarovsky, D.; Javanmardi, F.; Jenney, A. W. J.; Khorana, M.; Khusuwan, S.; Kisson, N.; Kobeissi, E.; Kostyanov, T.; Krapp, F.; Krumkamp, R.; Kumar, A.; Kyu, H. H.; Lim, C.; Lim, K.; Limmathurotsakul, D.; Loftus, M. J.; Lunn, M.; Ma, J.; Manoharan, A.; Marks, F.; May, J.; Mayxay, M.; Mturi, N.; Munera-Huertas, T.; Musicha, P.; Musila, L. A.; Mussi-Pinhata, M. M.; Naidu, R. N.; Nakamura, T.; Nanavati, R.; Nangia, S.; Newton, P.; Ngoun, C.; Novotney, A.; Nwakanma, D.; Obiero, C. W.; Ochoa, T. J.; Olivas-Martinez, A.; Olliaro, P.; Ooko, E.; Ortiz-Brizuela, E.; Ounchanum, P.; Pak, G. D.; Paredes, J. L.; Peleg, A. Y.; Perrone, C.; Phe, T.; Phommasone, K.; Plakkal, N.; Ponce-De-Leon, A.; Raad, M.; Ramdin, T.; Rattanaovong, S.; Riddell, A.; Roberts, T.; Robotham, J. V.; Roca, A.;

- Rosenthal, V. D.; Rudd, K. E.; Russell, N.; Sader, H. S.; Saengchan, W.; Schnall, J.; Scott, J. A. G.; Seekaew, S.; Sharland, M.; Shivamallappa, M.; Sifuentes-Osornio, J.; Simpson, A. J.; Steenkeste, N.; Stewardson, A. J.; Stoeva, T.; Tasak, N.; Thaiprakong, A.; Thwaites, G.; Tigoi, C.; Turner, C.; Turner, P.; Van Doorn, H. R.; Velaphi, S.; Vongpradith, A.; Vongsouvath, M.; Vu, H.; Walsh, T.; Walson, J. L.; Waner, S.; Wangrangsimakul, T.; Wannapinij, P.; Wozniak, T.; Young Sharma, T. E. M. W.; Yu, K. C.; Zheng, P.; Sartorius, B.; Lopez, A. D.; Stergachis, A.; Moore, C.; Dolecek, C.; Naghavi, M.. Global Burden of Bacterial Antimicrobial Resistance in 2019: A Systematic Analysis. *The Lancet* **2022**, 399 (10325), 629–655. [https://doi.org/10.1016/s0140-6736\(21\)02724-0](https://doi.org/10.1016/s0140-6736(21)02724-0).
17. Mai-Prochnow, A.; Clauson, M.; Hong, J.; Murphy, A. B.. Gram Positive and Gram Negative Bacteria Differ in Their Sensitivity to Cold Plasma. *Scientific Reports* **2016**, 6 (1), 38610. <https://doi.org/10.1038/srep38610>.
 18. Silhavy, T. J.; Kahne, D.; Walker, S.. The Bacterial Cell Envelope. *Cold Spring Harbor Perspectives in Biology* **2010**, 2 (5), a000414–a000414. <https://doi.org/10.1101/cshperspect.a000414>.
 19. Rice, L. B. Antimicrobial Resistance in Gram-Positive Bacteria. *American Journal of Infection Control* **2006**, 34 (5).
 20. Poole, K. Multidrug Resistance in Gram-Negative Bacteria. *Current Opinion in Microbiology* **2001**, 4 (5), 500–508.
 21. Hutchings, M. I.; Truman, A. W.; Wilkinson, B. Antibiotics: Past, Present and Future. *Current Opinion in Microbiology* **2019**, 51, 72–80.
 22. Nelson, M. L.; Dinardo, A.; Hochberg, J.; Armelagos, G. J.. Brief Communication: Mass Spectroscopic Characterization of Tetracycline in the Skeletal Remains of an Ancient Population from Sudanese Nubia 350-550 CE. *American Journal of Physical Anthropology* **2010**, 143 (1), 151–154. <https://doi.org/10.1002/ajpa.21340>.
 23. Winau, F.; Westphal, O.; Winau, R. Paul Ehrlich - In Search of the Magic Bullet. *Microb. Infect.* **2004**, 6, 786–789.

24. Kaufmann, S. Paul Ehrlich: Founder of Chemotherapy. *Nat. Rev. Drug Discov.* **2008**, 7, 373.
25. CDC - parasites - about parasites.
<https://www.cdc.gov/parasites/about.html#:~:text=A%20parasite%20is%20an%20organism,Entamoeba%20histolytica%20is%20a%20protozoan.> (accessed Mar 27, 2023).
26. McGregor, I. A.. The Significance of Parasitic Infections in Terms of Clinical Disease: A Personal View. *Parasitology* **1987**, 94 (S1), S159–S179.
<https://doi.org/10.1017/s0031182000085875>.
27. Eyayu, T.; Kiros, T.; Workineh, L.; Sema, M.; Damtie, S.; Hailemichael, W.; Dejen, E.; Tiruneh, T.. Prevalence of Intestinal Parasitic Infections and Associated Factors Among Patients Attending at Sanja Primary Hospital, Northwest Ethiopia: An Institutional-based Cross-sectional Study. *PLOS ONE* **2021**, 16 (2), e0247075. <https://doi.org/10.1371/journal.pone.0247075>.
28. Torgerson, P. R.; Devleesschauwer, B.; Praet, N.; Speybroeck, N.; Willingham, A. L.; Kasuga, F.; Rokni, M. B.; Zhou, X.-N.; Fèvre, E. M.; Sripa, B.; Gargouri, N.; Fürst, T.; Budke, C. M.; Carabin, H.; Kirk, M. D.; Angulo, F. J.; Havelaar, A.; De Silva, N.. World Health Organization Estimates of the Global and Regional Disease Burden of 11 Foodborne Parasitic Diseases, 2010: A Data Synthesis. *PLOS Medicine* **2015**, 12 (12), e1001920.
<https://doi.org/10.1371/journal.pmed.1001920>.
29. Malaria. https://www.who.int/news-room/questions-and-answers/item/malaria?gclid=CjwKCAjw_YShBhAiEiwAMomsEPAlkpx6jq5R7Q623wQ_yy3Eta3dNAaYKAWWh61bpJvYs0YtDUSeqEhoCjv0QAvD_BwE (accessed Mar 27, 2023).
30. Loeffel, M.; Ross, A.. The Relative Impact of Interventions on Sympatric Plasmodium Vivax and Plasmodium Falciparum Malaria: A Systematic Review. *PLOS Neglected Tropical Diseases* **2022**, 16 (6), e0010541.
<https://doi.org/10.1371/journal.pntd.0010541>.
31. Soulard, V.; Bosson-Vanga, H.; Lorthiois, A.; Roucher, C.; Franetich, J.-F.; Zanghi, G.; Bordessoulles, M.; Tefit, M.; Thellier, M.; Morosan, S.; Le Naour, G.;

- Capron, F.; Suemizu, H.; Snounou, G.; Moreno-Sabater, A.; Mazier, D.. Plasmodium Falciparum Full Life Cycle and Plasmodium Ovale Liver Stages in Humanized Mice. *Nature Communications* **2015**, 6 (1), 7690.
<https://doi.org/10.1038/ncomms8690>.
32. Venugopal, K.; Hentzschel, F.; Valkiūnas, G.; Marti, M. Plasmodium Asexual Growth and Sexual Development in the Haematopoietic Niche of the Host. *Nat. Rev. Microbiol.* **2020**, 18 (3), 177–189.
33. Suh, P. F.; Elanga-Ndille, E.; Tchouakui, M.; Sandeu, M. M.; Tagne, D.; Wondji, C.; Ndo, C.. Impact of Insecticide Resistance on Malaria Vector Competence: A Literature Review. *Malaria Journal* **2023**, 22 (1). <https://doi.org/10.1186/s12936-023-04444-2>.
34. Laurens, M. B.. RTS,S/AS01 Vaccine (mosquirix™): An Overview. *Human Vaccines & Immunotherapeutics* **2020**, 16 (3), 480–489.
<https://doi.org/10.1080/21645515.2019.1669415>.
35. Caminade, C.; Kovats, S.; Rocklov, J.; Tompkins, A. M.; Morse, A. P.; Colon-Gonzalez, F. J.; Stenlund, H.; Martens, P.; Lloyd, S. J. Impact of climate change on global malaria distribution. *Proc. Natl. Acad. Sci. USA.* **2014**, 111, 3286–3291.
36. Spry, C.; Kirk, K.; Saliba, K. J. Coenzyme a Biosynthesis: An Antimicrobial Drug Target. *FEMS Microbiology Reviews* **2008**, 32 (1), 56–106.
37. Strauss, E. Coenzyme A Biosynthesis and Enzymology. In *Comprehensive Natural Products II*; Lew, M., Liu, B., Eds.; Elsevier, **2010**; pp 351–410.
38. Goosen, R.; Strauss, E.. Simultaneous Quantification of Coenzyme A and Its Salvage Pathway Intermediates in in Vitro and Whole Cell-sourced Samples. *RSC Advances* **2017**, 7 (32), 19717–19724.
<https://doi.org/10.1039/c7ra00192d>.
39. Clifton, G.; Bryant, S. R.; Skinner, C. G. N'-(Substituted) Pantothenamides, Antimetabolites of Pantothenic Acid. *Arch. Biochem. Biophys.* **1970**, 137, 523–528.
40. Spry, C.; Macuamule, C.; Lin, Z.; Virga, K. G.; Lee, R. E.; Strauss, E.; Saliba, K. J. Pantothenamides Are Potent, On-Target Inhibitors of Plasmodium Falciparum

Growth When Serum Pantetheinase Is Inactivated. *PLoS. ONE*. **2013**, 8 (2), e54974.

41. Strauss, E.; Begley, T. P.. The Antibiotic Activity of N-pentylpantothenamide Results from Its Conversion to Ethyldethia-coenzyme A, a Coenzyme A Antimetabolite. *Journal of Biological Chemistry* **2002**, 277 (50), 48205–48209. <https://doi.org/10.1074/jbc.m204560200>.
42. Akinnusi, T. O.; Vong, K.; Auclair, K.. Geminal Dialkyl Derivatives of N-substituted Pantothenamides: Synthesis and Antibacterial Activity. *Bioorganic & Medicinal Chemistry* **2011**, 19 (8), 2696–2706. <https://doi.org/10.1016/j.bmc.2011.02.053>.
43. De Villiers, M.; Macuamule, C.; Spry, C.; Hyun, Y.-M.; Strauss, E.; Saliba, K. J.. Structural Modification of Pantothenamides Counteracts Degradation by Pantetheinase and Improves Antiplasmodial Activity. *ACS Medicinal Chemistry Letters* **2013**, 4 (8), 784–789. <https://doi.org/10.1021/ml400180d>.
44. Moolman, W. J. A.; De Villiers, M.; Strauss, E. Recent Advances in Targeting Coenzyme A Biosynthesis and Utilization for Antimicrobial Drug Development. *Biochem. Soc. Trans.* **2014**, 42, 1080–1086.
45. Zhang, Y.-M.; Frank, M. W.; Virga, K. G.; Lee, R. E.; Rock, C. O.; Jackowski, S.. Acyl Carrier Protein Is a Cellular Target for the Antibacterial Action of the Pantothenamide Class of Pantothenate Antimetabolites. *Journal of Biological Chemistry* **2004**, 279 (49), 50969–50975. <https://doi.org/10.1074/jbc.m409607200>.
46. Hoegl, A.; Darabi, H.; Tran, E.; Awuah, E.; Kerdo, E. S. C.; Habib, E.; Saliba, K. J.; Auclair, K. Stereochemical Modification of Geminal Dialkyl Substituents on Pantothenamides Alters Antimicrobial Activity. *Bioorg. Med. Chem. Lett.* **2014**, 24, 3274–3277.
47. Guan, J.; Hachey, M.; Puri, L.; Howieson, V.; Saliba, K. J.; Auclair, K. A Cross-Metathesis Approach to Novel Pantothenamide Derivatives. *Beilstein. J. Org. Chem.* **2016**, 12, 963–968.
48. Macuamule, C. J.; Tjhin, E. T.; Jana, C. E.; Barnard, L.; Koekemoer, L.; De Villiers, M.; Saliba, K. J.; Strauss, E. A Pantetheinase-Resistant Pantothenamide

- with Potent, on-Target, and Selective Antiplasmodial Activity. *Antimicrob. Agents. Chemother.* **2015**, *59*, 3666–3668.
49. Spry, C.; Barnard, L.; Kok, M.; Powell, A. K.; Mahesh, D.; Tjhin, E. T.; Saliba, K. J.; Strauss, E.; De Villiers, M. Toward a Stable and Potent Coenzyme A-Targeting Antiplasmodial Agent: Structure-Activity Relationship Studies of N-Phenethyl- α -Methyl-Pantothenamide. *ACS. Infect. Dis.* **2020**, *6*, 1844–1854.
 50. Guan, J.; Spry, C.; Tjhin, E.; Yang, P.; Kittikool, T.; Howieson, V.; Ling, H.; Starrs, L.; Duncan, D.; Burgio, G.; Saliba, K.; Auclair, K. Exploring Heteroaromatic Rings as a Replacement for the Labile Amide of Antiplasmodial Pantothenamides. *J. Med. Chem* **2021**.
<https://doi.org/https://doi.org/10.1021/acs.jmedchem.0c01755>.
 51. Barnard, L.; Mostert, K. J.; Van Otterlo, W. A. L.; Strauss, E. Developing Pantetheinase-Resistant Pantothenamide Antibacterials: Structural Modification Impacts on PanK Interaction and Mode of Action. *ACS Infect. Dis.* **2018**, *4*, 736–743.
 52. De Villiers, M.; Barnard, L.; Koekemoer, L.; Snoep, J. L.; Strauss, E.. Variation in Pantothenate Kinase Type Determines the Pantothenamide Mode of Action and Impacts on Coenzyme A Salvage Biosynthesis. *The FEBS Journal* **2014**, *281* (20), 4731–4753. <https://doi.org/10.1111/febs.13013>.
 53. Jansen, P. A. M.; van der Krieken, D. A.; Botman, P. N. M.; Blaauw, R. H.; Cavina, L.; Raaijmakers, E. M.; de Heuvel, E.; Sandrock, J.; Pennings, L. J.; Hermkens, P. H. H.; Zeeuwen, P. L. J. M.; Rutjes, F. P. J. T.; Schalkwijk, J. Stable Pantothenamide Bioisosteres: Novel Antibiotics for Gram-Positive Bacteria. *J. Antibiot.* **2019**, *72*, 682–692.
 54. Mercer, A. C.; Meier, J. L.; Hur, G. H.; Smith, A. R.; Burkart, M. D. Antibiotic Evaluation and in Vivo Analysis of Alkynyl Coenzyme A Antimetabolites in *Escherichia Coli*. *Bioorg. Med. Chem. Lett.* **2008**, *18*, 5991–5994.
 55. Hughes, S. J.; Barnard, L.; Mottaghi, K.; Tempel, W.; Antoshchenko, T.; Hong, B. S.; Allali-Hassani, A.; Smil, D.; Vedadi, M.; Strauss, E.; Park, H. W. Discovery of Potent Pantothenamide Inhibitors of *Staphylococcus Aureus* Pantothenate

Kinase Through a Minimal SAR Study: Inhibition Is Due to Trapping of the Product. *ACS Infect. Dis.* **2016**, 2, 627–641.

56. Schalkwijk, J.; Allman, E. L.; M Jansen, P. A.; de Vries, L. E.; J Verhoef, J. M.; Jackowski, S.; M Botman, P. N.; Beuckens-Schortinghuis, C. A.; J Koolen, K. M.; Bolscher, J. M.; Vos, M. W.; Miller, K.; Reeves, S. A.; Pett, H.; Trevitt, G.; Wittlin, S.; Scheurer, C.; Sax, S.; Fischli, C.; Angulo-Barturen, I.; Belén Jiménez-Díaz, M.; Josling, G.; A Kooij, T. W.; Bonnert, R.; Campo, B.; Blaauw, R. H.; J T Rutjes, F. P.; Sauerwein, R. W.; Llinás, M.; H Hermkens, P. H.; Dechering, K. J. Antimalarial Pantothenamide Metabolites Target Acetyl-Coenzyme A Biosynthesis in Plasmodium Falciparum. *Sci. Transl. Med.* **2019**, *11*, 9917.
57. Howieson, V. M.; Tran, E.; Hoegl, A.; Fam, H. L.; Fu, J.; Sivonen, K.; Li, X. X.; Auclair, K.; Saliba, K. J. Triazole Substitution of a Labile Amide Bond Stabilizes Pantothenamides and Improves Their Antiplasmodial Potency. *Antimicrob. Agents. Chemother.* **2016**, *60* (12), 7146–7152.
58. Ten health issues who will tackle this year. <https://www.who.int/news-room/spotlight/ten-threats-to-global-health-in-2019> (accessed Mar 28, 2023).
59. Choudhry, A. E.; Mandichak, T. L.; Broskey, J. P.; Egolf, R. W.; Kinsland, C.; Begley, T. P.; Seefeld, M. A.; Ku, T. W.; Brown, J. R.; Zalacain, M.; Ratnam, K. Inhibitors of Pantothenate Kinase: Novel Antibiotics for Staphylococcal Infections. *Antimicrob. Agents. Chemother.* **2003**, *47*, 2051–2055. <https://doi.org/1.>
60. Saliba, K. J.; Spry, C. Exploiting the Coenzyme A Biosynthesis Pathway for the Identification of New Antimalarial Agents: The Case for Pantothenamides. *Biochem. Soc. Trans.* **2014**, *42*, 1087–1093.
61. Chen, Y.; Rosenkranz, C.; Hirte, S.; Kirchmair, J.. Ring Systems in Natural Products: Structural Diversity, Physicochemical Properties, and Coverage by Synthetic Compounds. *Natural Product Reports* **2022**, *39* (8), 1544–1556. <https://doi.org/10.1039/d2np00001f>.
62. Aldeghi, M.; Malhotra, S.; Selwood, D. L.; Chan, A. W. E.. Two- and Three-dimensional Rings in Drugs. *Chemical Biology & Drug Design* **2014**, *83* (4), 450–461. <https://doi.org/10.1111/cbdd.12260>.

63. Jampilek, J.. Heterocycles in Medicinal Chemistry. *Molecules* **2019**, 24 (21), 3839. <https://doi.org/10.3390/molecules24213839>.
64. Annica Chu. Synthesis of thiazole-containing pantothenamide analogues as potential antimicrobial agents, Master of Science, McGill University, Montréal, QC, Canada, 2021. <https://escholarship.mcgill.ca/concern/theses/w0892g804>
65. Buchholz, C. R.; Pomerantz, W. C. K.. 19F NMR Viewed Through Two Different Lenses: Ligand-observed and Protein-observed 19F NMR Applications for Fragment-based Drug Discovery. *RSC Chemical Biology* **2021**, 2 (5), 1312–1330. <https://doi.org/10.1039/d1cb00085c>.
66. Inoue, M.; Sumii, Y.; Shibata, N.. Contribution of Organofluorine Compounds to Pharmaceuticals. *ACS Omega* **2020**, 5 (19), 10633–10640. <https://doi.org/10.1021/acsomega.0c00830>.
67. Victoria Virgilio. Synthesis of Pantothenamide-Mimicking Compounds as Novel Antibacterial and Antiplasmodial Agents, Master of Science, McGill University, Montréal, QC, Canada, June 2022. <https://escholarship.mcgill.ca/concern/theses/td96k759g>
68. WHO publishes list of bacteria for which new antibiotics are urgently needed. <https://www.who.int/news/item/27-02-2017-who-publishes-list-of-bacteria-for-which-new-antibiotics-are-urgently-needed> (accessed Apr 3, 2023).
69. Breijyeh, Z.; Jubeh, B.; Karaman, R.. Resistance of Gram-negative Bacteria to Current Antibacterial Agents and Approaches to Resolve It. *Molecules* **2020**, 25 (6), 1340. <https://doi.org/10.3390/molecules25061340>.
70. Acinetobacter in healthcare settings. [https://www.cdc.gov/hai/organisms/acinetobacter.html#:~:text=Acinetobacter%20baumannii%20can%20cause%20infections,\(sputum\)%20or%20open%20wounds](https://www.cdc.gov/hai/organisms/acinetobacter.html#:~:text=Acinetobacter%20baumannii%20can%20cause%20infections,(sputum)%20or%20open%20wounds) . (accessed Apr 3, 2023).
71. E. coli and Food Safety. <https://www.cdc.gov/foodsafety/communication/ecoli-and-food-safety.html#:~:text=Most%20E.,respiratory%20illness%2C%20and%20bloodstream%20infections>. (accessed Apr 3, 2023).

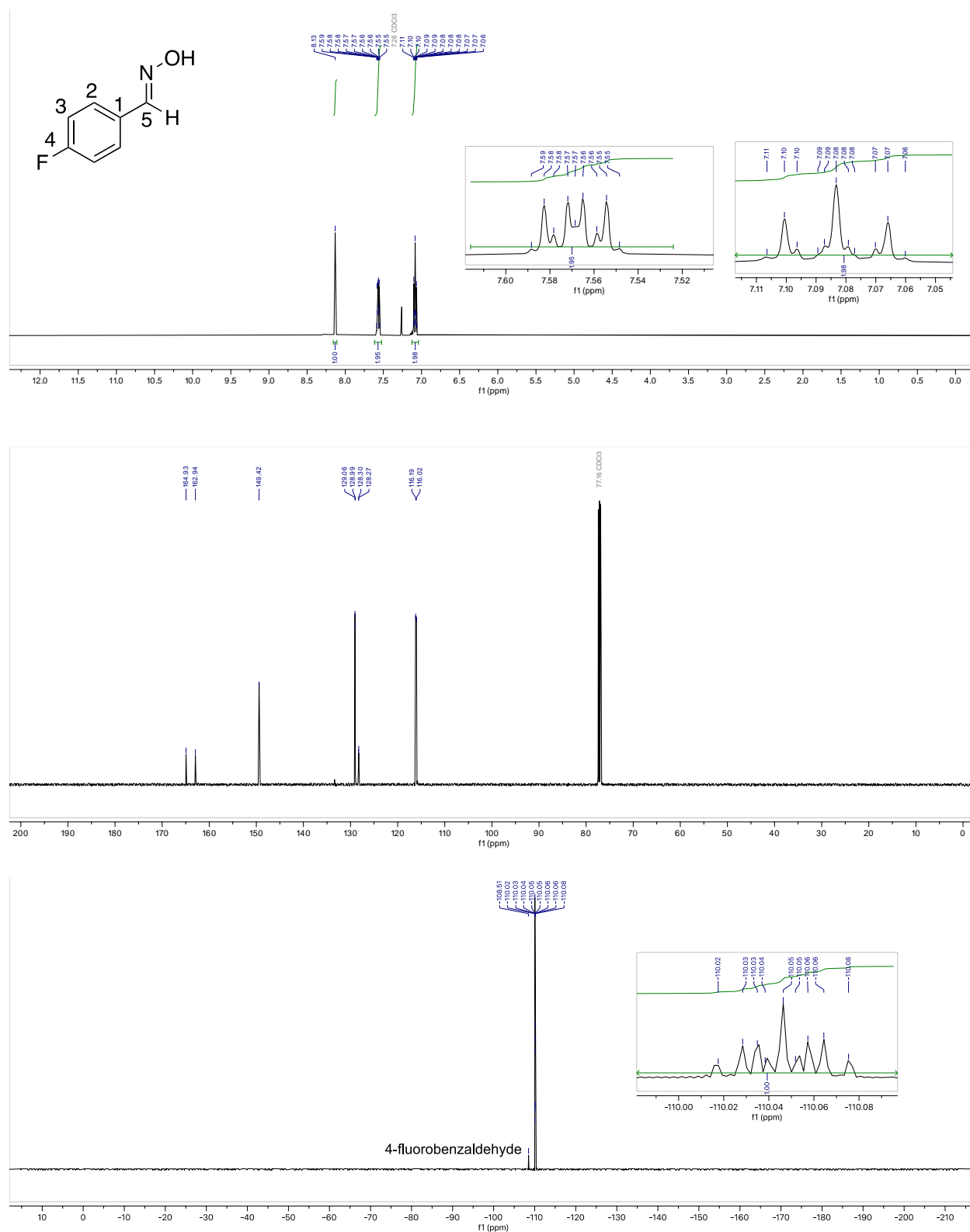
72. *Klebsiella pneumoniae* in healthcare settings.
<https://www.cdc.gov/hai/organisms/klebsiella/klebsiella.html> (accessed Apr 3, 2023).
73. *Pseudomonas aeruginosa* infection.
<https://www.cdc.gov/hai/organisms/pseudomonas.html#:~:text=Of%20the%20many%20different%20types,of%20the%20body%20after%20surgery.> (accessed Apr 3, 2023).
74. Kwiecinski, J. M.; Horswill, A. R. Staphylococcus Aureus Bloodstream Infections: Pathogenesis and Regulatory Mechanisms. *Current Opinion in Microbiology* **2020**, 53, 51–60.
75. Fàbrega, A.; Vila, J.. Salmonella Enterica Seroovar Typhimurium Skills to Succeed in the Host: Virulence and Regulation. *Clinical Microbiology Reviews* **2013**, 26 (2), 308–341. <https://doi.org/10.1128/cmr.00066-12>.
76. Kaur, P.. Deep Dive into a Drug Pump. *Nature Chemical Biology* **2022**.
<https://doi.org/10.1038/s41589-022-01201-5>.
77. CLSI. *Methods for Dilution Antimicrobial Susceptibility Tests for Bacteria That Grow Aerobically; Approved Standard - Tenth Edition*, M07-A10 ed.; *Clinical and Laboratory Standards Institute*: Wayne, PA, **2015**.
78. Fenton, C. S.; Buckley, T. C.. Minimum Inhibitory Concentrations of Erythromycin and Rifampin for *Rhodococcus Equi* During the Years 2007–2014. *Irish Veterinary Journal* **2015**, 68 (1). <https://doi.org/10.1186/s13620-015-0051-4>.
79. Mwai, L.; Kiara, S. M.; Abdirahman, A.; Pole, L.; Rippert, A.; Diriye, A.; Bull, P.; Marsh, K.; Borrmann, S.; Nzila, A.. In Vitro Activities of Piperaquine, Lumefantrine, and Dihydroartemisinin in Kenyan *Plasmodium Falciparum* Isolates and Polymorphisms in P Fcrt and P. *Antimicrobial Agents and Chemotherapy* **2009**, 53 (12), 5069–5073. <https://doi.org/10.1128/aac.00638-09>.
80. Armarego, W. L. F. and C. Chai (**2013**). Common Physical Techniques Used in Purification. *Purification of Laboratory Chemicals*: 1-70.
81. Li, X.; Wang, X.; Wang, Z.; Yan, X.; Xu, X., TBHP-induced iodocyclization with I2: atom economic synthesis of iodinated isoxazoles in water under mild conditions. *ACS Sustainable Chemistry & Engineering* **2019**, 7 (2), 1875-1878.

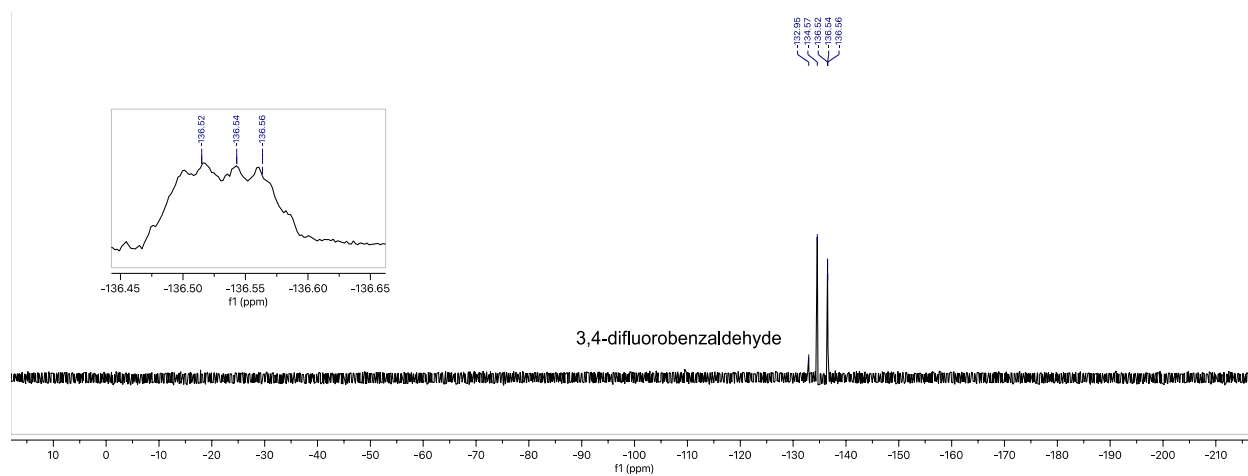
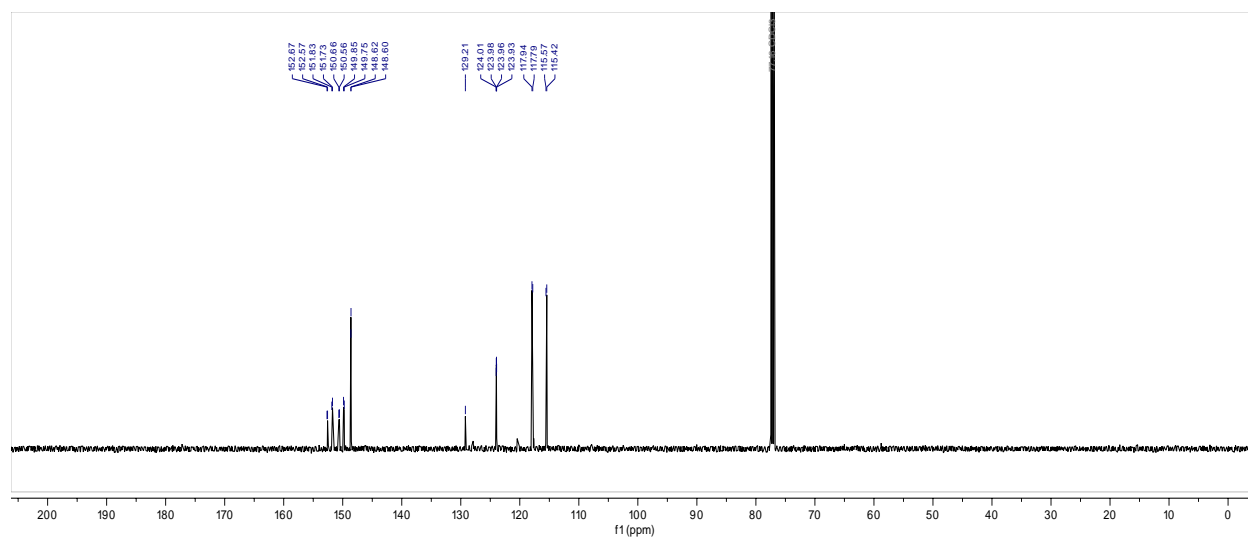
82. Di Nunno, L.; Vitale, P.; Scilimati, A.; Simone, L.; Capitelli, F. Stereoselective Dimerization Of 3-Arylisoxazoles To Cage-Shaped Bis-B-Lactams Syn 2,6-Diaryl-3,7-Diazatricyclo[4.2.0.0^{2,5}]Octan-4,8-Diones Induced By Hindered Lithium Amides. *Tetrahedron* **2007**, 63 (50), 12388-12395. DOI = <https://doi.org/10.1016/j.tet.2007.09.040>
83. Sit, S.; Conway, C.; Xie, K.; Bertekap, R.; Bourin, C.; Burris, K. Oxime Carbamate—Discovery Of A Series Of Novel FAAH Inhibitors. *Bioorganic & Medicinal Chemistry Letters* **2010**, 20 (3), 1272-1277. DOI = <https://doi.org/10.1016/j.bmcl.2009.11.080>
84. Ferreira-Silva, B.; Lavandera, I.; Kern, A.; Faber, K.; Kroutil, W. Chemo-Promiscuity Of Alcohol Dehydrogenases: Reduction Of Phenylacetaldoxime To The Alcohol. *Tetrahedron* **2010**, 66 (19), 3410-3414. DOI = <https://doi.org/10.1016/j.tet.2010.03.050>
85. Hinzmann, A.; Adebar, N.; Betke, T.; Leppin, M.; Gröger, H. Biotransformations In Pure Organic Medium: Organic Solvent-Labile Enzymes In The Batch And Flow Synthesis Of Nitriles. *European Journal of Organic Chemistry* **2019**, (41), 6911-6916. DOI = 10.1002/ejoc.201901168
86. Patel, N.; Schwarz, J.; Hou, X.; Hoover, D.; Xie, L.; Fliri, A.; Gallaschun, R.; Lazzaro, J.; Bryce, D.; Hoffmann, W.; Hanks, A.; McGinnis, D.; Marr, E.; Gazard, J.; Hajós, M.; Scialis, R.; Hurst, R.; Shaffer, C.; Pandit, J.; O'Donnell, C. Discovery And Characterization Of A Novel Dihydroisoxazole Class Of A-Amino-3-Hydroxy-5-Methyl-4-Isoxazolepropionic Acid (AMPA) Receptor Potentiators. *Journal of Medicinal Chemistry* **2013**, 56 (22), 9180-9191. DOI = <https://doi.org/10.1021/jm401274b>
87. Patel, N.; Schwarz, J.; Hou, X.; Hoover, D.; Xie, L.; Fliri, A.; Gallaschun, R.; Lazzaro, J.; Bryce, D.; Hoffmann, W.; Hanks, A.; McGinnis, D.; Marr, E.; Gazard, J.; Hajós, M.; Scialis, R.; Hurst, R.; Shaffer, C.; Pandit, J.; O'Donnell, C. Discovery And Characterization Of A Novel Dihydroisoxazole Class Of A-Amino-3-Hydroxy-5-Methyl-4-Isoxazolepropionic Acid (AMPA) Receptor Potentiators. *Journal of Medicinal Chemistry* **2013**, 56 (22), 9180-9191. DOI = <https://doi.org/10.1021/jm401274b>

88. Lazzaro, J.; Bryce, D.; Hoffmann, W.; Hanks, A.; McGinnis, D.; Marr, E.; Gazard, J.; Hajós, M.; Scialis, R.; Hurst, R.; Shaffer, C.; Pandit, J.; O'Donnell, C. Discovery And Characterization Of A Novel Dihydroisoxazole Class Of A-Amino-3-Hydroxy-5-Methyl-4-Isoxazolepropionic Acid (AMPA) Receptor Potentiators. *Journal of Medicinal Chemistry* **2013**, *56* (22), 9180-9191. DOI = <https://doi.org/10.1021/jm401274b>
89. Castellano, S.; Kuck, D.; Viviano, M.; Yoo, J.; López-Vallejo, F.; Conti, P.; Tamborini, L.; Pinto, A.; Medina-Franco, J.; Sbardella, G. Synthesis And Biochemical Evaluation Of Δ^2 -Isoxazoline Derivatives As DNA Methyltransferase 1 Inhibitors. *Journal of Medicinal Chemistry* **2011**, *54* (21), 7663-7677. DOI = 10.1021/jm2010404
90. Hewitt, R.; Lim, Y.; Ong, M. Improved Synthesis Of Glucosinolates. *Synthesis* **2018**, *50* (08), 1640-1650. DOI = 10.1055/s-0036-1591895
91. CLSI. *Methods for Dilution Antimicrobial Susceptibility Tests for Bacteria That Grow Aerobically; Approved Standard - Tenth Edition*, M07-A10 ed.; *Clinical and Laboratory Standards Institute: Wayne, PA*, **2015**.
92. Smilkstein, M.; Sriwilaijaroen, N.; Kelly, J. X.; Wilairat, P.; Riscoe, M. Simple and Inexpensive Fluorescence-Based Technique for High-Throughput Antimalarial Drug Screening. *Antimicrob. Agents. Chemother.* **2004**, *48*, 1803–1806.

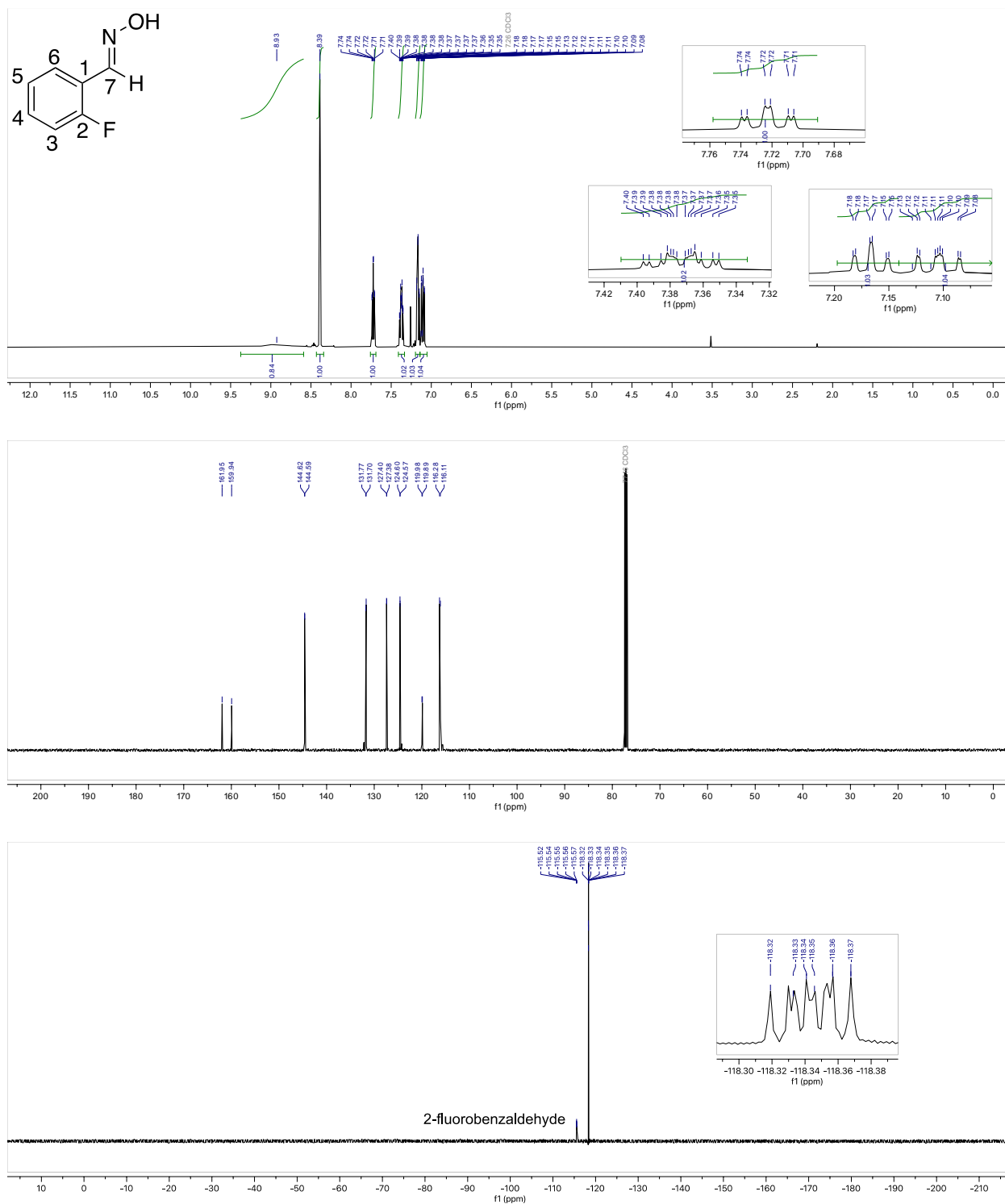
Appendix

Compound 3.2a

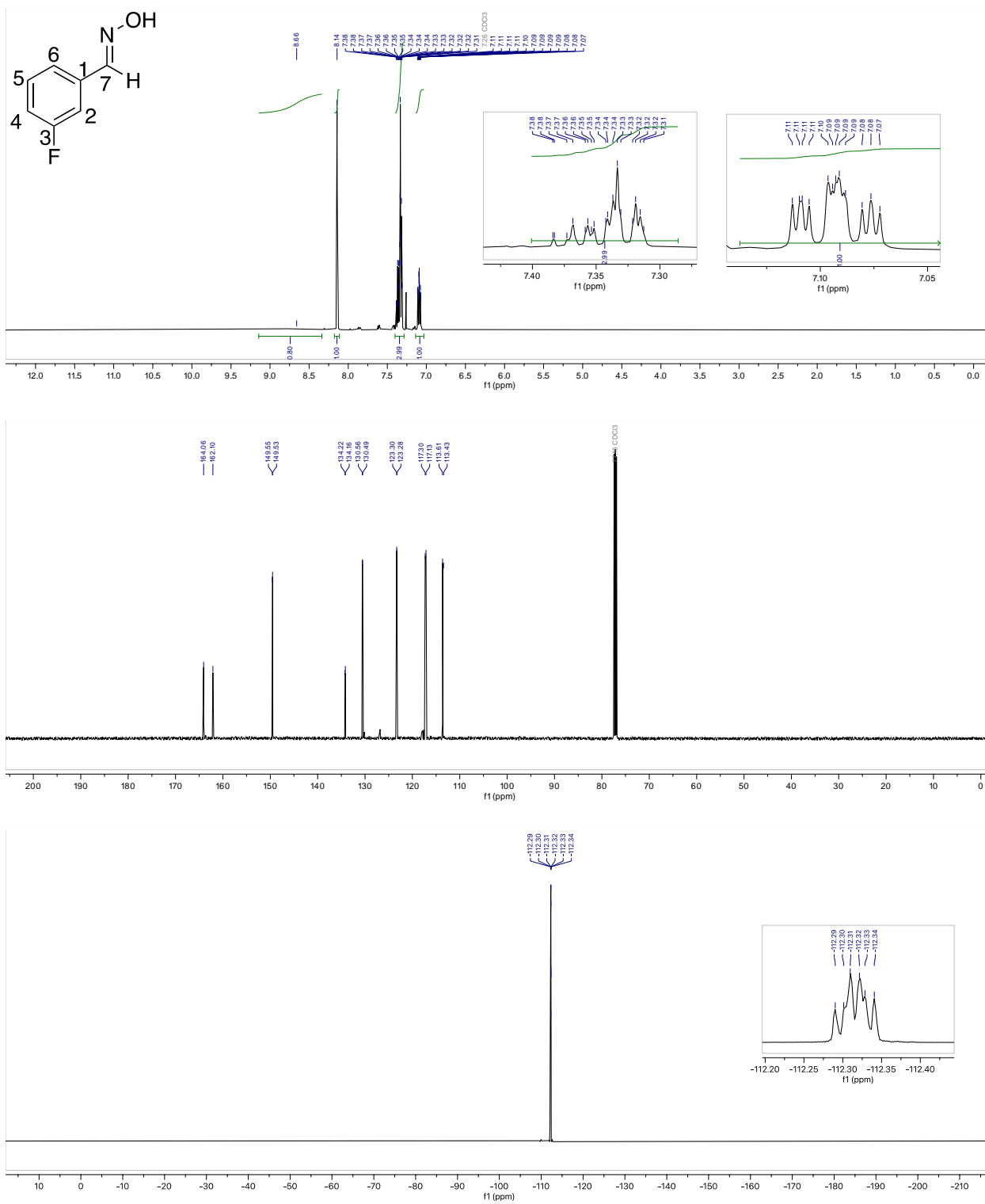




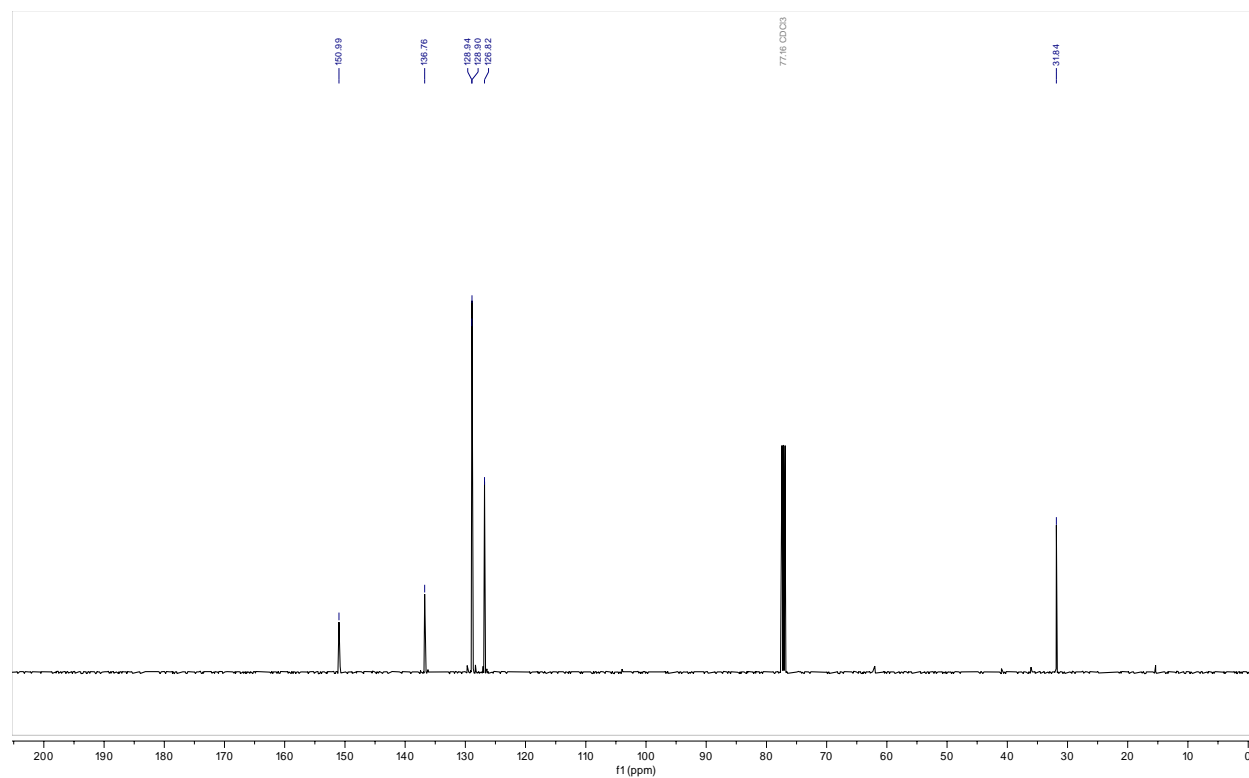
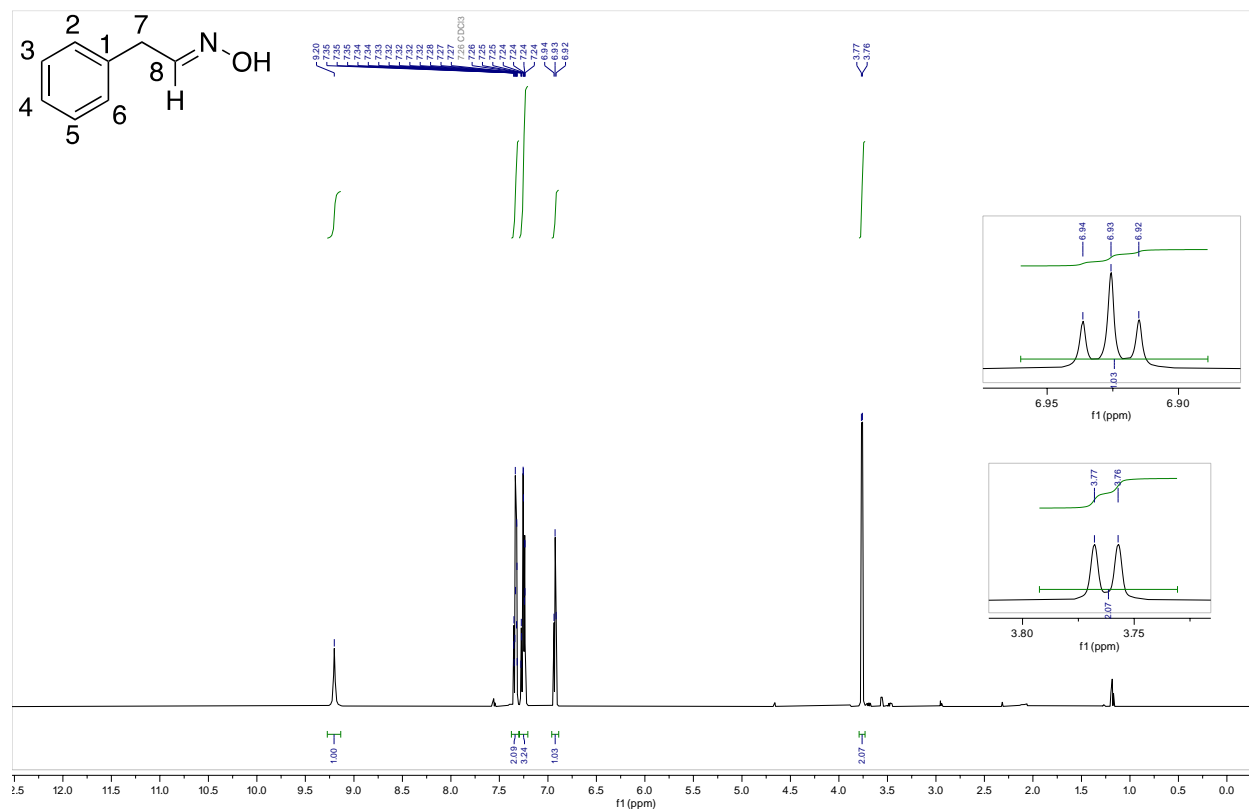
Compound 3.2c



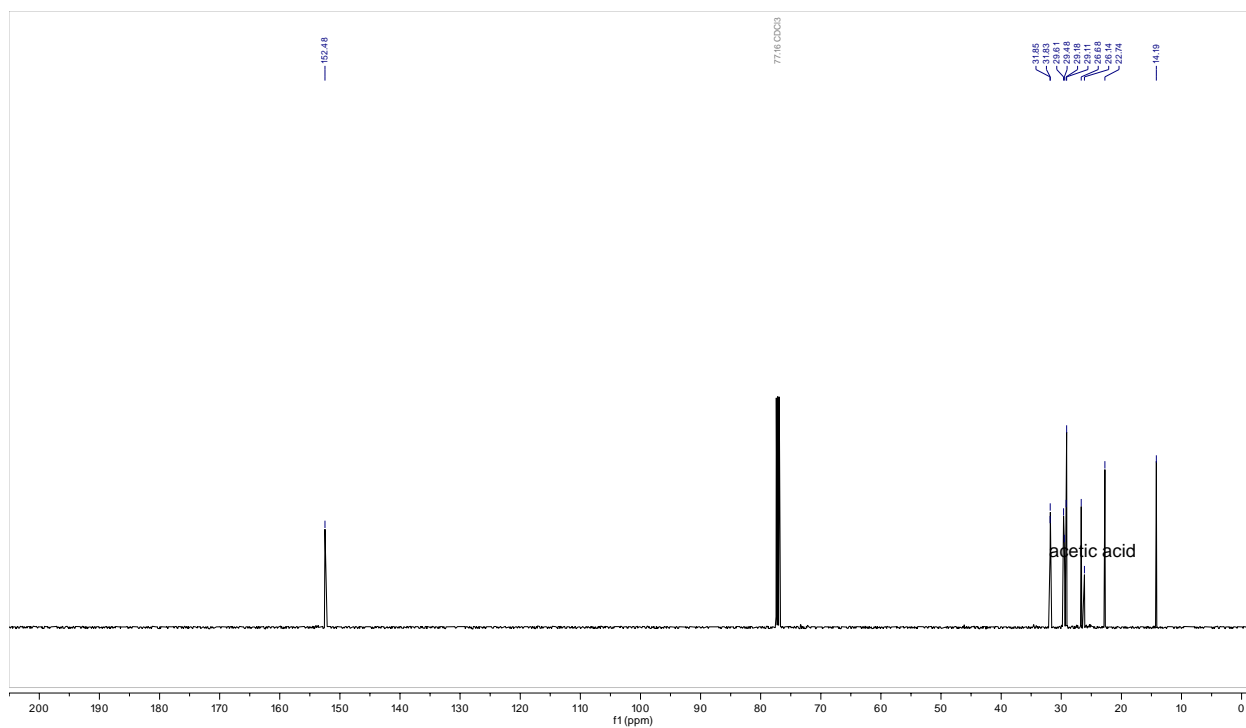
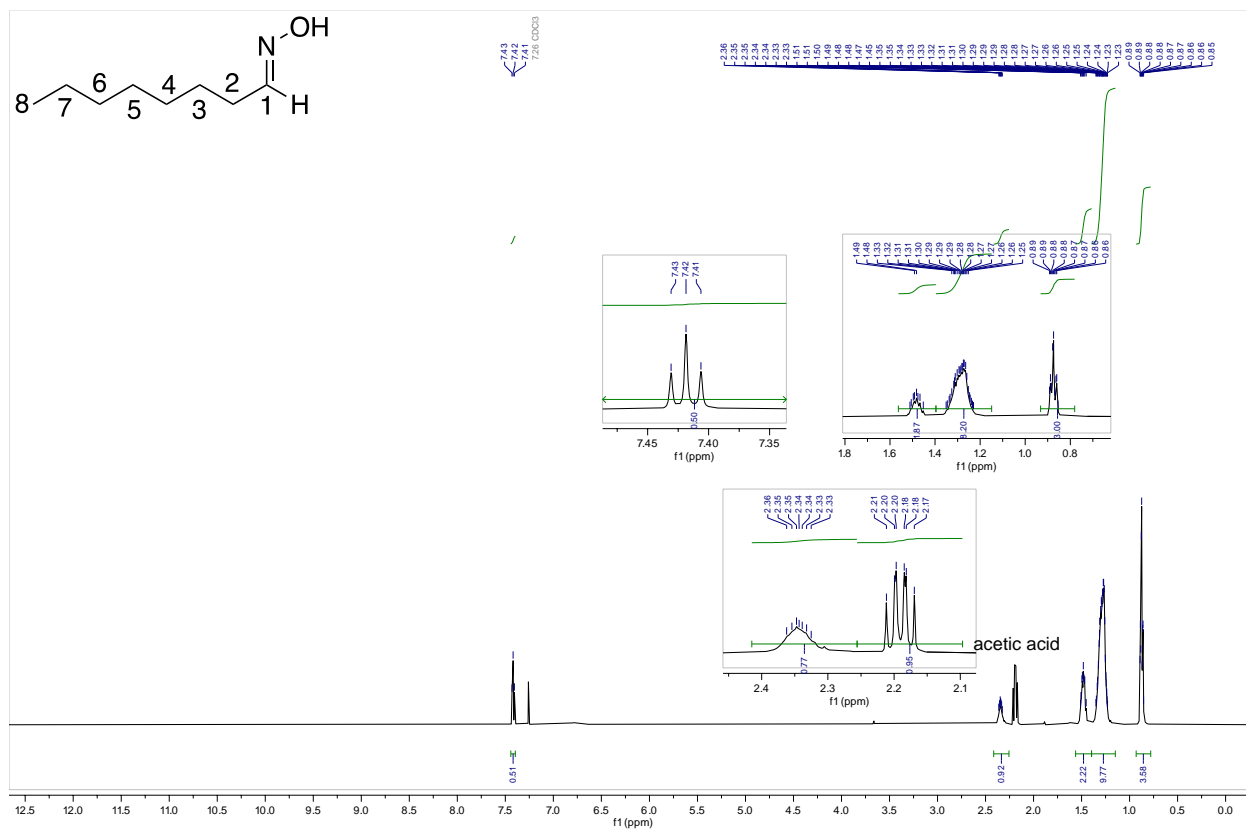
Compound 3.2d



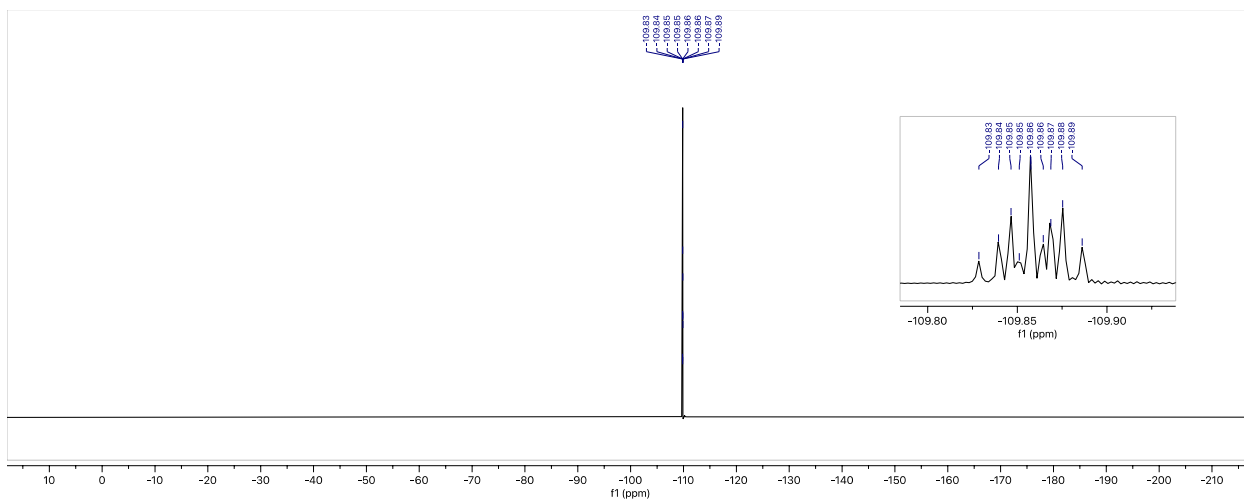
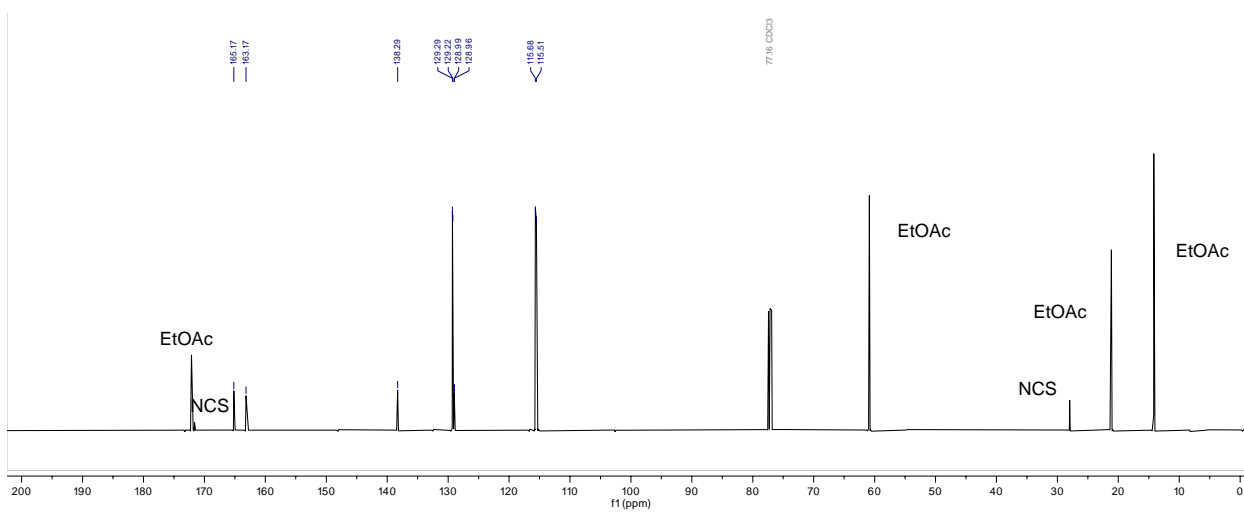
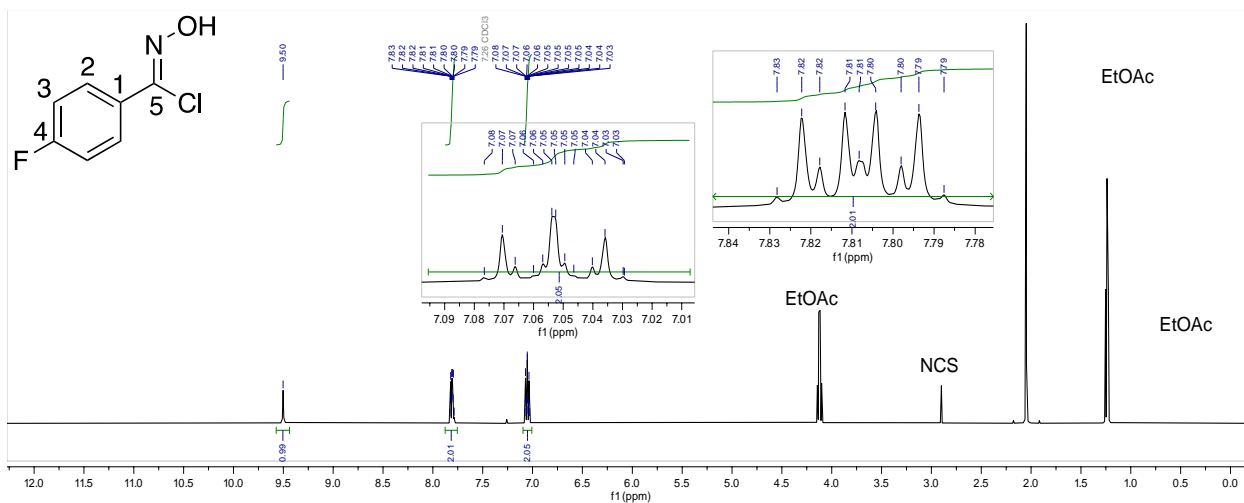
Compound 3.2e



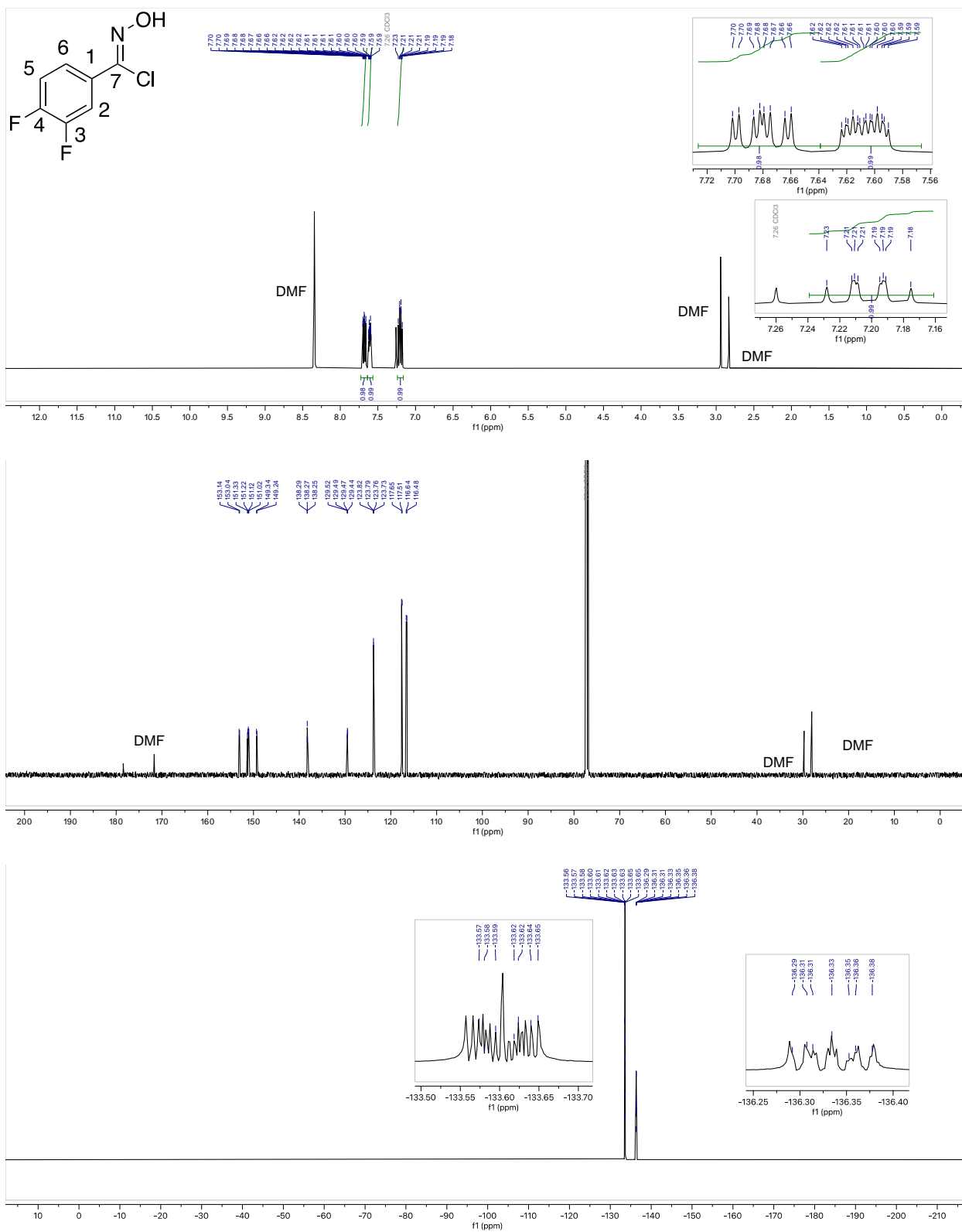
Compound 3.2f



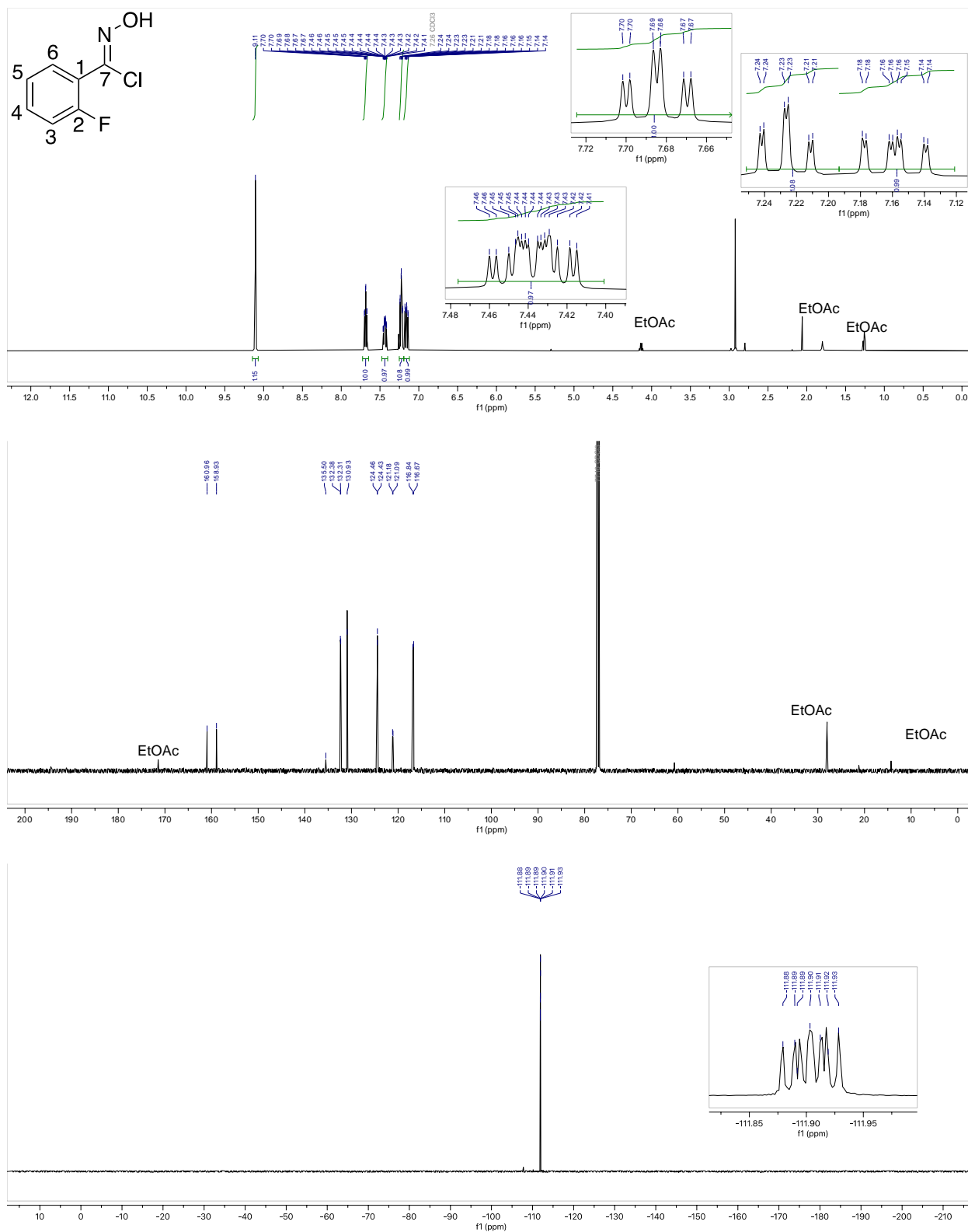
Compound 3.3a



Compound 3.3b



Compound 3.3c



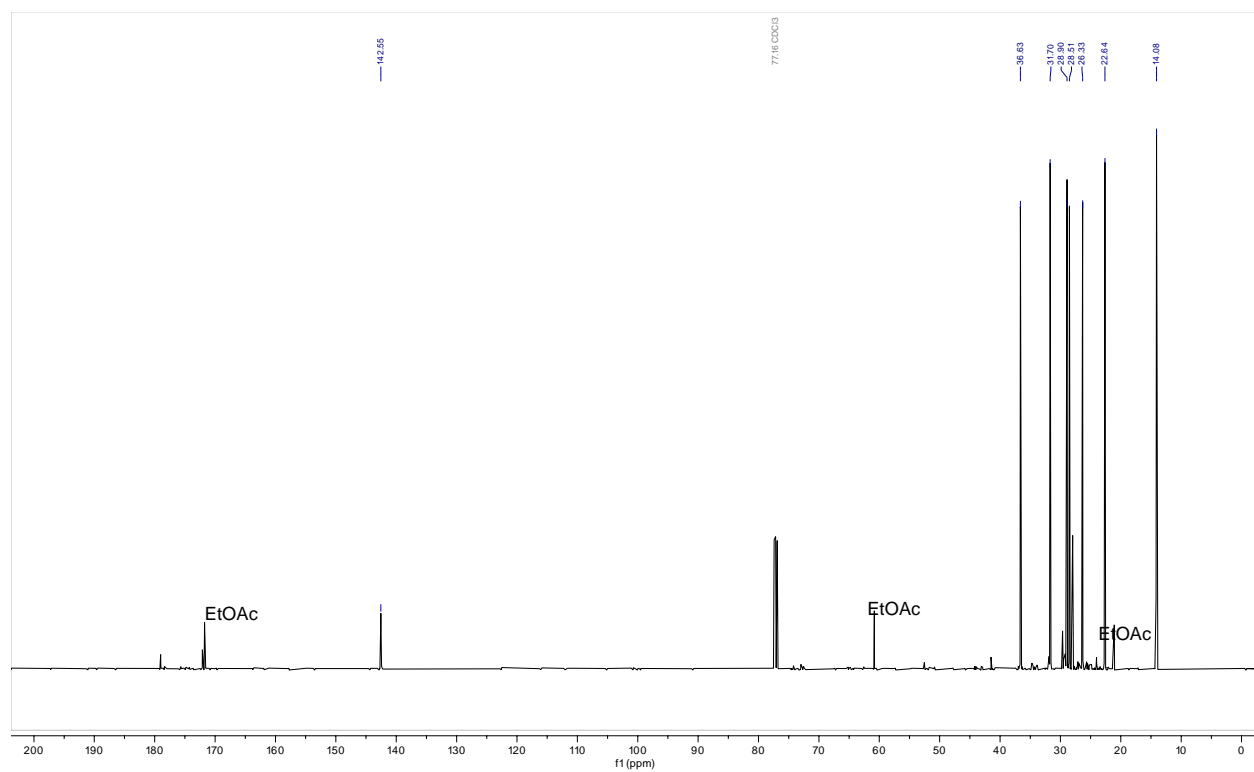
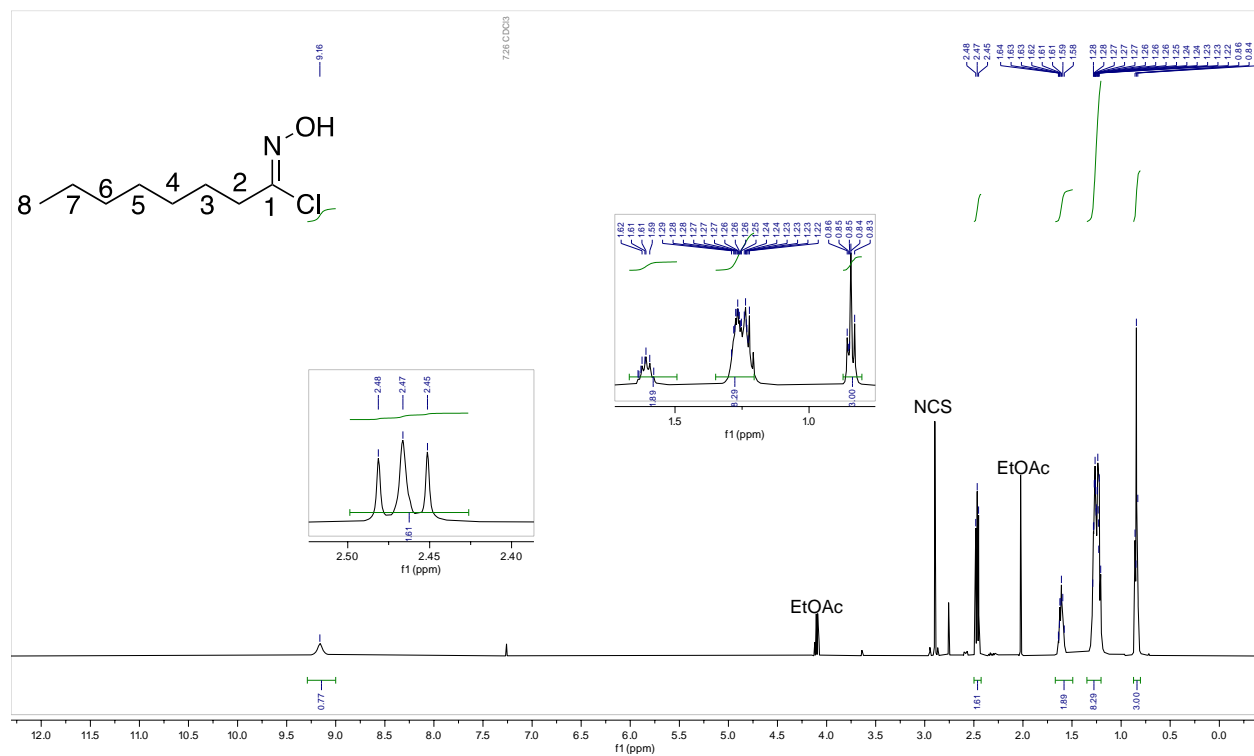
Chemical Structure: 2-(4-fluorophenyl)-2-hydroxypropanenitrile. The structure shows a benzene ring with a fluorine atom at position 4 and a 2-hydroxypropanenitrile group at position 1. Protons are numbered 1 through 6, and the carbon of the nitrile group is numbered 7.

¹H NMR Spectrum (400 MHz, CDCl₃): The spectrum shows peaks for the compound and solvent. The aromatic region (7.1-7.7 ppm) contains multiplets for protons 1-6. The nitrile proton (7.26 ppm) is a singlet. The hydroxyl proton (9.46 ppm) is a broad singlet. The solvent peaks for EtOAc (1.2, 2.0, 2.3 ppm) and DMF (2.9 ppm) are present. Integration values are shown below the peaks.

¹³C NMR Spectrum (100 MHz, CDCl₃): The spectrum shows peaks for the compound and solvent. The aromatic carbons (114-135 ppm) are in the range of 114.25 to 135.03 ppm. The nitrile carbon (118.12 ppm) is a sharp peak. The solvent peaks for EtOAc (12.1, 19.1, 35.1 ppm) and DMF (29.8 ppm) are present.

¹⁵N NMR Spectrum (400 MHz, CDCl₃): The spectrum shows peaks for the compound and solvent. The nitrile nitrogen (112.48 ppm) is a sharp peak. The solvent peaks for EtOAc (12.1, 19.1, 35.1 ppm) and DMF (29.8 ppm) are present.

Compound 3.3f

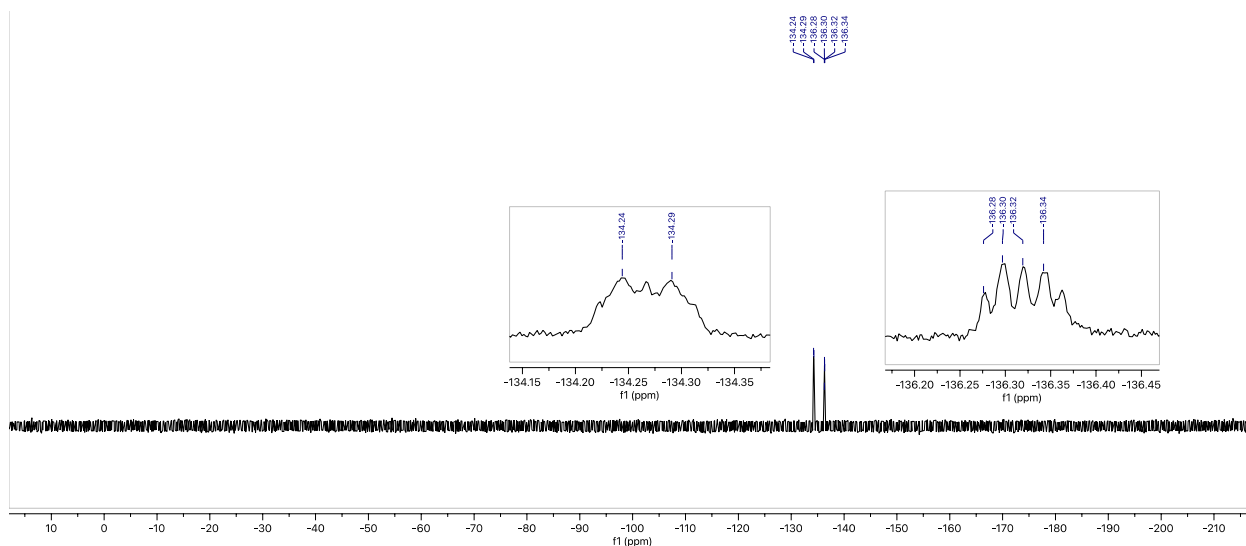
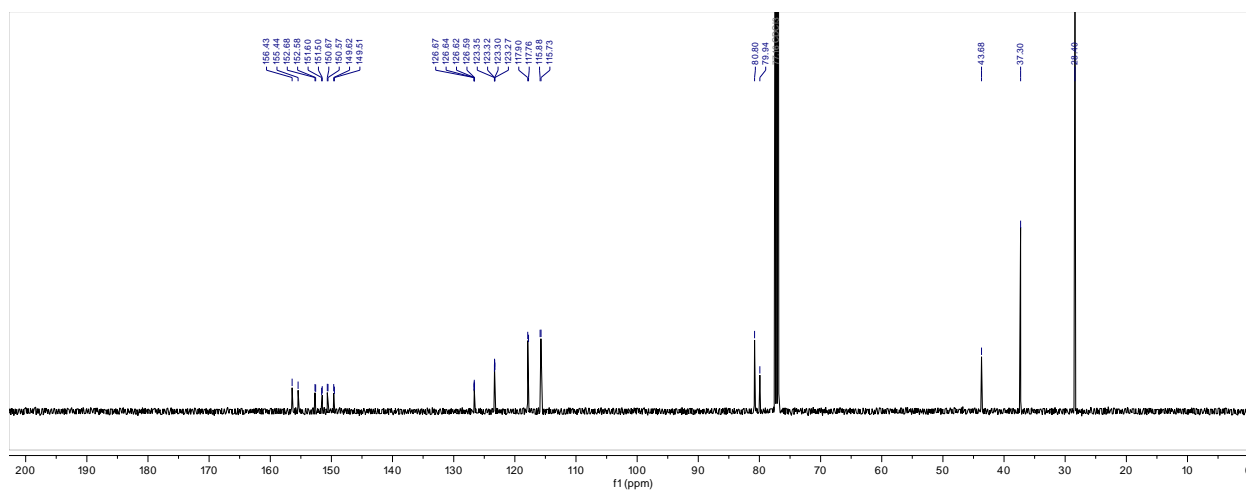
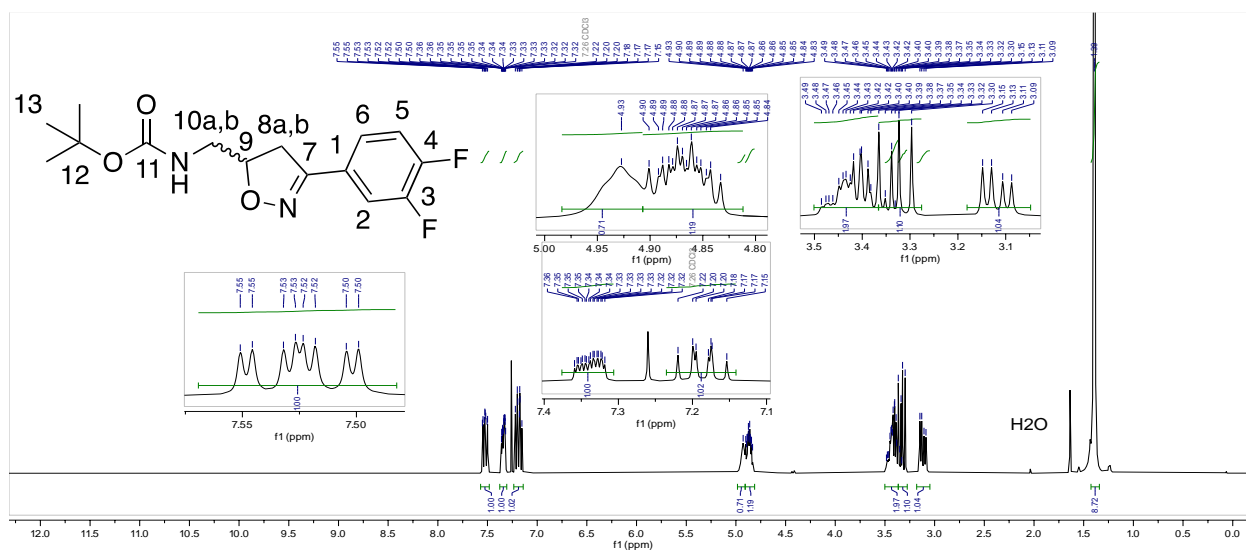


Chemical structure of compound 11 is shown at the top left. The structure is a 4-fluorophenyl group attached to a 5-membered ring containing an oxygen atom and a nitrogen atom. The 5-membered ring is further substituted with a tert-butyl group and a carbonyl group. The atoms are numbered 1 through 11.

¹H NMR (400 MHz, CDCl₃)

Chemical shift (ppm): 8.87, 8.86, 8.85, 8.84, 8.83, 8.82, 8.81, 8.80, 8.79, 8.78, 8.77, 8.76, 8.75, 8.74, 8.73, 8.72, 8.71, 8.70, 8.69, 8.68, 8.67, 8.66, 8.65, 8.64, 8.63, 8.62, 8.61, 8.60, 8.59, 8.58, 8.57, 8.56, 8.55, 8.54, 8.53, 8.52, 8.51, 8.50, 8.49, 8.48, 8.47, 8.46, 8.45, 8.44, 8.43, 8.42, 8.41, 8.40, 8.39, 8.38, 8.37, 8.36, 8.35, 8.34, 8.33, 8.32, 8.31, 8.30, 8.29, 8.28, 8.27, 8.26, 8.25, 8.24, 8.23, 8.22, 8.21, 8.20, 8.19, 8.18, 8.17, 8.16, 8.15, 8.14, 8.13, 8.12, 8.11, 8.10, 8.09, 8.08, 8.07, 8.06, 8.05, 8.04, 8.03, 8.02, 8.01, 8.00, 7.99, 7.98, 7.97, 7.96, 7.95, 7.94, 7.93, 7.92, 7.91, 7.90, 7.89, 7.88, 7.87, 7.86, 7.85, 7.84, 7.83, 7.82, 7.81, 7.80, 7.79, 7.78, 7.77, 7.76, 7.75, 7.74, 7.73, 7.72, 7.71, 7.70, 7.69, 7.68, 7.67, 7.66, 7.65, 7.64, 7.63, 7.62, 7.61, 7.60, 7.59, 7.58, 7.57, 7.56, 7.55, 7.54, 7.53, 7.52, 7.51, 7.50, 7.49, 7.48, 7.47, 7.46, 7.45, 7.44, 7.43, 7.42, 7.41, 7.40, 7.39, 7.38, 7.37, 7.36, 7.35, 7.34, 7.33, 7.32, 7.31, 7.30, 7.29, 7.28, 7.27, 7.26, 7.25, 7.24, 7.23, 7.22, 7.21, 7.20, 7.19, 7.18, 7.17, 7.16, 7.15, 7.14, 7.13, 7.12, 7.11, 7.10, 7.09, 7.08, 7.07, 7.06, 7.05, 7.04, 7.03, 7.02, 7.01, 7.00, 6.99, 6.98, 6.97, 6.96, 6.95, 6.94, 6.93, 6.92, 6.91, 6.90, 6.89, 6.88, 6.87, 6.86, 6.85, 6.84, 6.83, 6.82, 6.81, 6.80, 6.79, 6.78, 6.77, 6.76, 6.75, 6.74, 6.73, 6.72, 6.71, 6.70, 6.69, 6.68, 6.67, 6.66, 6.65, 6.64, 6.63, 6.62, 6.61, 6.60, 6.59, 6.58, 6.57, 6.56, 6.55, 6.54, 6.53, 6.52, 6.51, 6.50, 6.49, 6.48, 6.47, 6.46, 6.45, 6.44, 6.43, 6.42, 6.41, 6.40, 6.39, 6.38, 6.37, 6.36, 6.35, 6.34, 6.33, 6.32, 6.31, 6.30, 6.29, 6.28, 6.27, 6.26, 6.25, 6.24, 6.23, 6.22, 6.21, 6.20, 6.19, 6.18, 6.17, 6.16, 6.15, 6.14, 6.13, 6.12, 6.11, 6.10, 6.09, 6.08, 6.07, 6.06, 6.05, 6.04, 6.03, 6.02, 6.01, 6.00, 5.99, 5.98, 5.97, 5.96, 5.95, 5.94, 5.93, 5.92, 5.91, 5.90, 5.89, 5.88, 5.87, 5.86, 5.85, 5.84, 5.83, 5.82, 5.81, 5.80, 5.79, 5.78, 5.77, 5.76, 5.75, 5.74, 5.73, 5.72, 5.71, 5.70, 5.69, 5.68, 5.67, 5.66, 5.65, 5.64, 5.63, 5.62, 5.61, 5.60, 5.59, 5.58, 5.57, 5.56, 5.55, 5.54, 5.53, 5.52, 5.51, 5.50, 5.49, 5.48, 5.47, 5.46, 5.45, 5.44, 5.43, 5.42, 5.41, 5.40, 5.39, 5.38, 5.37, 5.36, 5.35, 5.34, 5.33, 5.32, 5.31, 5.30, 5.29, 5.28, 5.27, 5.26, 5.25, 5.24, 5.23, 5.22, 5.21, 5.20, 5.19, 5.18, 5.17, 5.16, 5.15, 5.14, 5.13, 5.12, 5.11, 5.10, 5.09, 5.08, 5.07, 5.06, 5.05, 5.04, 5.03, 5.02, 5.01, 5.00, 4.99, 4.98, 4.97, 4.96, 4.95, 4.94, 4.93, 4.92, 4.91, 4.90, 4.89, 4.88, 4.87, 4.86, 4.85, 4.84, 4.83, 4.82, 4.81, 4.80, 4.79, 4.78, 4.77, 4.76, 4.75, 4.74, 4.73, 4.72, 4.71, 4.70, 4.69, 4.68, 4.67, 4.66, 4.65, 4.64, 4.63, 4.62, 4.61, 4.60, 4.59, 4.58, 4.57, 4.56, 4.55, 4.54, 4.53, 4.52, 4.51, 4.50, 4.49, 4.48, 4.47, 4.46, 4.45, 4.44, 4.43, 4.42, 4.41, 4.40, 4.39, 4.38, 4.37, 4.36, 4.35, 4.34, 4.33, 4.32, 4.31, 4.30, 4.29, 4.28, 4.27, 4.26, 4.25, 4.24, 4.23, 4.22, 4.21, 4.20, 4.19, 4.18, 4.17, 4.16, 4.15, 4.14, 4.13, 4.12, 4.11, 4.10, 4.09, 4.08, 4.07, 4.06, 4.05, 4.04, 4.03, 4.02, 4.01, 4.00, 3.99, 3.98, 3.97, 3.96, 3.95, 3.94, 3.93, 3.92, 3.91, 3.90, 3.89, 3.88, 3.87, 3.86, 3.85, 3.84, 3.83, 3.82, 3.81, 3.80, 3.79, 3.78, 3.77, 3.76, 3.75, 3.74, 3.73, 3.72, 3.71, 3.70, 3.69, 3.68, 3.67, 3.66, 3.65, 3.64, 3.63, 3.62, 3.61, 3.60, 3.59, 3.58, 3.57, 3.56, 3.55, 3.54, 3.53, 3.52, 3.51, 3.50, 3.49, 3.48, 3.47, 3.46, 3.45, 3.44, 3.43, 3.42, 3.41, 3.40, 3.39, 3.38, 3.37, 3.36, 3.35, 3.34, 3.33, 3.32, 3.31, 3.30, 3.29, 3.28, 3.27, 3.26, 3.25, 3.24, 3.23, 3.22, 3.21, 3.20, 3.19, 3.18, 3.17, 3.16, 3.15, 3.14, 3.13, 3.12, 3.11, 3.10, 3.09, 3.08, 3.07, 3.06, 3.05, 3.04, 3.03, 3.02, 3.01, 3.00, 2.99, 2.98, 2.97, 2.96, 2.95, 2.94, 2.93, 2.92, 2.91, 2.90, 2.89, 2.88, 2.87, 2.86, 2.85, 2.84, 2.83, 2.82, 2.81, 2.80, 2.79, 2.78, 2.77, 2.76, 2.75, 2.74, 2.73, 2.72, 2.71, 2.70, 2.69, 2.68, 2.67, 2.66, 2.65, 2.64, 2.63, 2.62, 2.61, 2.60, 2.59, 2.58, 2.57, 2.56, 2.55, 2.54, 2.53, 2.52, 2.51, 2.50, 2.49

Compound 3.4b

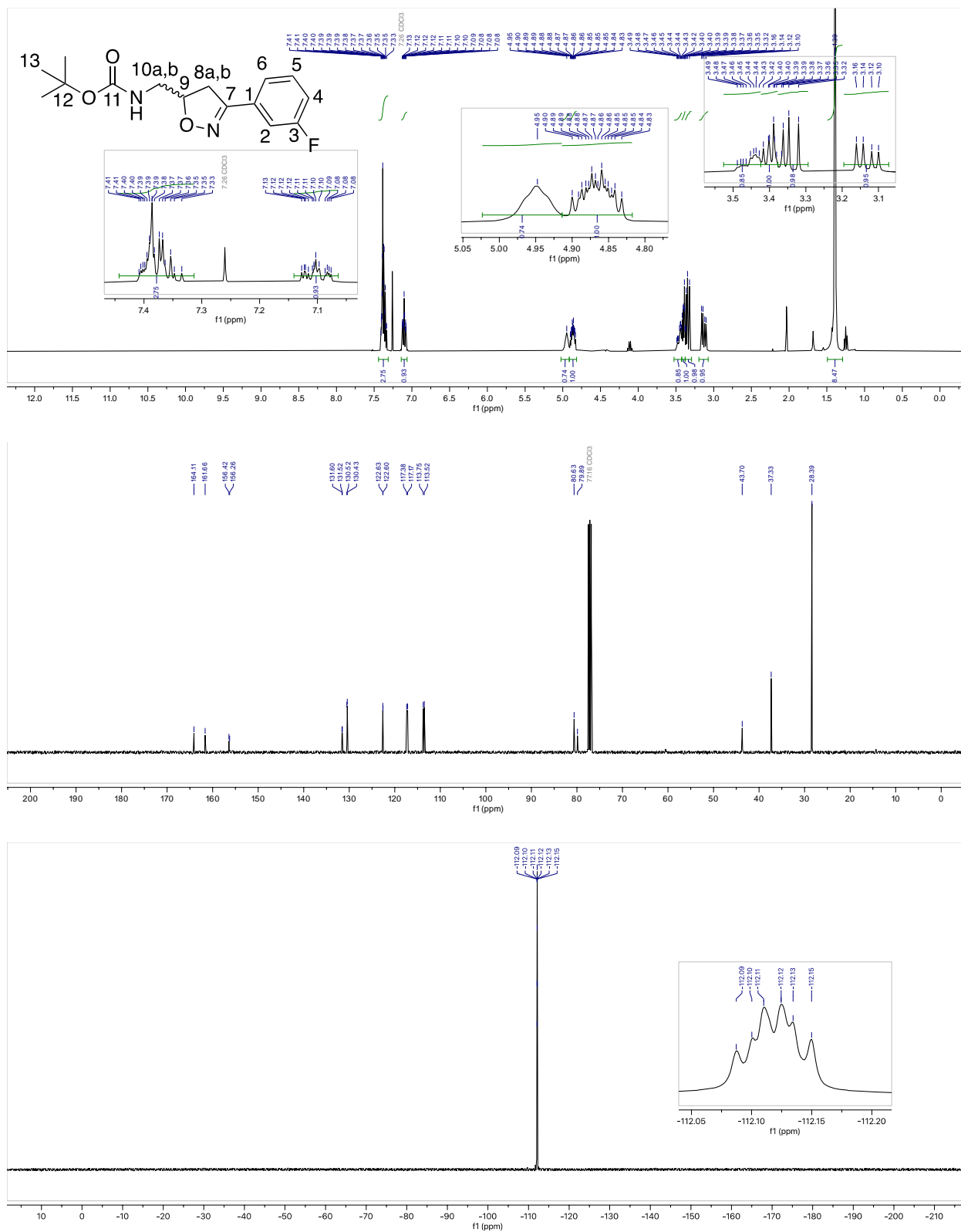


Chemical structure of compound 13 is shown at the top left. The structure is a 2-fluorophenyl derivative with a 1,3-dioxolane ring and a 2,2,4,4-tetramethyl-1,3-dioxolane-5-carboxamide group. The atoms are numbered 1 through 13.

¹H NMR (400 MHz, CDCl₃)

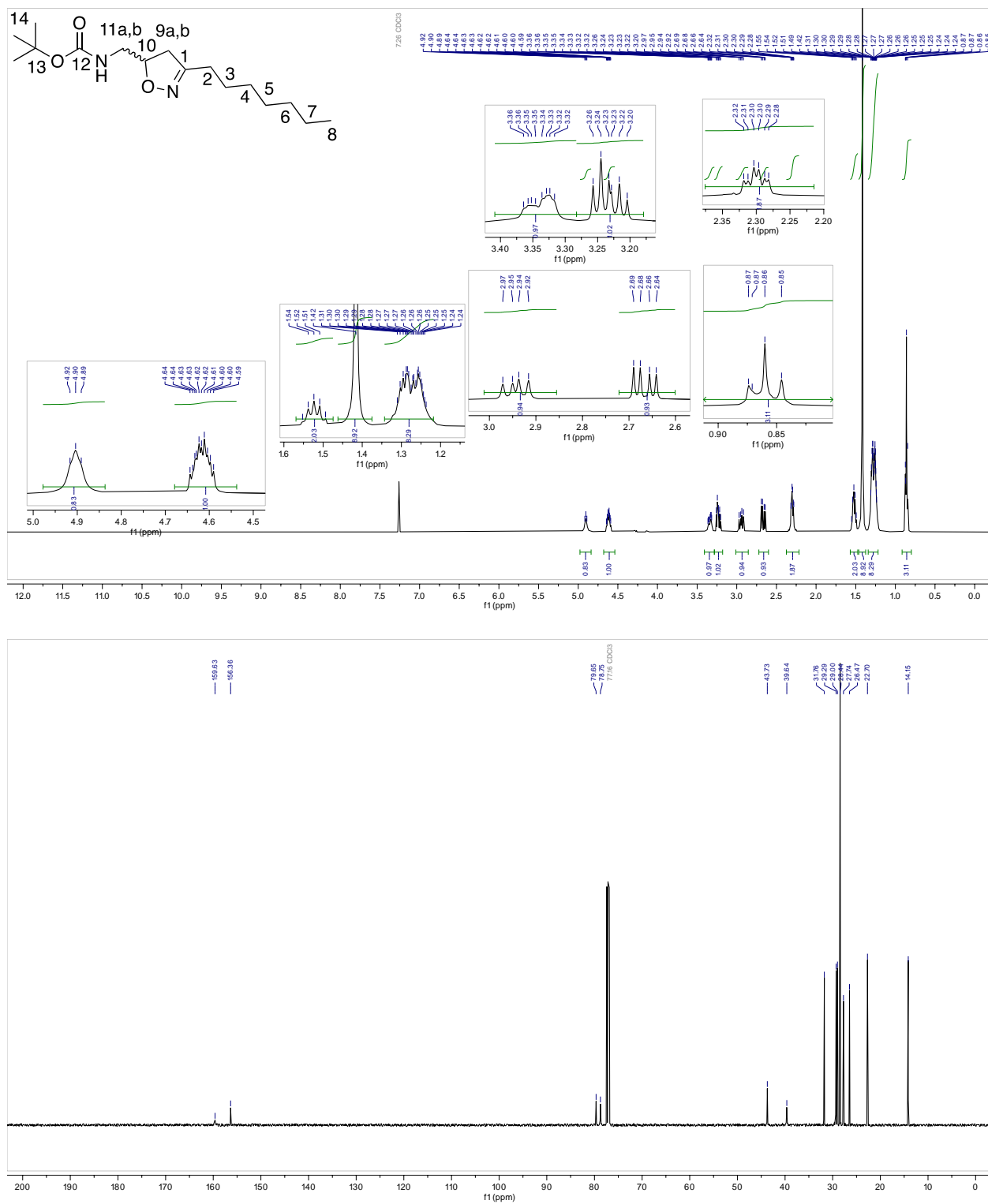
Chemical shift (ppm): 7.81, 7.80, 7.78, 7.77, 7.76, 7.75, 7.74, 7.73, 7.72, 7.71, 7.70, 7.69, 7.68, 7.67, 7.66, 7.65, 7.64, 7.63, 7.62, 7.61, 7.60, 7.59, 7.58, 7.57, 7.56, 7.55, 7.54, 7.53, 7.52, 7.51, 7.50, 7.49, 7.48, 7.47, 7.46, 7.45, 7.44, 7.43, 7.42, 7.41, 7.40, 7.39, 7.38, 7.37, 7.36, 7.35, 7.34, 7.33, 7.32, 7.31, 7.30, 7.29, 7.28, 7.27, 7.26, 7.25, 7.24, 7.23, 7.22, 7.21, 7.20, 7.19, 7.18, 7.17, 7.16, 7.15, 7.14, 7.13, 7.12, 7.11, 7.10, 7.09, 7.08, 7.07, 7.06, 7.05, 7.04, 7.03, 7.02, 7.01, 7.00, 6.99, 6.98, 6.97, 6.96, 6.95, 6.94, 6.93, 6.92, 6.91, 6.90, 6.89, 6.88, 6.87, 6.86, 6.85, 6.84, 6.83, 6.82, 6.81, 6.80, 6.79, 6.78, 6.77, 6.76, 6.75, 6.74, 6.73, 6.72, 6.71, 6.70, 6.69, 6.68, 6.67, 6.66, 6.65, 6.64, 6.63, 6.62, 6.61, 6.60, 6.59, 6.58, 6.57, 6.56, 6.55, 6.54, 6.53, 6.52, 6.51, 6.50, 6.49, 6.48, 6.47, 6.46, 6.45, 6.44, 6.43, 6.42, 6.41, 6.40, 6.39, 6.38, 6.37, 6.36, 6.35, 6.34, 6.33, 6.32, 6.31, 6.30, 6.29, 6.28, 6.27, 6.26, 6.25, 6.24, 6.23, 6.22, 6.21, 6.20, 6.19, 6.18, 6.17, 6.16, 6.15, 6.14, 6.13, 6.12, 6.11, 6.10, 6.09, 6.08, 6.07, 6.06, 6.05, 6.04, 6.03, 6.02, 6.01, 6.00, 5.99, 5.98, 5.97, 5.96, 5.95, 5.94, 5.93, 5.92, 5.91, 5.90, 5.89, 5.88, 5.87, 5.86, 5.85, 5.84, 5.83, 5.82, 5.81, 5.80, 5.79, 5.78, 5.77, 5.76, 5.75, 5.74, 5.73, 5.72, 5.71, 5.70, 5.69, 5.68, 5.67, 5.66, 5.65, 5.64, 5.63, 5.62, 5.61, 5.60, 5.59, 5.58, 5.57, 5.56, 5.55, 5.54, 5.53, 5.52, 5.51, 5.50, 5.49, 5.48, 5.47, 5.46, 5.45, 5.44, 5.43, 5.42, 5.41, 5.40, 5.39, 5.38, 5.37, 5.36, 5.35, 5.34, 5.33, 5.32, 5.31, 5.30, 5.29, 5.28, 5.27, 5.26, 5.25, 5.24, 5.23, 5.22, 5.21, 5.20, 5.19, 5.18, 5.17, 5.16, 5.15, 5.14, 5.13, 5.12, 5.11, 5.10, 5.09, 5.08, 5.07, 5.06, 5.05, 5.04, 5.03, 5.02, 5.01, 5.00, 4.99, 4.98, 4.97, 4.96, 4.95, 4.94, 4.93, 4.92, 4.91, 4.90, 4.89, 4.88, 4.87, 4.86, 4.85, 4.84, 4.83, 4.82, 4.81, 4.80, 4.79, 4.78, 4.77, 4.76, 4.75, 4.74, 4.73, 4.72, 4.71, 4.70, 4.69, 4.68, 4.67, 4.66, 4.65, 4.64, 4.63, 4.62, 4.61, 4.60, 4.59, 4.58, 4.57, 4.56, 4.55, 4.54, 4.53, 4.52, 4.51, 4.50, 4.49, 4.48, 4.47, 4.46, 4.45, 4.44, 4.43, 4.42, 4.41, 4.40, 4.39, 4.38, 4.37, 4.36, 4.35, 4.34, 4.33, 4.32, 4.31, 4.30, 4.29, 4.28, 4.27, 4.26, 4.25, 4.24, 4.23, 4.22, 4.21, 4.20, 4.19, 4.18, 4.17, 4.16, 4.15, 4.14, 4.13, 4.12, 4.11, 4.10, 4.09, 4.08, 4.07, 4.06, 4.05, 4.04, 4.03, 4.02, 4.01, 4.00, 3.99, 3.98, 3.97, 3.96, 3.95, 3.94, 3.93, 3.92, 3.91, 3.90, 3.89, 3.88, 3.87, 3.86, 3.85, 3.84, 3.83, 3.82, 3.81, 3.80, 3.79, 3.78, 3.77, 3.76, 3.75, 3.74, 3.73, 3.72, 3.71, 3.70, 3.69, 3.68, 3.67, 3.66, 3.65, 3.64, 3.63, 3.62, 3.61, 3.60, 3.59, 3.58, 3.57, 3.56, 3.55, 3.54, 3.53, 3.52, 3.51, 3.50, 3.49, 3.48, 3.47, 3.46, 3.45, 3.44, 3.43, 3.42, 3.41, 3.40, 3.39, 3.38, 3.37, 3.36, 3.35, 3.34, 3.33, 3.32, 3.31, 3.30, 3.29, 3.28, 3.27, 3.26, 3.25, 3.24, 3.23, 3.22, 3.21, 3.20, 3.19, 3.18, 3.17, 3.16, 3.15, 3.14, 3.13, 3.12, 3.11, 3.10, 3.09, 3.08, 3.07, 3.06, 3.05, 3.04, 3.03, 3.02, 3.01, 3.00, 2.99, 2.98, 2.97, 2.96, 2.95, 2.94, 2.93, 2.92, 2.91, 2.90, 2.89, 2.88, 2.87, 2.86, 2.85, 2.84, 2.83, 2.82, 2.81, 2.80, 2.79, 2.78, 2.77, 2.76, 2.75, 2.74, 2.73, 2.72, 2.71, 2.70, 2.69, 2.68, 2.67, 2.66, 2.65, 2.64, 2.63, 2.62, 2.61, 2.60, 2.59, 2.58, 2.57, 2.56, 2.55, 2.54, 2.53, 2.52, 2.51, 2.50, 2.49, 2.48, 2.47, 2.46, 2.45, 2.44, 2.43, 2.42, 2.41, 2.40, 2.39, 2.38, 2.37, 2.36, 2.35, 2.34, 2.33, 2.32, 2.31, 2.30, 2.29, 2.28, 2.27, 2.26, 2.25, 2.24, 2.23, 2.22, 2.21, 2.20, 2.19, 2.18, 2.17, 2.16, 2.15, 2.14, 2.13, 2.12, 2.11, 2.10, 2.09, 2.08, 2.07, 2.06, 2.05, 2.04, 2.03, 2.02, 2.01, 2.00, 1.99, 1.98, 1.97, 1.96, 1.95, 1.94, 1.93, 1.92, 1.91, 1.90, 1.89, 1.88, 1.87, 1.86, 1.85, 1.84, 1.83, 1.82, 1.81, 1.80, 1.79, 1.78, 1.77, 1.76, 1.75, 1.74, 1.73, 1.72, 1.71, 1.70, 1.69, 1.68, 1.67, 1.66, 1.65, 1.6

Compound 3.4d

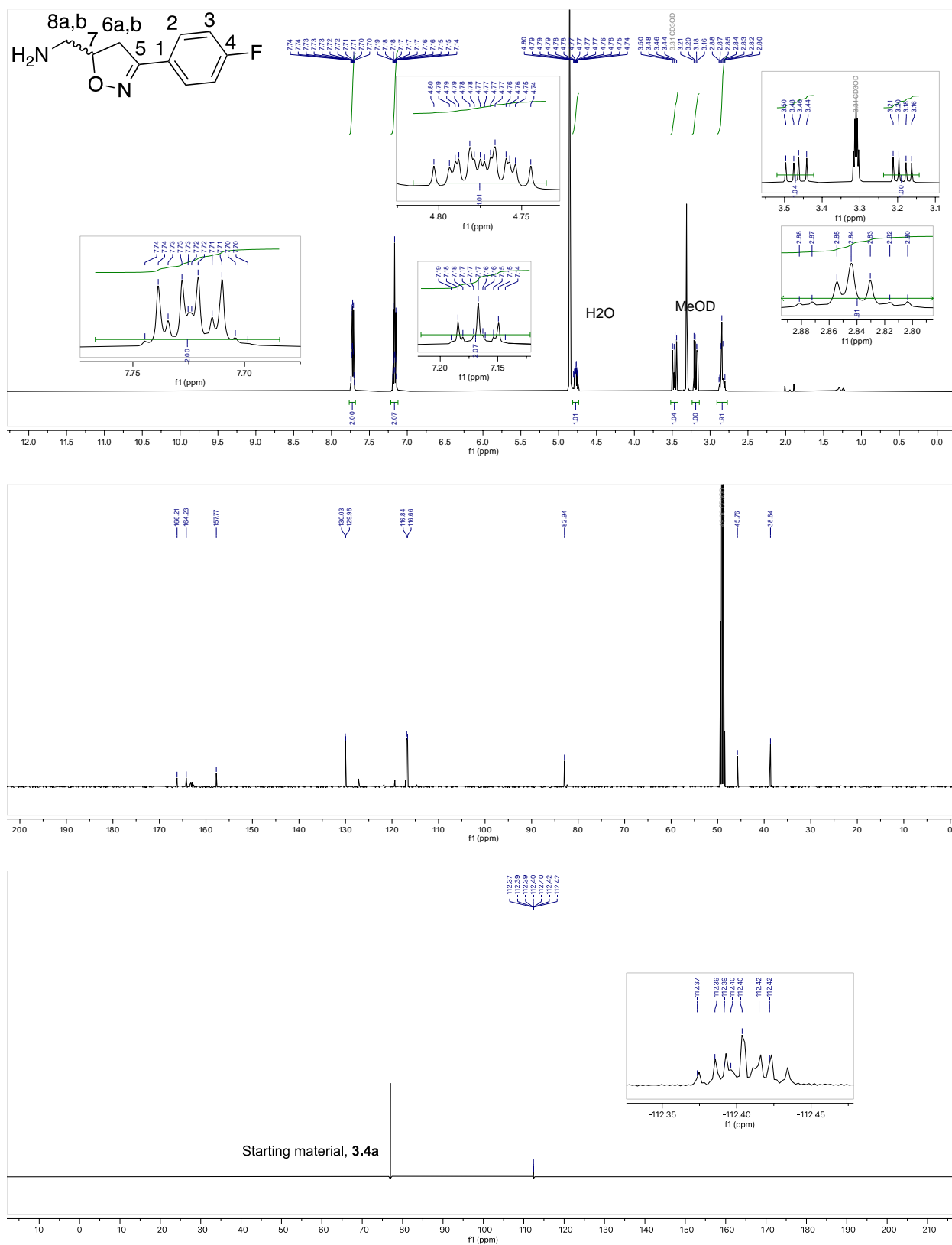


[illegible]

Compound 3.4f



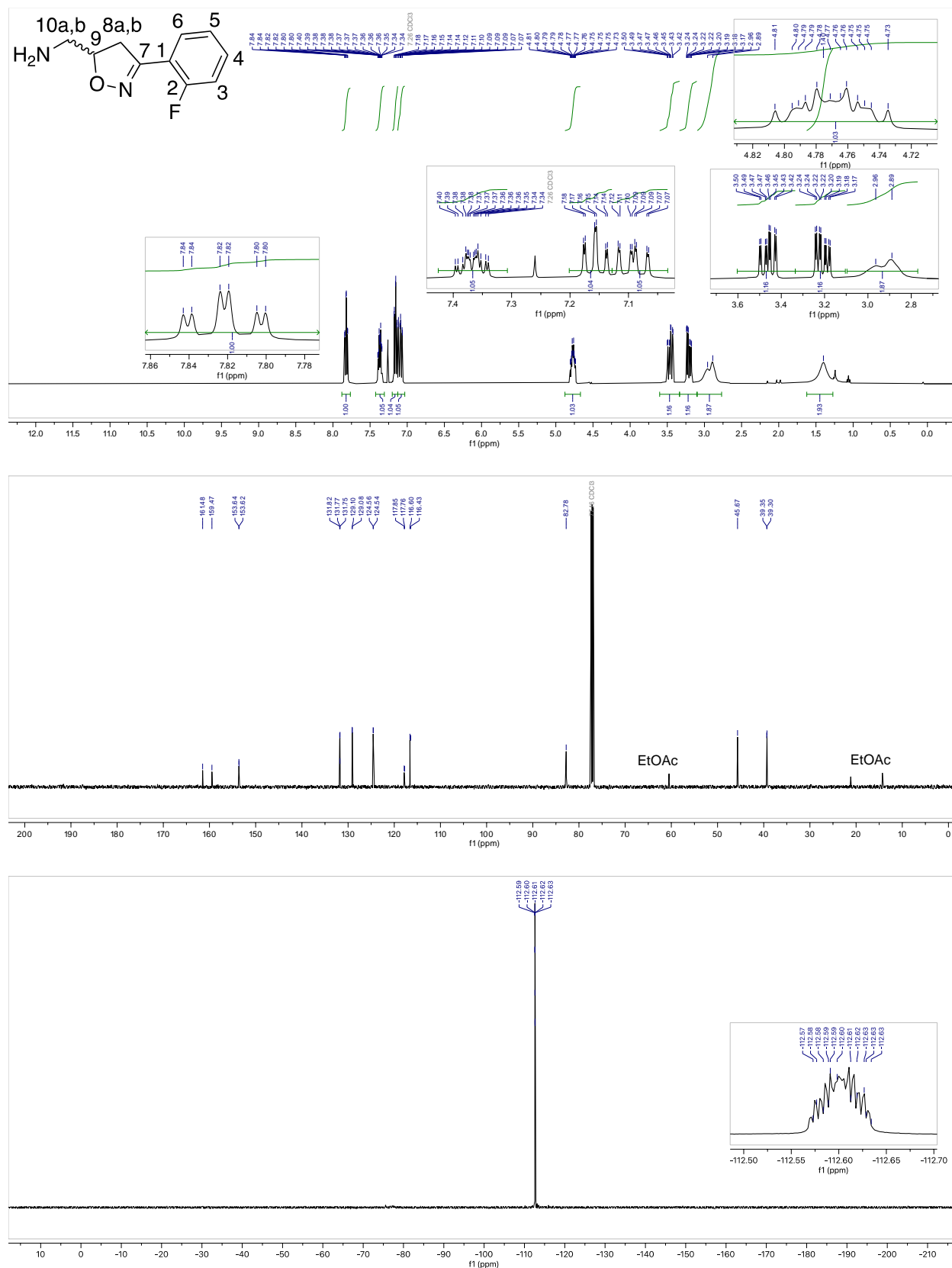
Compound 3.5a



Chemical structure of 10a,b is shown in the top left corner. The structure is a 2,4-difluorophenyl derivative with a 1,3,4-oxadiazole ring and a 10a,b label. The structure is labeled with 10a,b, 8a,b, 6, 5, 4, 3, 2, 1, 7, 9, and 10a,b.

¹H NMR (400 MHz, DMSO-d₆) spectrum (top) shows peaks at 8.00 (d, 1H), 7.87 (d, 1H), 7.85 (d, 1H), 7.84 (d, 1H), 7.83 (d, 1H), 7.74 (d, 1H), 7.70 (d, 1H), 7.68 (d, 1H), 7.67 (d, 1H), 7.66 (d, 1H), 7.65 (d, 1H), 4.87 (d, 1H), 4.86 (d, 1H), 4.85 (d, 1H), 4.84 (d, 1H), 4.83 (d, 1H), 4.82 (d, 1H), 3.57 (d, 1H), 3.55 (d, 1H), 3.51 (d, 1H), 3.42 (d, 1H), 3.38 (d, 1H), 3.37 (d, 1H), 3.33 (d, 1H), 2.97 (d, 1H), 2.95 (d, 1H), 2.93 (d, 1H), 2.92 (d, 1H), 2.91 (d, 1H), 2.90 (d, 1H), 2.89 (d, 1H), 2.88 (d, 1H), 2.87 (d, 1H), 2.86 (d, 1H), 2.85 (d, 1H), 2.84 (d, 1H), 2.83 (d, 1H), 2.82 (d, 1H), 2.81 (d, 1H), 2.80 (d, 1H), 2.79 (d, 1H), 2.78 (d, 1H), 2.77 (d, 1H), 2.76 (d, 1H), 2.75 (d, 1H), 2.74 (d, 1H), 2.73 (d, 1H), 2.72 (d, 1H), 2.71 (d, 1H), 2.70 (d, 1H), 2.69 (d, 1H), 2.68 (d, 1H), 2.67 (d, 1H), 2.66 (d, 1H), 2.65 (d, 1H), 2.64 (d, 1H), 2.63 (d, 1H), 2.62 (d, 1H), 2.61 (d, 1H), 2.60 (d, 1H), 2.59 (d, 1H), 2.58 (d, 1H), 2.57 (d, 1H), 2.56 (d, 1H), 2.55 (d, 1H), 2.54 (d, 1H), 2.53 (d, 1H), 2.52 (d, 1H), 2.51 (d, 1H), 2.50 (d, 1H), 2.49 (d, 1H), 2.48 (d, 1H), 2.47 (d, 1H), 2.46 (d, 1H), 2.45 (d, 1H), 2.44 (d, 1H), 2.43 (d, 1H), 2.42 (d, 1H), 2.41 (d, 1H), 2.40 (d, 1H), 2.39 (d, 1H), 2.38 (d, 1H), 2.37 (d, 1H), 2.36 (d, 1H), 2.35 (d, 1H), 2.34 (d, 1H), 2.33 (d, 1H), 2.32 (d, 1H), 2.31 (d, 1H), 2.30 (d, 1H), 2.29 (d, 1H), 2.28 (d, 1H), 2.27 (d, 1H), 2.26 (d, 1H), 2.25 (d, 1H), 2.24 (d, 1H), 2.23 (d, 1H), 2.22 (d, 1H), 2.21 (d, 1H), 2.20 (d, 1H), 2.19 (d, 1H), 2.18 (d, 1H), 2.17 (d, 1H), 2.16 (d, 1H), 2.15 (d, 1H), 2.14 (d, 1H), 2.13 (d, 1H), 2.12 (d, 1H), 2.11 (d, 1H), 2.10 (d, 1H), 2.09 (d, 1H), 2.08 (d, 1H), 2.07 (d, 1H), 2.06 (d, 1H), 2.05 (d, 1H), 2.04 (d, 1H), 2.03 (d, 1H), 2.02 (d, 1H), 2.01 (d, 1H), 2.00 (d, 1H), 1.99 (d, 1H), 1.98 (d, 1H), 1.97 (d, 1H), 1.96 (d, 1H), 1.95 (d, 1H), 1.94 (d, 1H), 1.93 (d, 1H), 1.92 (d, 1H), 1.91 (d, 1H), 1.90 (d, 1H), 1.89 (d, 1H), 1.88 (d, 1H), 1.87 (d, 1H), 1.86 (d, 1H), 1.85 (d, 1H), 1.84 (d, 1H), 1.83 (d, 1H), 1.82 (d, 1H), 1.81 (d, 1H), 1.80 (d, 1H), 1.79 (d, 1H), 1.78 (d, 1H), 1.77 (d, 1H), 1.76 (d, 1H), 1.75 (d, 1H), 1.74 (d, 1H), 1.73 (d, 1H), 1.72 (d, 1H), 1.71 (d, 1H), 1.70 (d, 1H), 1.69 (d, 1H), 1.68 (d, 1H), 1.67 (d, 1H), 1.66 (d, 1H), 1.65 (d, 1H), 1.64 (d, 1H), 1.63 (d, 1H), 1.62 (d, 1H), 1.61 (d, 1H), 1.60 (d, 1H), 1.59 (d, 1H), 1.58 (d, 1H), 1.57 (d, 1H), 1.56 (d, 1H), 1.55 (d, 1H), 1.54 (d, 1H), 1.53 (d, 1H), 1.52 (d, 1H), 1.51 (d, 1H), 1.50 (d, 1H), 1.49 (d, 1H), 1.48 (d, 1H), 1.47 (d, 1H), 1.46 (d, 1H), 1.45 (d, 1H), 1.44 (d, 1H), 1.43 (d, 1H), 1.42 (d, 1H), 1.41 (d, 1H), 1.40 (d, 1H), 1.39 (d, 1H), 1.38 (d, 1H), 1.37 (d, 1H), 1.36 (d, 1H), 1.35 (d, 1H), 1.34 (d, 1H), 1.33 (d, 1H), 1.32 (d, 1H), 1.31 (d, 1H), 1.30 (d, 1H), 1.29 (d, 1H), 1.28 (d, 1H), 1.27 (d, 1H), 1.26 (d, 1H), 1.25 (d, 1H), 1.24 (d, 1H), 1.23 (d, 1H), 1.22 (d, 1H), 1.21 (d, 1H), 1.20 (d, 1H), 1.19 (d, 1H), 1.18 (d, 1H), 1.17 (d, 1H), 1.16 (d, 1H), 1.15 (d, 1H), 1.14 (d, 1H), 1.13 (d, 1H), 1.12 (d, 1H), 1.11 (d, 1H), 1.10 (d, 1H), 1.09 (d, 1H), 1.08 (d, 1H), 1.07 (d, 1H), 1.06 (d, 1H), 1.05 (d, 1H), 1.04 (d, 1H), 1.03 (d, 1H), 1.02 (d, 1H), 1.01 (d, 1H), 1.00 (d, 1H), 0.99 (d, 1H), 0.98 (d, 1H), 0.97 (d, 1H), 0.96 (d, 1H), 0.95 (d, 1H), 0.94 (d, 1H), 0.93 (d, 1H), 0.92 (d, 1H), 0.91 (d, 1H), 0.90 (d, 1H), 0.89 (d, 1H), 0.88 (d, 1H), 0.87 (d, 1H), 0.86 (d, 1H), 0.85 (d, 1H), 0.84 (d, 1H), 0.83 (d, 1H), 0.82 (d, 1H), 0.81 (d, 1H), 0.80 (d, 1H), 0.79 (d, 1H), 0.78 (d, 1H), 0.77 (d, 1H), 0.76 (d, 1H), 0.75 (d, 1H), 0.74 (d, 1H), 0.73 (d, 1H), 0.72 (d, 1H), 0.71 (d, 1H), 0.70 (d, 1H), 0.69 (d, 1H), 0.68 (d, 1H), 0.67 (d, 1H), 0.66 (d, 1H), 0.65 (d, 1H), 0.64 (d, 1H), 0.63 (d, 1H), 0.62 (d, 1H), 0.61 (d, 1H), 0.60 (d, 1H), 0.59 (d, 1H), 0.58 (d, 1H), 0.57 (d, 1H), 0.56 (d, 1H), 0.55 (d, 1H), 0.54 (d, 1H), 0.53 (d, 1H), 0.52 (d, 1H), 0.51 (d, 1H), 0.50 (d, 1H), 0.49 (d, 1H), 0.48 (d, 1H), 0.47 (d, 1H), 0.46 (d, 1H), 0.45 (d, 1H), 0.44 (d, 1H), 0.43 (d, 1H), 0.42 (d, 1H), 0.41 (d, 1H), 0.40 (d, 1H), 0.39 (d, 1H), 0.38 (d, 1H), 0.37 (d, 1H), 0.36 (d, 1H), 0.35 (d, 1H), 0.34 (d, 1H), 0.33 (d, 1H), 0.32 (d, 1H), 0.31 (d, 1H), 0.30 (d, 1H), 0.29 (d, 1H), 0.28 (d, 1H), 0.27 (d, 1H), 0.26 (d, 1H), 0.25 (d, 1H), 0.24 (d, 1H), 0.23 (d, 1H), 0.22 (d, 1H), 0.21 (d, 1H), 0.20 (d, 1H), 0.19 (d, 1H), 0.18 (d, 1H), 0.17 (d, 1H), 0.16 (d, 1H), 0.15 (d, 1H), 0.14 (d, 1H), 0.13 (d, 1H), 0.12 (d, 1H), 0.11 (d, 1H), 0.10 (d, 1H), 0.09 (d, 1H), 0.08 (d, 1H), 0.07 (d, 1H), 0.06 (d, 1H), 0.05 (d, 1H), 0.04 (d, 1H), 0.03 (d, 1H), 0.02 (d, 1

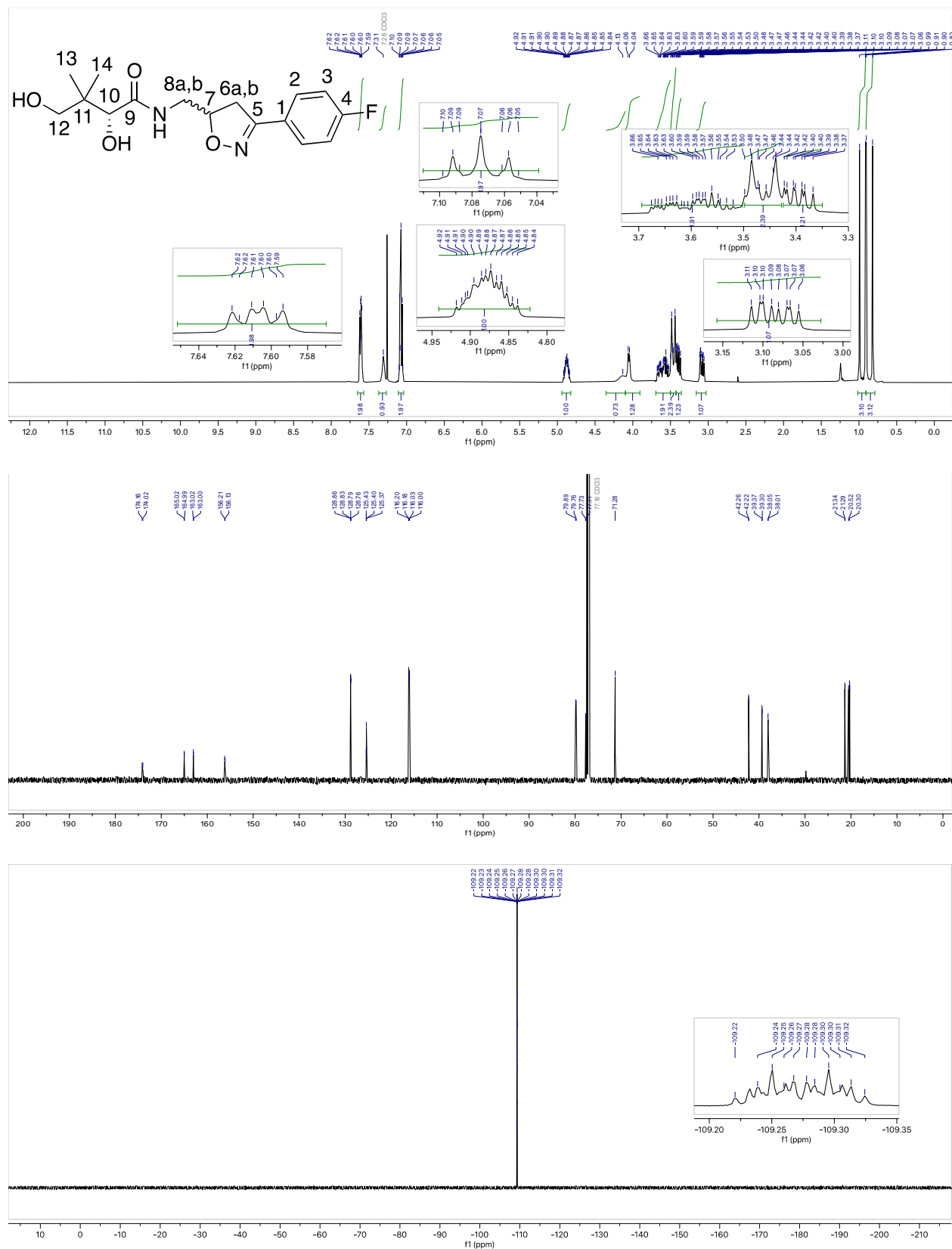
Compound 3.5c



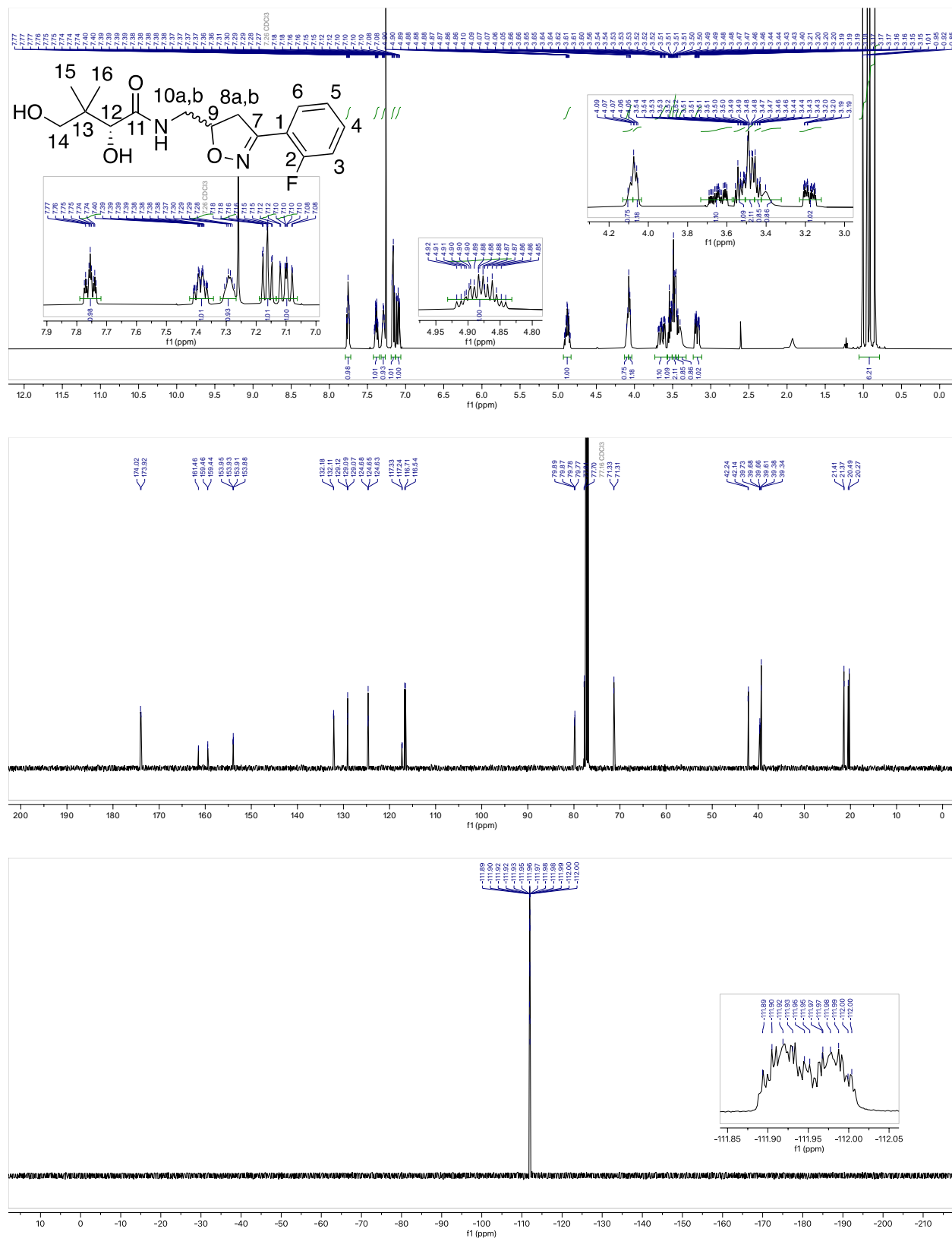
Chemical structure of compound 10a,b is shown in the top left corner. The structure is a 2,4-difluorophenyl derivative with a 1,2,3,4-tetrahydro-1H-benzoxazole ring system. The numbering of the atoms is as follows: 10a,b (NH₂), 8a,b (CH₂), 6 (CH), 5 (CH), 4 (CH), 3 (CH), 2 (CH), 1 (CH), 7 (CH), 9 (CH), and 10 (CH).

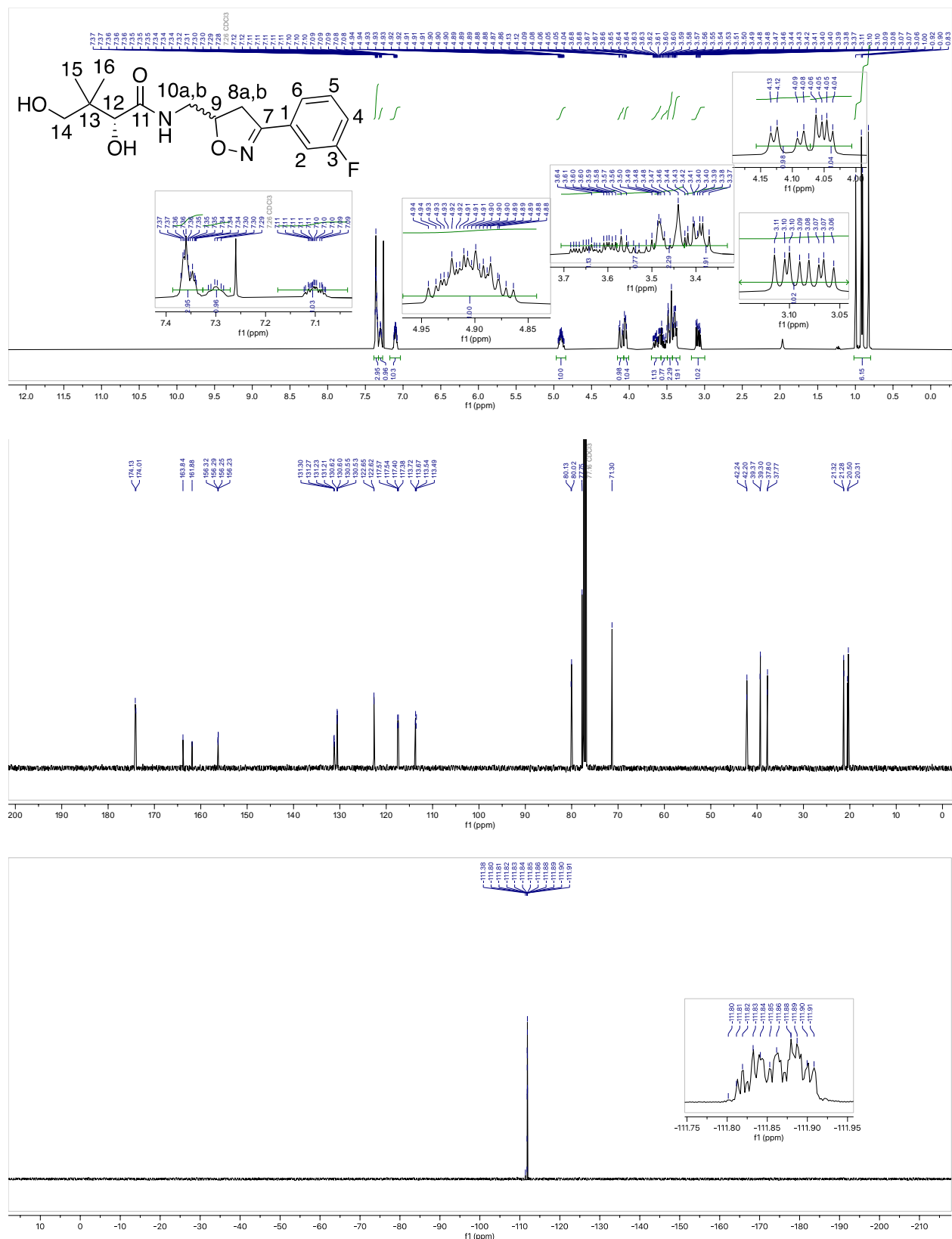
The ¹H NMR spectrum (top) shows peaks in the aromatic region (6.8-7.5 ppm) and aliphatic region (2.8-3.4 ppm). The ¹³C NMR spectrum (bottom) shows peaks in the aromatic region (112-183 ppm) and aliphatic region (45-57 ppm).

¹H NMR (400 MHz, CDCl₃) peaks (ppm): 7.42, 7.41, 7.40, 7.39, 7.38, 7.37, 7.36, 7.35, 7.34, 7.33, 7.32, 7.31, 7.30, 7.29, 7.28, 7.27, 7.26, 7.25, 7.24, 7.23, 7.22, 7.21, 7.20, 7.19, 7.18, 7.17, 7.16, 7.15, 7.14, 7.13, 7.12, 7.11, 7.10, 7.09, 7.08, 7.07, 7.06, 7.05, 7.04, 7.03, 7.02, 7.01, 7.00, 6.99, 6.98, 6.97, 6.96, 6.95, 6.94, 6.93, 6.92, 6.91, 6.90, 6.89, 6.88, 6.87, 6.86, 6.85, 6.84, 6.83, 6.82, 6.81, 6.80, 6.79, 6.78, 6.77, 6.76, 6.75, 6.74, 6.73, 6.72, 6.71, 6.70, 6.69, 6.68, 6.67, 6.66, 6.65, 6.64, 6.63, 6.62, 6.61, 6.60, 6.59, 6.58, 6.57, 6.56, 6.55, 6.54, 6.53, 6.52, 6.51, 6.50, 6.49, 6.48, 6.47, 6.46, 6.45, 6.44, 6.43, 6.42, 6.41, 6.40, 6.39, 6.38, 6.37, 6.36, 6.35, 6.34, 6.33, 6.32, 6.31, 6.30, 6.29, 6.28, 6.27, 6.26, 6.25, 6.24, 6.23, 6.22, 6.21, 6.20, 6.19, 6.18, 6.17, 6.16, 6.15, 6.14, 6.13, 6.12, 6.11, 6.10, 6.09, 6.08, 6.07, 6.06, 6.05, 6.04, 6.03, 6.02, 6.01, 6.00, 5.99, 5.98, 5.97, 5.96, 5.95, 5.94, 5.93, 5.92, 5.91, 5.90, 5.89, 5.88, 5.87, 5.86, 5.85, 5.84, 5.83, 5.82, 5.81, 5.80, 5.79, 5.78, 5.77, 5.76, 5.75, 5.74, 5.73, 5.72, 5.71, 5.70, 5.69, 5.68, 5.67, 5.66, 5.65, 5.64, 5.63, 5.62, 5.61, 5.60, 5.59, 5.58, 5.57, 5.56, 5.55, 5.54, 5.53, 5.52, 5.51, 5.50, 5.49, 5.48, 5.47, 5.46, 5.45, 5.44, 5.43, 5.42, 5.41, 5.40, 5.39, 5.38, 5.37, 5.36, 5.35, 5.34, 5.33, 5.32, 5.31, 5.30, 5.29, 5.28, 5.27, 5.26, 5.25, 5.24, 5.23, 5.22, 5.21, 5.20, 5.19, 5.18, 5.17, 5.16, 5.15, 5.14, 5.13, 5.12, 5.11, 5.10, 5.09, 5.08, 5.07, 5.06, 5.05, 5.04, 5.03, 5.02, 5.01, 5.00, 4.99, 4.98, 4.97, 4.96, 4.95, 4.94, 4.93, 4.92, 4.91, 4.90, 4.89, 4.88, 4.87, 4.86, 4.85, 4.84, 4.83, 4.82, 4.81, 4.80, 4.79, 4.78, 4.77, 4.76, 4.75, 4.74, 4.73, 4.72, 4.71, 4.70, 4.69, 4.68, 4.67, 4.66, 4.65, 4.64, 4.63, 4.62, 4.61, 4.60, 4.59, 4.58, 4.57, 4.56, 4.55, 4.54, 4.53, 4.52, 4.51, 4.50, 4.49, 4.48, 4.47, 4.46, 4.45, 4.44, 4.43, 4.42, 4.41, 4.40, 4.39, 4.38, 4.37, 4.36, 4.35, 4.34, 4.33, 4.32, 4.31, 4.30, 4.29, 4.28, 4.27, 4.26, 4.25, 4.24, 4.23, 4.22, 4.21, 4.20, 4.19, 4.18, 4.17, 4.16, 4.15, 4.14, 4.13, 4.12, 4.11, 4.10, 4.09, 4.08, 4.07, 4.06, 4.05, 4.04, 4.03, 4.02, 4.01, 4.00, 3.99, 3.98, 3.97, 3.96, 3.95, 3.94, 3.93, 3.92, 3.91, 3.90, 3.89, 3.88, 3.87, 3.86, 3.85, 3.84, 3.83, 3.82, 3.81, 3.80, 3.79, 3.78, 3.77, 3.76, 3.75, 3.74, 3.73, 3.72, 3.71, 3.70, 3.69, 3.68, 3.67, 3.66, 3.65, 3.64, 3.63, 3.62, 3.61, 3.60, 3.59, 3.58, 3.57, 3.56, 3.55, 3.54, 3.53, 3.52, 3.51, 3.50, 3.49, 3.48, 3.47, 3.46, 3.45, 3.44, 3.43, 3.42, 3.41, 3.40, 3.39, 3.38, 3.37, 3.36, 3.35, 3.34, 3.33, 3.32, 3.31, 3.30, 3.29, 3.28, 3.27, 3.26, 3.25, 3.24, 3.23, 3.22, 3.21, 3.20, 3.19, 3.18, 3.17, 3.16, 3.15, 3.14, 3.13, 3.12, 3.11, 3.10, 3.09, 3.08, 3.07, 3.06, 3.05, 3.04, 3.03, 3.02, 3.01, 3.00, 2.99, 2.98, 2.97, 2.96, 2.95, 2.94, 2.93, 2.92, 2.91, 2.90, 2.89, 2.88, 2.87, 2.86, 2.85, 2.84, 2.83, 2.82, 2.81, 2.80, 2.79, 2.78, 2.77, 2.76, 2.75, 2.74, 2.73, 2.72, 2.71, 2.70, 2.69, 2.68, 2.67, 2.66, 2.65, 2.64, 2.63, 2.62, 2.61, 2.60, 2.59, 2.58, 2.57, 2.56, 2.55, 2.54, 2.53, 2.52, 2.51, 2.50, 2.49, 2.48, 2.47, 2.46, 2.45, 2.44, 2.43, 2.42, 2.41, 2.40, 2.39, 2.38, 2.37, 2.36, 2.35, 2.34, 2.33, 2.32, 2.31, 2.30, 2.29, 2.28, 2.27, 2.26, 2.25, 2.24, 2.23, 2.22, 2.21, 2.20, 2.19, 2.18, 2.17, 2.16, 2.15, 2.14, 2.13, 2.12, 2.11, 2.10, 2.09, 2.08, 2.07, 2.06, 2.05, 2.04, 2.03, 2.02, 2.01, 2.00, 1.99, 1.98, 1.97, 1.96, 1.95, 1.94, 1.93, 1.92, 1.91, 1.90, 1.89, 1.88, 1.87, 1.86, 1.85, 1.84, 1.83, 1.82, 1.81, 1.80, 1.79, 1.78, 1.77, 1.76, 1.75, 1.74, 1.73, 1.72, 1.71, 1.70, 1.69, 1.68, 1.67, 1.66, 1.65, 1.64, 1.63, 1.62, 1.61, 1.60, 1.59, 1.58, 1.57, 1.56, 1.55, 1.54, 1.53, 1.52, 1.51, 1.50, 1.49, 1.48, 1.47, 1.46, 1.45, 1.44, 1.43, 1.42, 1.41, 1.40, 1.39, 1.38, 1.37, 1.36, 1.35, 1.34, 1.33, 1.32, 1.31, 1.30, 1.29, 1.28, 1.27, 1.26, 1.25, 1.24, 1.23, 1.22,

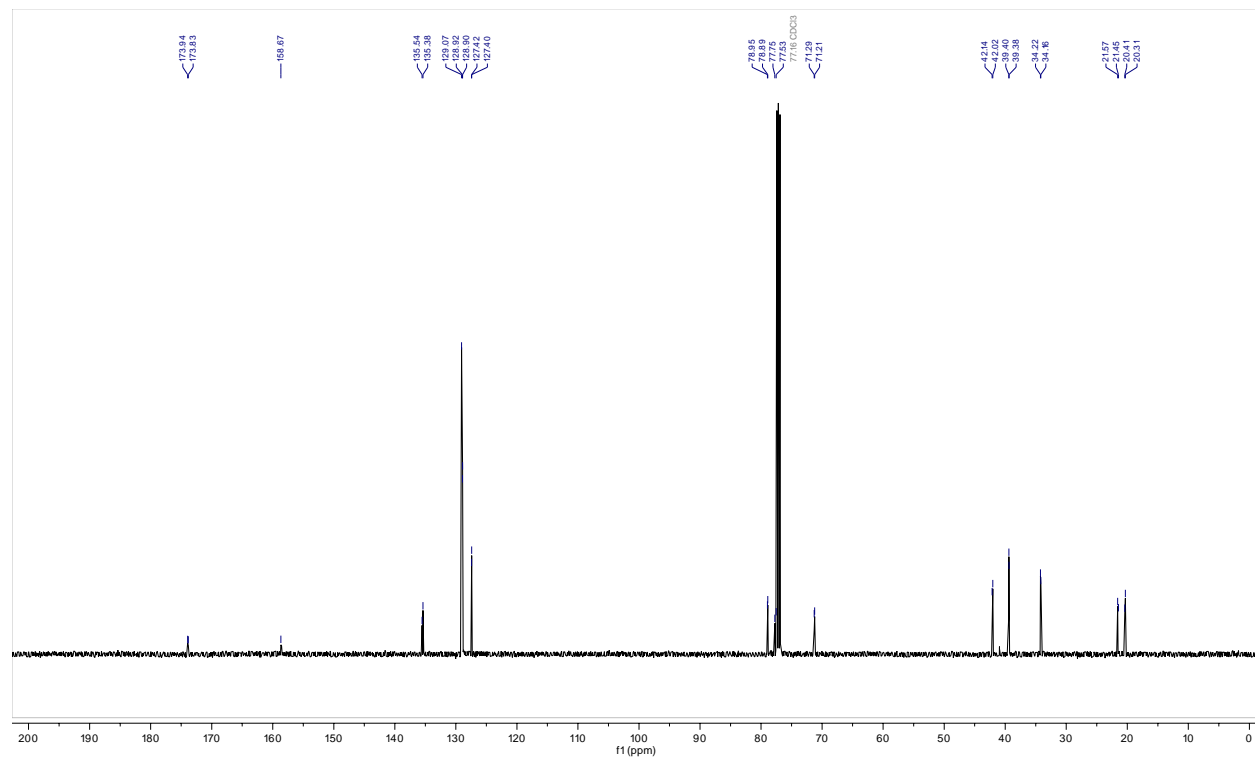
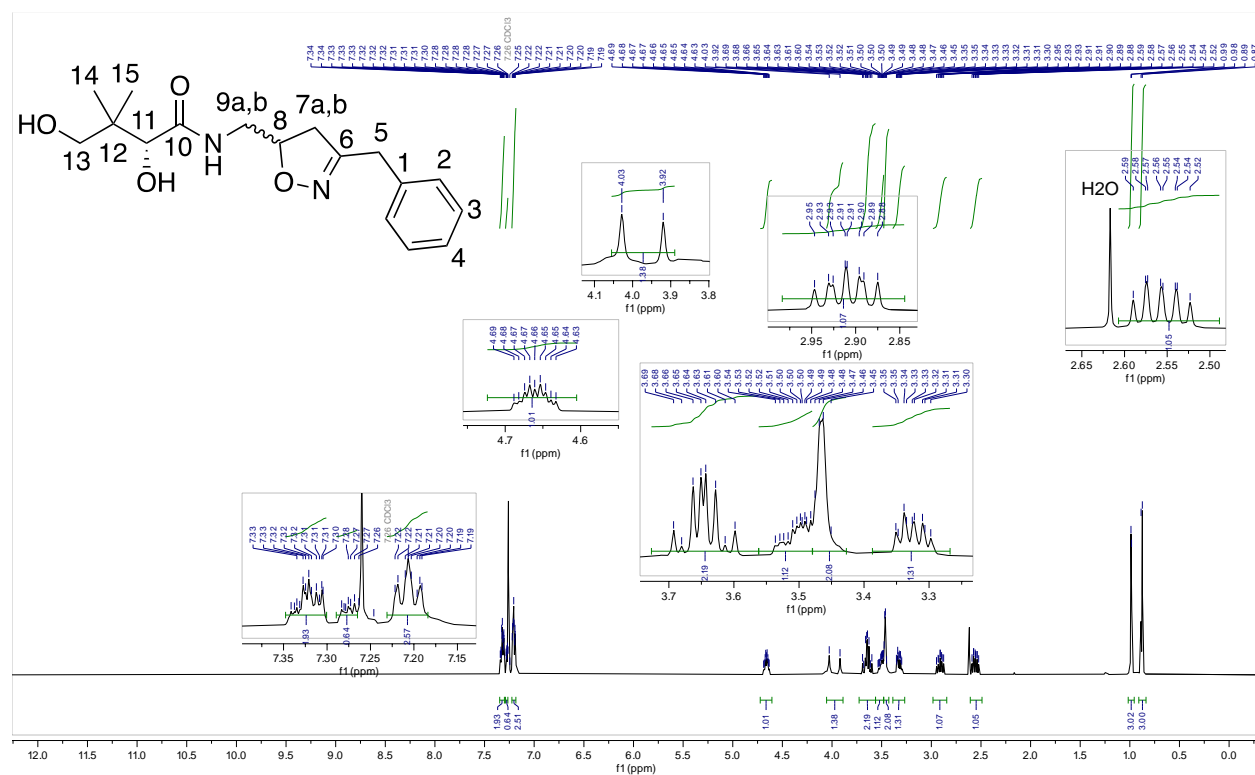


Compound 3c





Compound 3e



Compound 3f

